

Complex Mechanisms of KCNQ Channel Activation by State-dependent Modulators

By

Caroline Kaiyun Wang

A thesis submitted in partial fulfillment of the requirements for the degree of

Master of Science

Department of Pharmacology

University of Alberta

© Caroline Kaiyun Wang, 2018

ABSTRACT

Epilepsy is among the most common neurological diseases, but approximately 30% of epileptics are unresponsive to available drugs, and many more suffer significant side effects. One reason for the persisting large fraction of drug-resistant or drug-intolerant patients may be that most drug development in this field has been limited towards just a few molecular targets. I investigated a new class of anti-epileptic drugs that targets voltage-gated potassium channels of the KCNQ family, mutations of which have been implicated in neonatal forms of epilepsy. The KCNQ channel activator retigabine (RTG) was only recently approved (~2011) for use as an antiepileptic in humans. However, RTG has little subtype specificity between KCNQ2-5, and efforts are underway to develop improved retigabine derivatives with better specificity. To do this, a deeper understanding of the mechanism behind KCNQ channel openers is needed. My research compares the mechanisms of RTG and a 'second-generation' KCNQ channel opener, ICA-069673 (ICA73), which is suggested to have a distinct binding site and mechanism from RTG. In Chapter 3, we investigated the state- and use-dependent properties of ICA73 and RTG on KCNQ2 channel activation. Using whole-cell patch clamp electrophysiology and fast-solution switching, we characterized the relationship between drug binding and channel activation, and found that ICA73 preferentially binds to open channels at more depolarized voltages, while RTG can readily access both open and closed channels, and is thus available to bind across a broader range of voltages. Additionally, we found that an alanine to proline mutation in KCNQ2, previously shown to alter ICA73 sensitivity, results in faster ICA73 unbinding despite the drug retaining state-dependent binding. Both ICA73 and RTG bound in a use-dependent manner during rapid, successive depolarizations. In Chapter 4, we found that a mixture of ICA73 and RTG synergistically enhanced KCNQ channel activation in *Xenopus* oocytes using two-electrode voltage clamp. In an *in vivo* model of zebrafish larvae, RTG showed a clear, dose-dependent inhibition of seizure activity; ICA73 did not. Instead, another KCNQ opener, ML-213, was an

exceptionally powerful anticonvulsant drug in larvae, cells, and oocytes. Further investigation of ML-213 actions on KCNQ2 W236F and KCNQ2 F168L, mutations known to disrupt RTG or ICA73 sensitivity respectively, showed that ML-213 sensitivity was most severely disrupted in W236F. Finally, in Chapter 5, we aligned sequences of KCNQ2 with that of KCNQ5, an ICA73-insensitive subtype, and identified several mutations that had altered ICA73 sensitivity. The KCNQ2 mutants K116P, I173T, and G186K exhibited attenuated ICA73-induced gating shifts. Collectively, the results from this thesis highlight fundamental differences in the mechanism of two KCNQ2 openers, ICA73 and RTG, which may be exploited for clinical therapy.

PREFACE

This thesis is an original work by Caroline Wang. No part of this thesis has been previously published. Chapter 3 of this thesis is submitted for publication at The Journal of General Physiology. Caroline Wang performed all of the experiments, analyzed the data, and contributed to manuscript composition and project design. Harley Kurata was the primary author who conceptualized and designed the research project. The *in vivo* work with zebrafish larvae in Chapter 4 was done in collaboration with Richard Kanyo, Laszlo Locskai, and Ted Allison. Caroline Wang and Harley Kurata designed the experiments; Richard Kanyo performed the experiments and analyzed the data. Laszlo Locskai contributed to data analysis and performed statistical measurements. All other work in Chapter 4 was performed by Caroline Wang. All work in Chapter 5 was performed primarily by Caroline Wang, with contributions from Harley Kurata in project design, and from Runying Yang in technical assistance with mutagenesis.

Two papers not included in this thesis have been submitted for publication at The Journal of General Physiology and are currently undergoing revisions. These include “Functional stoichiometry of KCNQ channel openers I: pore-targeted openers” by Michael Yau, Robin Kim, Caroline Wang, Runying Yang, Stephan Pless and Harley Kurata, and “Functional stoichiometry of KCNQ channel openers II: voltage sensor-targeted openers” by Alice Wang, Michael Yau, Caroline Wang, Runying Yang, Stephan Pless and Harley Kurata.

ACKNOWLEDGEMENTS

I would like to thank my supervisor, Harley Kurata, for his invaluable mentorship throughout the course of my graduate studies. It is rare to encounter a supervisor who is both a friend to and an inspiration for young scientists. You are both. I feel incredibly lucky to have worked with you, and am convinced that I could not have picked a better lab. I am also grateful for the guidance provided by my committee members, Peter Smith and Warren Gallin. Additionally, I would like to thank my friends and lab mates with whom I shared many wonderful memories – Mikaela Burgos, Victoria Baronas, Robin Kim, Alice Wang, Damayantee Das, Jihee Yoo, Jingru Li, Daniel Fajonyomi, Tarek Ammar, Nazlee Sharmin, Runying Yang, and Camilla Lund. You all have made my stay in Edmonton such a fun and fulfilling experience, and I will always cherish our friendship. Finally, thank you to my family, who have always shown me unwavering love and support in all my endeavors.

TABLE OF CONTENTS

ABSTRACT	II
PREFACE	IV
ACKNOWLEDGEMENTS	V
TABLE OF CONTENTS	VI
LIST OF TABLES	VIII
LIST OF FIGURES	IX
LIST OF ABBREVIATIONS	X
CHAPTER 1 : INTRODUCTION	1
POTASSIUM CHANNEL OVERVIEW	1
<i>Channel structure</i>	1
<i>Ion selectivity and permeation</i>	3
<i>Voltage sensing and gating</i>	4
KCNQ CHANNEL OVERVIEW	6
<i>KCNQ channel regulation</i>	6
<i>PIP₂</i>	7
<i>KCNQ1 channels are linked to cardiac disease</i>	10
<i>KCNQ4 channels are important for hearing</i>	11
<i>KCNQ2 and KCNQ3 are the molecular correlates of the M-current</i>	12
<i>KCNQ5 may also contribute to the M-current</i>	16
KCNQ PHARMACOLOGY	17
<i>Retigabine: a first-in-class KCNQ pore site activator</i>	18
<i>Other pore site activators</i>	20
<i>Voltage sensing domain activators</i>	22
STATE- AND USE-DEPENDENCE	24
SCOPE OF THESIS INVESTIGATION	26
CHAPTER 2 : MATERIALS AND METHODS	28
<i>Whole cell patch clamp</i>	28
<i>Two-electrode voltage clamp</i>	28
<i>Fast-solution switching</i>	28
<i>Drug solutions</i>	29
<i>Chemical structures of drugs</i>	29
<i>Ion channel constructs and transfection in cells</i>	30
<i>Harvesting oocytes & mRNA injections</i>	30
<i>Zebrafish activity measurements</i>	31

<i>Statistics</i>	32
CHAPTER 3 : STATE- AND USE-DEPENDENT BINDING OF KCNQ CHANNEL OPENERS	33
INTRODUCTION	33
RESULTS	36
<i>ICA73 binding is occluded in the KCNQ2 closed state</i>	36
<i>ICA73 binding site access tracks voltage-dependent activation</i>	38
<i>Retigabine readily accesses KCNQ2 closed states</i>	40
<i>Channel closure requires ICA73 unbinding</i>	42
<i>A voltage sensor mutation accelerates ICA73 unbinding</i>	44
<i>Both RTG and ICA73 promote channel opening with high frequency stimulation</i>	46
DISCUSSION	48
CHAPTER 4 : SYNERGISTIC ACTIONS OF ANTICONVULSANT KCNQ CHANNEL OPENERS	52
BACKGROUND	52
RESULTS	54
<i>ICA73 and RTG have synergistic actions in oocytes expressing KCNQ2/3 channels</i>	54
<i>KCNQ channel opener effects in an in vivo model</i>	56
<i>ML213 effects on pore and voltage sensor mutants</i>	59
DISCUSSION	60
CHAPTER 5 : PROBING FOR SPECIFIC VOLTAGE SENSOR RESIDUES REQUIRED FOR ICA73 EFFECT	64
BACKGROUND	64
RESULTS	66
<i>KCNQ5 is insensitive to ICA73</i>	66
<i>ICA73 effects are diminished in three voltage sensor mutants</i>	67
DISCUSSION	69
CHAPTER 6 : GENERAL DISCUSSION & CONCLUSION	71
<i>General discussion</i>	71
<i>Conclusion</i>	76
REFERENCES	77

LIST OF TABLES

Table 1.1 KCNQ openers.	17
Table 2.1 Chemical structures of drugs	29

LIST OF FIGURES

Figure 1.1 KCNQ channel structure.	2
Figure 1.2 The K⁺ channel pore.	4
Figure 1.3 KCNQ channels are regulated by muscarinic signaling.	8
Figure 2.1 Fast-solution switching	29
Figure 3.1 ICA73 is excluded from channel closed states and binds to open channel states.	37
Figure 3.2 ICA73 binding tracks KCNQ2 channel opening.	38
Figure 3.3 RTG can bind to both open and closed channel states.	40
Figure 3.4 RTG binds before channels open.	41
Figure 3.5 RTG increases the speed of channel opening and re-opening while ICA73 does not affect channel opening kinetics.	43
Figure 3.6 ICA73 binding to KCNQ2[A181P] also tracks channel opening.	44
Figure 3.7 Rate of ICA73 binding to WT KCNQ2 and KCNQ2[A181P] channels.	45
Figure 3.8 ICA73 unbinds from KCNQ2 [A181P] faster at various voltages.	46
Figure 3.9 Use-dependent activation by ICA73 and RTG.	47
Figure 3.10 Model of ICA73 versus RTG binding.	50
Figure 4.1 Low to intermediate concentrations of ICA73 and RTG synergistically activate KCNQ channels.	55
Figure 4.2 KCNQ opener effects in zebrafish larvae.	56
Figure 4.3 ML-213 is a strong KCNQ channel opener and effective anticonvulsant.	58
Figure 4.4 ML213 sensitivity in pore and voltage sensor mutants.	59
Figure 5.1 ICA73 sensitivity of KCNQ5 and residue differences.	67
Figure 5.2 ICA73 effects in three voltage sensor mutants.	68

LIST OF ABBREVIATIONS

BFNC/S – benign familial neonatal convulsions/seizures
EE – epileptic encephalopathy
RTG – retigabine
ICA73 – ICA-069673
Kv – voltage-gated potassium
Kir – inwardly rectifying potassium
AED – antiepileptic drug
PIP₂ – phosphatidylinositol 4,5-bisphosphate
PLC – phospholipase C
IP₃ – inositol triphosphate
DAG – diacylglycerol
GPCR – G-protein coupled receptor
M1 – muscarinic acetylcholine 1
PKC – protein kinase C
LQT – long QT

DFNA2 – deafness nonsyndromic autosomal dominant 2
JLNS – Jervell-Lange-Nielsen syndrome
RWS – Romano-Ward syndrome
VSD – voltage sensor domain
VS – voltage sensor
PD – pore domain
LA – local anesthetic
P_o – open probability
ZnPy – zinc pyrithione
PTZ – pentylenetetrazol
WT – wildtype
HEK – human embryonic kidney
VCF – voltage clamp fluoremetry
CaM – calmodulin
SQT – short QT

CHAPTER 1 : INTRODUCTION

POTASSIUM CHANNEL OVERVIEW

Potassium channels are ubiquitously expressed in eukaryotic, eubacterial and archaeal genomes, and make up the largest family of ion channels in invertebrates (Littleton and Ganetzky, 2000; Miller, 2000). These channels underlie electrical signaling and play diverse roles in a number of physiological processes. These range from regulating behaviors of excitable cells of the brain, pancreas, and muscle, to working in non-excitable organs and playing roles in electrolyte balance, immunity, and mechanosensation (Miller, 2000). Potassium channels can be classified into two broad categories: the six-transmembrane voltage gated (K_V) channels, and the two-transmembrane inward rectifier (K_{IR}) channels (Miller, 2000). Variations in the structure of these two classes give rise to other potassium channels, such as the calcium-activated potassium channels with 7-transmembrane domains, and the two-pore channels (Miller, 2000).

Channel structure

The crystal structure of KcsA, a bacterial two transmembrane K^+ channel served as an early template for modelling the pore-forming domain of K_V channels (Doyle et al., 1998; Lu et al., 2001). Since then, high-resolution structures of other K_V channels have steadily emerged. Recent work by members of the MacKinnon group elucidated the cryo-electron microscopy (EM) structure of KCNQ1, a member of the KCNQ (K_V7) family. KCNQ1 has a classical K_V transmembrane topology: four-fold symmetry consistent with its tetrameric structure, with each subunit consisting of six transmembrane helices (S1-S6), along with a cytosolic N- and C-terminal domain. The C-terminal tail contains four intracellular helices (A-D) that serves as a platform for interactions with regulatory molecules (Sun and MacKinnon, 2017). The first four transmembrane segments of each subunit (S1-S4) form the voltage sensor module that controls channel gating in response to membrane voltage (Sun and MacKinnon, 2017). The remaining two

transmembrane segments (S5-S6), along with a re-entrant loop (P-loop) linking the two segments, make up the channel pore (Sun and MacKinnon, 2017). At the P-loop sits a hydrophilic selectivity filter containing the K⁺ selectivity signature sequence T/SxxTxGYG; some mutations in this signature sequence eliminates channel selectivity for K⁺ ions (Heginbotham et al., 1994; Sun and MacKinnon, 2017).

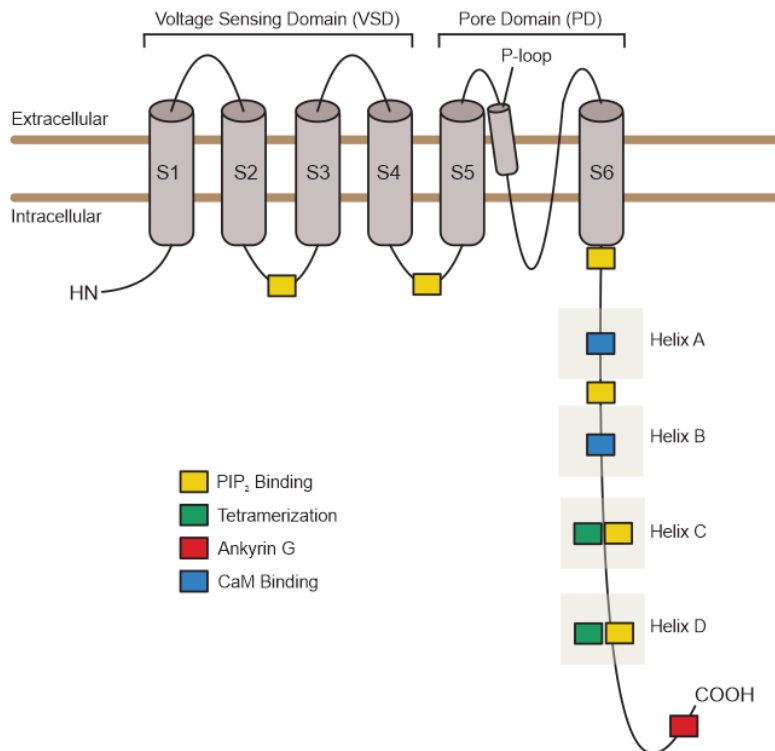


Figure 1.1 KCNQ channel structure. KCNQ channels contain six transmembrane domains. S1-S4 make up the voltage sensing domain, with positively charged residues in the S4 comprising the main voltage sensor. S5-S6 make up the pore domain that contains a P-loop that imparts K⁺ ion selectivity. Amino and carboxylic terminals are both intracellular; the carboxylic tail contains four helices (A-D), which contain regions important for tetramerization or binding to regulatory factors including PIP₂, ankyrin G, and CaM. Figure modelled from (Barrese et al., 2018).

Disease-causing mutations often affect channel function by disrupting channel gating and/or permeation. Understanding mechanisms of normal ion channel gating and permeation will thus help to better understand the molecular basis for disease phenotypes.

Ion selectivity and permeation

Potassium channels exhibit a >1000 fold selectivity for K⁺ ions over Na⁺ ions despite similar atomic radii (1.33Å for K⁺ and 0.95Å for Na⁺) (Armstrong and Hille, 1998; MacKinnon, 2003). A closer look at the architecture of the channel tells us how these proteins can paradoxically have such high selectivity for K⁺ ions while maintaining a high throughput rate of the ion through the pore. When closed, the channel pore structure resembles an ‘inverted teepee’, with four transmembrane helices crossing each other to form a gate. The selectivity filter sits at the wide end of this teepee (Doyle et al., 1998). The pore is 45Å long, 10Å wide at its center and narrows to 3Å wide at the selectivity filter (Doyle et al., 1998). While the central cavity and internal pore is hydrophobic, the selectivity filter is hydrophilic (Doyle et al., 1998). Ions predominantly occupy alternating sites in the cavity site and the selectivity filter (Doyle et al., 1998). K⁺ ions entering the selectivity filter from the cavity center must dehydrate, but are well stabilized energetically by electronegative moieties from backbone carbonyl groups pointing into the selectivity filter that mimic water oxygen atoms (Doyle et al., 1998). High selectivity for K⁺ is preserved because these electronegative moieties create a cavity into which a dehydrated K⁺ ion would fit, but for which Na⁺ fits too loosely to be energetically favorable (Doyle et al., 1998). The entrance of a second K⁺ ion into the selectivity filter introduces electrostatic repulsion between the two closely spaced ions. This repulsion overcomes the stabilizing interaction between the channel and the ion, resulting in a rapidly ejected ion through the pore (Doyle et al., 1998).

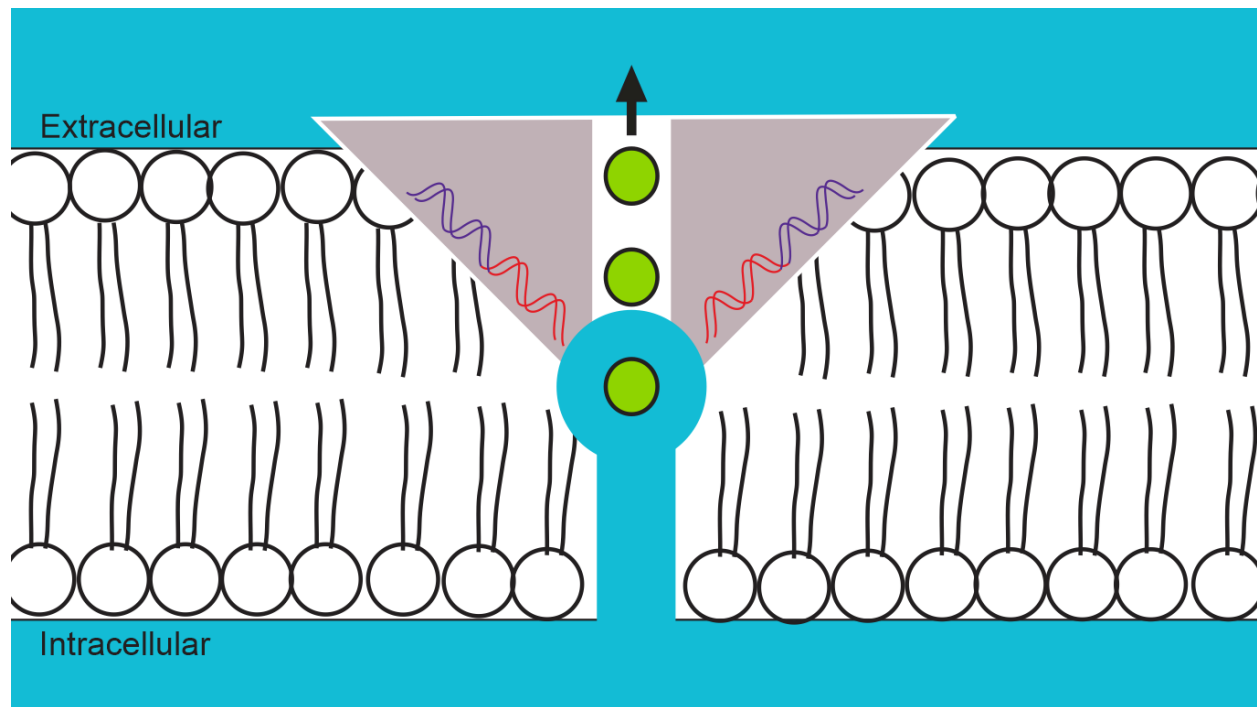


Figure 1.2 The K⁺ channel pore. The center cavity (blue) is continuous with the cytosol. K⁺ ions (green) sitting in the center cavity are stabilized by electronegative moieties from backbone carbonyl groups. A K⁺ ion entering the more narrow selectivity filter (white) propels the other ion through the pore. Note that the pore itself is passive, and the direction of ion flow depends on electrochemical gradient. Figure modelled from (Doyle et al., 1998).

Voltage sensing and gating

How is membrane depolarization coupled to ion conduction? Charged amino acids, called gating charges, move through the membrane electric field in response to membrane potential changes to produce a transient gating current and couple electric work to channel opening (Bezannila, 2008). The Shaker K⁺ channel from *Drosophila melanogaster*, named because of the shaking phenotype mutant flies adopt under anesthesia, was the first K⁺ channel cloned and served as a prototype for modelling voltage sensing. In Shaker, 12-14 elementary charges make up the gating charge (Aggarwal and MacKinnon, 1996). These charges are carried primarily by the first four arginines on the S4 helix of the voltage sensor (R362, R365, R368, R371), with minor contributions by other basic residues on the S4 (K374) and an acidic residue in S2 (E293)

(Aggarwal and MacKinnon, 1996; Schoppa et al., 1992; Seoh et al., 1996). The energetic costs of burying these gating charges in the membrane core of the protein are minimized by salt bridge interactions with acidic residues in other transmembrane domains, and by the fact that only a subset of the charged residues happen to be within the membrane core of the protein at any one time (Larsson et al., 1996). The overall voltage-dependence and size of gating charge varies between different channel types, depending on the magnitude of the charge carried by voltage sensor residues, and the strength of the electric field where the charges move (Bezaniilla, 2008).

In K_v channels, the movement of the voltage sensor is tightly coupled to the intracellular channel gate that regulates pore access (Liu et al., 1997; Long et al., 2005). This is accomplished by key residues – a glycine and a PXP motif – in the inner pore helix (S6). The pore glycine acts as a gating hinge: when the channel is closed, the helices are straight; upon channel opening, the helices are bent at this hinge point to permit flow of ions (MacKinnon, 2003). Also in the pore, a PXP motif bends the inner S6 helix, allowing the S6 to extensively interact with the S4-S5 linker of the same subunit and couple voltage sensor activation to pore opening (Long et al., 2005). In KCNQ channels, this PXP motif is replaced by a PAG motif (Seeböhm et al., 2006). Mutations in the PXP motif or PAG motif alter channel gating and uncouple voltage sensor movement from pore movement (Long et al., 2005; Seeböhm et al., 2006). In summary, changes in membrane voltage are sensed by basic charges on the channel's S4 helix. When the membrane depolarizes, the S4 helix moves upwards and outwards through the membrane. This movement pulls up on the S4-S5 linker, which in turn pulls the intracellular gating hinge in the S6 helix open. Hyperpolarization of the membrane induces a reverse sequence of actions: the voltage sensors displace inwards, pushing down on the S4-S5 linker which compresses the inner S6 helices to close access to the pore (Long et al., 2005).

KCNQ CHANNEL OVERVIEW

My research focuses on a specific family of K_V channels, the K_V7 channels, also known as KCNQ channels. Five members make up the KCNQ family: KCNQ1-5, whose genes are located at chromosomal loci *11p15*, *20q13*, *8q24*, *1p34*, and *6p13* respectively (Barrese et al., 2018). Each of these genes encode a channel subunit made up of 650-940 amino acids (Barrese et al., 2018). KCNQ channels are tetrameric proteins whose subunits assemble into both homomeric and heteromeric channels. KCNQ1 forms homomeric channels to contribute to repolarization of the cardiac action potential (Robbins, 2001a). KCNQ2, 3, and 5, the neuronal isoforms of the channel, heteromerize to regulate neurotransmitter release and action potential firing (Robbins, 2001a). KCNQ4 and 5 also heteromerize in smooth muscle of the vasculature, bladder, uterus and gastrointestinal tract where they modulate contractility (Barrese et al., 2018). KCNQ subunits may also associate with auxiliary subunits that modulate channel kinetics, expression, function, and pharmacology. For example, KCNQ1 associates with transmembrane, non-pore forming proteins of the KCNE family to modulate their activation properties in the heart (Barrese et al., 2018; Robbins, 2001b). Interaction with KCNE1 prominently slows activation kinetics, shifts the voltage-dependence of KCNQ1 activation to more depolarized voltages, and increases channel expression and single-channel conductance (Barrese et al., 2018). In contrast, the association of KCNE proteins with neuronal KCNQ2/3 is less characterized and may only have modest effects (~5mV depolarizing shift) (Tinel et al., 2000).

KCNQ channel regulation

All KCNQ channels have an elongated intracellular C-terminal domain organized into four helices (A-D) (Barrese et al., 2018). These helices serve as the primary site for interactions with regulatory factors, and as the platform for channel tetramerization (Barrese et al., 2018). One key element of KCNQ regulation comes from their absolute requirement for PIP₂ for channel

regulation. Thus, $G_{q/11}$ -coupled receptor activation and subsequent PLC-mediated PIP_2 hydrolysis is an important physiological regulatory mechanism that controls KCNQ function.

PIP₂

PIP_2 is an anionic lipid located in the inner leaflet of the membrane that makes up <1% of the total pool of phospholipids (Zaydman and Cui, 2014). It is synthesized in two ATP-dependent steps by the phosphorylation of PI to PIP, and again to PIP_2 by PI_4 -kinase and PI_5 -kinase respectively (Suh and Hille, 2007). All KCNQ subtypes require PIP_2 for channel activation. Inside-out patches from KCNQ2/3 channels expressed in oocytes exhibit current ‘run-down’ following depletion of PIP_2 , which is restored with application of PIP_2 to the intracellular side (Zhang et al., 2003). Introduction of intracellular hydrolysable ATP is necessary for PIP_2 synthesis and recovery of M-current, while application of wortmannin, a PI_4 -kinase inhibitor, reduces M-current (Suh and Hille, 2002). Translocatable enzymes that cleave membrane PIP_2 in response to a chemical cue without affecting concentrations of downstream effectors DAG, IP_3 or calcium led to a rapid, complete, and irreversible suppression of current (Suh et al., 2006). Rather than changing single channel conductance or ionic selectivity, PIP_2 increases P_O by facilitating coupling of voltage sensor activation and pore opening (Li et al., 2005; Zaydman et al., 2013a). In a voltage sensor activated, pore closed, PIP_2 -free state, KCNQ1 has a disengaged connection between its S4 helix and S4-S5 linker, with this region partially extending into a loop. Overall, this results in an S4-S5 linker that has diminished contact with S6. This loop coincides with a potential PIP_2 binding pocket, consistent with idea that PIP_2 binding facilitates voltage sensor-pore coupling (Sun and MacKinnon, 2017).

PIP_2 concentrations in the membrane are modulated by the activity of $G_{q/11}$ -protein coupled receptors. Activation of these receptors activates phosphoinositide-specific phospholipase C- β (PLC- β), resulting in a cascade of intracellular events (see Fig. 1.3 below). Activated PLC- β catalyzes the hydrolysis of membrane PIP_2 into IP_3 and DAG (Delmas and Brown,

2005; Rhee, 2001). The loss of PIP_2 inhibits KCNQ current, while the production of IP_3 leads to IP_3 binding on its receptors and release of intracellular calcium stores. Elsewhere, DAG activates protein kinase C (PKC) and triggers other downstream cascades (Delmas and Brown, 2005; Rhee, 2001). The loss of PIP_2 by maximal receptor activation can be large (>95%) and rapid, although levels are recoverable (Delmas and Brown, 2005; Horowitz et al., 2005; Suh and Hille, 2008; Suh et al., 2006).

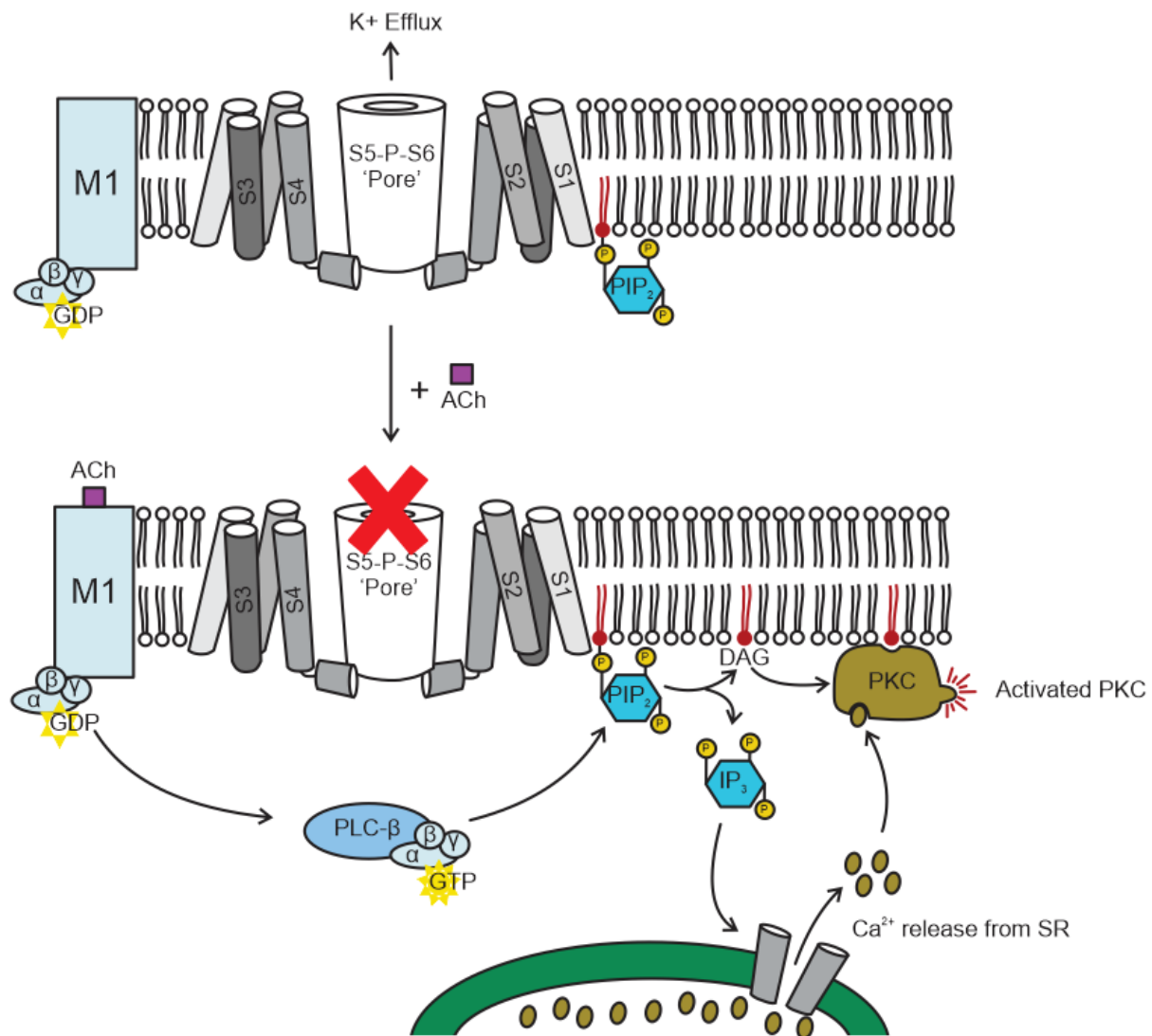


Figure 1.3 KCNQ channels are regulated by muscarinic signaling. In the absence of muscarinic receptor stimulation, membrane PIP_2 interacts with channel and allows for K^+ conductance. Activation of muscarinic receptors leads to PLC activation, PIP_2 membrane cleavage, activated PKC and calcium efflux from the sarcoplasmic reticulum (SR) downstream. Dissociation of PIP_2 inhibits KCNQ conductance.

Sensitivity to PIP₂ varies amongst KCNQ subtypes. KCNQ3 is most sensitive (EC₅₀ = 2.6 μM); KCNQ2 and KCNQ4 are a hundred-fold less so (EC₅₀ = 205 μM and 215 μM for KCNQ2 and KCNQ4 respectively) (Li et al., 2005). Heteromeric KCNQ2/3 channels show intermediate PIP₂ sensitivities (EC₅₀ ~40 μM) (Li et al., 2005). Such differential affinities account for the differences in maximum open probabilities (P_o) of the KCNQ channel subtypes (Li et al., 2005). For example, KCNQ3 channels may open with near-unity with the concentration of PIP₂ present in cells, but this same concentration might only partially activate KCNQ2 channels (Delmas and Brown, 2005). Thus, depending on the channel composition, KCNQ channels exhibit drastically different responses to muscarinic stimulation and PIP₂ depletion (Delmas and Brown, 2005).

The key PIP₂ interaction sites are clustered around the voltage sensor-pore interface. This interface is made up of contributions by residues from the S2-S3 linker, the S4-S5 linker, the S6, and the proximal C-terminus (Zaydman and Cui, 2014). Mutations of these mostly positively charged residues resulted in severe weakening of channel affinity to PIP₂ and subsequent loss of voltage sensor activation-coupled pore opening (Park et al., 2005; Rodriguez-Menchaca et al., 2012; Thomas et al., 2011; Zaydman et al., 2013b; Zhang et al., 2003). Two other proposed interaction sites for PIP₂ are the Helix A-B linker, and the distal C-terminus. Mutations in the Helix A-B linker reduce P_o values at 0 mV by ~50%, and chimeric studies between KCNQ3 (high PIP₂ affinity) and KCNQ4 (low PIP₂ affinity) show PIP₂ having more similar affinity to channels from which the Helix A-B linker originated, than from the background channel (Hernandez et al., 2008). Because the Helix A-B linker also serves as the binding site for CaM, CaM binding may regulate PIP₂ interaction with the channel (Tobelaim et al., 2017). Finally, mutations in the distal C-terminus R539W, R555C decreased affinity of KCNQ1/KCNE1 channels to exogenous PIP₂ (Park et al., 2005). Mutations that disrupt PIP₂ binding have been described as one pathogenic mechanism in KCNQ-related diseases. Alternatively, drugs that increase channel sensitivity to PIP₂ to promote its coupling effects represent valuable therapies in such pathologies.

KCNQ SUBTYPES AND PATHOLOGIES

The functional significance of the KCNQ family of channels is highlighted by the fact that KCNQ genes map directly to human disease loci. Their physiological correlates are diverse and wide-ranging, encompassing chronic and neuropathic pain, hearing, neuronal excitability, and cardiac function. KCNQ modulators thus have potential for treating a variety of clinical diseases.

KCNQ1 channels are linked to cardiac disease

KCNQ1 was the first KCNQ subtype cloned. It was first linked to Long QT (LQT) syndrome when positional cloning methods identified *kcnq1* as the gene responsible for LQT1 syndrome, an inherited cardiac arrhythmia (Wang et al., 1996). Mutations in *kcnq1* are also associated with other cardiac diseases, including familial atrial fibrillation, and short QT syndromes (Robbins, 2001a; Sun and MacKinnon, 2017). In the heart, KCNQ1 co-assembles with KCNE1, a 130-AA, single-transmembrane protein, to produce the cardiac slowly activating delayed rectifier I_{ks} current (Barhanin et al., 1996; Sanguinetti et al., 1996). Loss of function mutations in KCNQ1 and KCNE1 result in LQT, a cardiac disease characterized by prolonged repolarization of the cardiac action potential. This manifests as a prolonged QT interval on the electrocardiogram and susceptibility to syncope, seizures, and ventricular tachyarrhythmia in patients (Jervell and Lange-Nielsen, 1957). There are two forms of inherited LQT1 associated with KCNQ1/KCNE1 defect: Romano-Ward syndrome (RWS), an autosomal dominant LQT, and Jervell-Lange-Nielsen syndrome (JLNS), an autosomal recessive LQT associated with congenital deafness (Romano, 1965; Wang et al., 1998a). Alternatively, gain of function mutations in KCNQ1 lead to SQT, and familial atrial fibrillation.

Other KCNQ1 roles

KCNQ1 is also enriched in the cochlea of the inner ear, where it regulates ionic homeostasis (Neyroud et al., 1997). During auditory stimulation, K^+ ions move from the endolymph into hair

cells and then into supporting cells (Wang and Li, 2016). KCNQ1 channels maintain a high K^+ concentration in the endolymph by allowing K^+ recycling back into the endolymph from the stria vascularis (Neyroud et al., 1997). Mutations in KCNQ1/KCNE1 can cause deafness-related symptoms in JLNS, highlighting its functional importance in the inner ear (Neyroud et al., 1997).

KCNQ4 channels are important for hearing

KCNQ4 is another KCNQ subtype with important physiological roles in the inner ear: it localizes specifically to outer hair cells of the cochlea to mediate the $I_{K_{oh}}$ current, and to Type I hair cells of the vestibular apparatus where it mediates the I_{KL} current, both outwardly rectifying K^+ currents in the inner ear. KCNQ4 also influences K^+ concentrations in synapses to regulate fusion of synaptic vesicles (Kharkovets et al., 2000). Mutations in KCNQ4 are directly linked to deafness nonsyndromic autosomal dominant 2 (DFNA2), a subtype of sensorineural progressive hearing loss that affects high frequency-hearing first (Wang and Li, 2016).

Other KCNQ4 roles

In addition to hearing, KCNQ4 modulates stimulus-excitation coupling in touch sensation (Heidenreich et al., 2012). Mechanoreceptors in lanceolate and circular nerve endings around hair follicles, and in Meissner corpuscles in non-hairy skin express KCNQ4. Here, the channel dampens the firing of these rapidly adapting sensory structures so that low-frequency stimuli are not detected as well as higher frequency stimuli (Heidenreich et al., 2012). KCNQ4 also has roles in the heart, where its localization to cardiac mitochondria allows it to regulate mitochondrial membrane potential. The channel's activation increases mitochondrial permeability to K^+ ions, depolarizing the membrane and subsequently inhibiting mitochondrial calcium uptake (Testai et al., 2016). Because KCNQ4 activation opposes calcium overload and subsequent triggers of apoptosis, pharmacological activation of these channels may be a novel therapeutic strategy for cardioprotection (Testai et al., 2016). In the vasculature, KCNQ4 heteromerizes with KCNQ5 to regulate vascular tone. These channel subunits are present in the smooth muscle of many arteries,

including mesenteric, renal, cerebral, coronary, and penile tissues, as well as the smooth muscle of the gastrointestinal tract, uterus, corpus cavernosum, lungs, and bladder (Barrese et al., 2018). Contractility of smooth muscle predominately occurs through influx of calcium through voltage-gated calcium channels; KCNQ subunits modulate the amount of calcium influx and subsequent contractility by regulating the resting membrane potential of these cells (Barrese et al., 2018). The vasodilatory effects of KCNQ4/5 raises the possibility of KCNQ activators as treatment for pathologies such as pulmonary hypertension, cerebral vasospasm, and erectile dysfunction (Chadha et al., 2014; Jepps et al., 2016; Joshi et al., 2009). On the other hand, KCNQ blockers may be valuable therapies for urinary retention, in which decreased contractility of the bladder detrusor muscle inhibits bladder emptying (Anderson et al., 2013).

KCNQ2 and KCNQ3 are the molecular correlates of the M-current

KCNQ2 and 3 form channels that conduct the M-current, so named because of its propensity to be regulated by muscarinic signaling (Wang et al., 1998b). The M-current is a slowly activating and deactivating potassium current that was originally identified in frog, then shown to also be present in mammalian sympathetic neurons (Brown and Adams, 1980; Constanti and Brown, 1981). M-currents are non-inactivating potassium currents that take tens to hundreds of milliseconds to activate at moderately depolarized potentials (Brown and Adams, 1980; Constanti and Brown, 1981). These channels are activated at subthreshold potentials greater than -60mV to generate an outward potassium current (Brown and Adams, 1980; Constanti and Brown, 1981). Pharmacologically, M-current is inhibited by stimulation of receptors coupled to GPCR and G_{q/G11} proteins. These include receptors for acetylcholine, glutamate, histamine, serotonin, nucleotides, and peptide factors such as bradykinin and angiotensin (Brown and Passmore, 2009). M-currents are blocked by two specific inhibitors, linopirdine and XE-991 (Brown and Adams, 1980; Brown and Passmore, 2009; Constanti and Brown, 1981; Wang et al., 1998a).

While all KCNQ family members (Q1-Q5) form M-like currents in heterologous expression systems, heteromeric KCNQ2/3 channels, with possible contribution by heteromeric Q3/5 channels, have been identified as the molecular correlates of the M-current in native neurons (Brown and Passmore, 2009; Lerche et al., 2000; Schroeder et al., 2000; Wang et al., 1998a; Wickenden et al., 2001). Heteromerization of KCNQ2 and KCNQ3 subunits results in channels conducting at least 10 fold greater currents than either homomer alone due to enhanced channel expression and increased P_o (Schroeder et al., 1998; Wang et al., 1998a). When expressed alone, KCNQ3 subunits remain in the endoplasmic reticulum and are unable to traffic efficiently to the membrane (Gómez-Posada et al., 2010). Instead of a conserved threonine amongst eukaryotic potassium channels, KCNQ3 expresses an alanine at position 315 in the inner pore vestibule (Gómez-Posada et al., 2010). It is this singular amino acid that prevents KCNQ3 from expressing functional homomeric channels, while KCNQ3 [A315T] can efficiently traffic to the plasma membrane (Gómez-Posada et al., 2010). Since KCNQ3 is poorly expressed by itself, the expression patterns of KCNQ2 primarily regulate M-current (Wang et al., 1998a).

M-channels are expressed in central, peripheral and sensory neurons. In the brain, M-channels are expressed broadly throughout the cerebral and cerebellar cortices and the hippocampus, where they exert strong inhibitory influences on neuronal excitation (Brown and Passmore, 2009; Pan et al., 2006). Peripherally, M-channels are expressed in the dorsal root ganglia, where they strongly reduce the responses of nociceptive neurons to exert analgesia (Passmore et al., 2003). The role of M-channels is determined largely by their subcellular localization to nerve terminals, perisomatic regions, or axon initial segments. At nerve terminals, M-channels regulate neurotransmitter release (Martire et al., 2004). At the perisomatic region, M-current mediates medium afterhyperpolarizations and spike-frequency adaptations, which are important for determining discharge patterns and frequency (Gu et al., 2005; Otto et al., 2006; Peters et al., 2005). At axon initial segments, M-channels co-localize with Na_v channels through an ankyrin-G binding motif in their C-terminal tails to regulate action potential thresholds and

propagation (Pan et al., 2006). M-channels have two underlying features that allow them to strongly influence neuronal excitability. First, their activation at subthreshold potentials allows for channels to be partially activated at voltages near the resting membrane potential, and to thus suppress spontaneous firing (Gunthorpe et al., 2012). Second, their slow activation kinetics means that while they are too slow to prevent individual action potentials from firing, they can modulate the afterpotential to regulate the excitability of the cell following an action potential to limit the occurrence of burst firing (Gu et al., 2005; Yue and Yaari, 2004).

KCNQ2 and KCNQ3 mutations give rise to a neonatal epilepsies

KCNQ2 and 3 were first linked to epileptic disorders when a form of neonatal epilepsy, benign familial neonatal convulsions (BFNC), was mapped to a specific chromosomal region on the long arm of chromosome 20 (Leppert et al., 1989). Subsequent genetic linkage studies using a BFNC family mapped the locus of this gene, which was found to have significant homology to *KCNQ1* and thus named *KCNQ2* (Biervert et al., 1998). The BFNC family studied had a loss-of-function mutation in *KCNQ2*: a five base-pair insertion in the protein, leading to a premature stop codon and truncation of the channel (Biervert et al., 1998). Genetic analysis of other BFNC families soon identified more disease-causing mutations in *KCNQ2* (Singh et al., 1998). The genetic heterogeneity of BFNC was highlighted by the identification of a new locus on chromosome 8 that was also linked to the disease (Lewis et al., 1993; Steinlein et al., 1995). The gene implicated was eventually identified as *KCNQ3*, with a mutation (G263V) identified in a BFNC family (Charlier et al., 1998). Since then, many other *KCNQ2* and *KCNQ3* mutations have been identified, giving rise to neonatal epilepsies with a spectrum of phenotypes that range from mild to more severe. Milder loss-of-function mutations (haploinsufficiency) in both *KCNQ2* and *KCNQ3* result in BFNC. On the other hand, more serious impairment of channel function, limited to mutations in *KCNQ2*, cause severe forms of epileptic encephalopathy (EE).

BFNC is a benign, autosomal dominant form of childhood epilepsy affecting 1 out of every 100 000 people. Clinically, patients experience seizures that begin within the first week after birth but that remit by 16 months (Weckhuysen et al., 2013). These seizures are tonic, with motor and autonomic components and are often accompanied by apnea (Weckhuysen et al., 2013). Patients with BFNC generally have favorable prognosis, although some patients (~16%) may have increased risk of seizures in later life (Weckhuysen et al., 2013). Mutations responsible for BFNC lie mostly in KCNQ2, although there are several present in KCNQ3 (Millichap et al., 2016). These mutations are scattered throughout all regions of the channel, from the voltage sensor to the pore to the C-terminus. Mutations are diverse, ranging from missense to frameshift to truncation mutations (Millichap et al., 2016). These mutations result in subtle to modest loss of channel function (Millichap et al., 2016). As low as a 20% reduction of channel current is sufficient for BFNC, implying that M-current function is critical for early life, but that compensatory mechanisms in later development prevent the recurrence of seizures (Schroeder et al., 1998).

A more severe form of childhood epilepsy is KCNQ2 encephalopathy. As in BFNC, patients exhibit seizures within the first week of life. Unlike BFNC, however, these seizures do not remit and are extremely therapy-resistant (Weckhuysen et al., 2012). Patients experience profound developmental delay, motor impairment and speech and communication problems (Millichap et al., 2016; Weckhuysen et al., 2012). Other neurological impairments include hypotonia, dysphagia, dystonia, and spastic quadriplegia (Millichap et al., 2016; Weckhuysen et al., 2012). KCNQ2 encephalopathy mutations are clustered around “hot spots” in the S4 voltage sensor, the pore, and regions of C-terminus that bind to PIP₂ and CaM (Millichap et al., 2016). These mutations are nearly always single nucleotide substitutions resulting in missense mutations that severely impair channel function by affecting channel voltage dependence, PIP₂ interaction, or subcellular localizations to key sites (Barrese et al., 2018; Millichap et al., 2016).

KCNQ5 may also contribute to the M-current

KCNQ5 was cloned in 2000 by two independent groups, and found to share approximately 40% overall identity to other KCNQ subunits (Lerche et al., 2000; Schroeder et al., 2000). KCNQ5 mRNA localized mainly to the brain and to skeletal muscle, and smooth muscle including the urinary bladder (Lerche et al., 2000; Schroeder et al., 2000; Svalø et al., 2015). Its broad expression in the brain and periphery mirrors that of KCNQ2 and KCNQ3 – KCNQ5 transcripts are found in the cerebral cortex, hippocampus, putamen, occipital lobe, frontal lobe and temporal lobe, as well as peripheral sympathetic neurons (Lerche et al., 2000; Schroeder et al., 2000). KCNQ5 can heteromerize with KCNQ3 subunits to create channels with 4-5 fold greater currents, but KCNQ5 likely only contributes to M-current heterogeneity, rather than M-current directly, by sequestering the amount of KCNQ3 available to heteromerize with KCNQ2, thus regulating levels of the more “efficient” KCNQ2/3 heteromers (Lerche et al., 2000; Schroeder et al., 2000).

KCNQ5 in epilepsy

The physiological importance of KCNQ5 is still unclear at this time. Unlike other KCNQ subtypes, the KCNQ5 gene did not map directly to a human disease. Recently, however, heterozygous missense mutations in KCNQ5 have been identified in four patients with congenital neurological disorders of intellectual disability or epileptic encephalopathy (Lehman et al., 2017). These mutations include three loss-of-function mutations in the S1, S6, and C-terminus (V145G, L341I, and S448I respectively) with altered gating and reduced expression relative to homomeric KCNQ5 channels (Lehman et al., 2017). One gain-of-function mutation in the C-terminus, KCNQ5 [P369R], was present in the most severely affected child (Lehman et al., 2017). This mutation caused a 30mV hyperpolarizing shift in channel gating, accelerated activation and slowed deactivation (Lehman et al., 2017). The P369R mutant possibly increases neuronal excitability through a mechanism involving hyperactivation of hyperpolarization-activated non-selective cation channels, resulting in secondary depolarizations (Lehman et al., 2017).

KCNQ PHARMACOLOGY

The development of KCNQ channel drugs stemmed from initial identification that flupirtine enhances KCNQ current in dorsal root ganglion neurons to mediate analgesia (Szelenyi, 2013). Since then, the discovery of alternate therapeutic targets for KCNQ activators in cardiac disease, tinnitus, and epilepsy has led to an explosion of novel KCNQ modulators. These activators can be categorized by their site of action: one class of drugs binds to the channel pore, and includes the prototype KCNQ opener retigabine; another class of drugs binds to the channel voltage sensor to modulate its gating properties.

Compound Name	Site of Action	Selectivity
Flupirtine	Pore	KCNQ2-5
Retigabine	Pore	KCNQ2-5
BMS-204352	Pore	KCNQ2-5
Acrylamide-S1	Pore	KCNQ2-5
ML-213	Pore	KCNQ2-5
Zinc pyrithione	Pore, different site than RTG	KCNQ1-5 except KCNQ3
ICA-27243	VSD	KCNQ2, KCNQ2/3, KCNQ4
ICA-069673	VSD	KCNQ2, KCNQ4
Diclofenac	VSD	KCNQ2-5
Meclofenamate	VSD	KCNQ2/3
Ztz240	VSD	KCNQ2, KCNQ4, KCNQ5
NH29	VSD	KCNQ2, KCNQ2/3 > KCNQ4 > KCNQ5

Table 1.1 KCNQ openers. Molecules and drugs that activate KCNQ channels, their postulated site of action, and subtype selectivity. VSD = voltage sensing domain.

Retigabine: a first-in-class KCNQ pore site activator

Among the drugs that bind the channel pore, retigabine is the first and only drug to date that had been approved for use in humans as an antiepileptic. Early development of RTG began in the 1980s, from quantitative structural optimization of the congener compound flupirtine (Gunthorpe et al., 2012). Its efficacy in animal models of epilepsy and pharmaceutical profile led to its further development as an antiepileptic over flupirtine (Gunthorpe et al., 2012). Initially, the target of retigabine was unknown, although early studies showed that it lacked activity at conventional antiepileptic targets, including sodium and calcium channels, and only activated GABA receptors at high concentrations (Gunthorpe et al., 2012). Hints of its target came from the finding that the drug increased K⁺ conductance, although the specific channel was still unknown (Rundfeldt, 1997). Following cloning of the KCNQ channels, RTG was found to non-selectively activate KCNQ2-5 subtypes (Main et al., 2000; Tatulian and Brown, 2003; Tatulian et al., 2001; Wickenden et al., 2000). RTG is most potent on KCNQ3 and least potent on KCNQ4 and KCNQ5, with heteromeric channels displaying intermediate potencies to the drug (Gunthorpe et al., 2012). RTG activates channels with EC₅₀'s ranging from 0.6μM to 6.4μM (Gunthorpe et al., 2012).

RTG increases channel open probability, without changing the number of functional channels and/or the slope conductance (Tatulian and Brown, 2003). This results in KCNQ channel activation observable through three features: a gating shift wherein the voltage dependence of channel activation was shifted to more hyperpolarized potentials, an increase in the rate of channel activation, and a decrease in the rate of channel deactivation (Main et al., 2000; Tatulian et al., 2001; Wickenden et al., 2000). The M-current plays a physiologically significant role in dampening neuronal excitation; retigabine enhances this braking mechanism by recruiting activated M-channels (~30-40% in perforated patches) at resting membrane potentials to hyperpolarize the membrane and suppress action potential discharge (Tatulian et al., 2001).

Mapping the RTG binding site

Chimeric channels consisting of RTG-sensitive KCNQ2 and RTG-insensitive KCNQ1 were used to probe the structural determinants of the RTG binding site. A tryptophan pore residue, W236 (KCNQ2 numbering), was identified as essential for RTG effect which is likely mediated through a hydrogen bond interaction between the carbonyl group on RTG and the tryptophan side chain (Kim et al., 2015; Wuttke et al., 2005). A set of auxiliary residues in the S5 and S6 domain (L272, L314, L338, and G301) were also found lining the hydrophobic binding pocket for RTG in structural models of KCNQ3 (Lange et al., 2009). With the exception of Leu272, these amino acids are conserved across all KCNQ channels except for KCNQ1, which may account for its RTG insensitivity (Lange et al., 2009). Consistent with the hypothesis that RTG is an open channel stabilizer, the models show that when the channel is closed, S5 and S6 are parallel and exclude RTG from docking (Wuttke et al., 2005). When open, the S6 helix kinks at the gating hinge and a simultaneous conformational change of S5 allows for the hydrophobic pocket to form and RTG to bind (Wuttke et al., 2005). These models provide an attractive hypothesis for how RTG may bind to the activation gate of the channel to stabilize the open conformation.

Synthetic modifications of RTG moieties can finely tune the potency of the drug at the pore site. Because the carbonyl group on RTG forms a hydrogen bond with the indole nitrogen of the tryptophan side chain, the more polar the carbonyl group, the stronger is its propensity to accept a H-bond and the more potent the drug (Kim et al., 2015; Kumar et al., 2016). Correspondingly, increasing the electronegativity of the tryptophan side chain through fluorination increases RTG potency as the side chain becomes a better H-bond donor (Kim et al., 2015).

RTG as an antiepileptic drug

RTG is an effective anticonvulsant in a variety of animal models of epilepsy. RTG inhibited amygdala-kindled focal and secondarily generalized seizures in adult rats, and was comparable or superior to other antiepileptic drugs in suppressing seizures in kindling models of the rat

hippocampus (Large et al., 2012). RTG was also effective in maximal electroshock-induced rodents, a model of generalized tonic clonic seizures (Large et al., 2012). In models of pharmacoresistent epilepsy, RTG blocked seizures and was more potent than levetiracetam and valproate (Large et al., 2012). The drug's efficacy as an anticonvulsant in humans was established in two multicenter, randomized, double-blinded human clinical trials, RESTORE 1 and RESTORE 2 (Brodie et al., 2010; French et al., 2011). 1200mg of retigabine daily showed a mean reduction in seizure frequency of 45% compared to placebo (Brodie et al., 2010; French et al., 2011). However, the overall discontinuation rate of RTG was 17-30% higher than those of other antiepileptic drugs in clinical trials (Amabile and Vasudevan, 2013). These were likely due to side effects, including dizziness, somnolence, fatigue, confusion, ataxia, blurred vision, tremor, speech disorder (Brodie et al., 2010; French et al., 2011). The drug also bound to KCNQ subtypes in the bladder epithelium, leading to reports of urinary retention in 8.5% of patients across seven clinical trials (Amabile and Vasudevan, 2013). Starting in 2010, RTG was approved as an adjunct treatment for partial-onset seizures in adult patients in the United States, followed by approval in Canada and Europe (Martyn-St James et al., 2012). Concerns about risks of retinal abnormality, potential vision loss, and skin discoloration seen after long-term use, however, led to a FDA black box warning for the drug in 2013 (Millichap et al., 2016). In 2017, RTG's production stopped due to low usage amongst patients. RTG's nonspecificity will be an important point to improve upon in designs of future KCNQ openers for epilepsy.

Other pore site activators

BMS-204352 and acrylamide-S1 are two other KCNQ activators that potentiate current and induce hyperpolarizing shifts in the voltage dependence of channel activation (Bentzen et al., 2006; Schröder et al., 2001). Both are nonselective KCNQ activators that depend on the conserved pore tryptophan residue for their effects (Bentzen et al., 2006; Schröder et al., 2001). One pore activator that retains sensitivity on KCNQ2 W236L is zinc pyridone (ZnPy). Interestingly, this

compound has diminished effects on other pore mutants (KCNQ2 L249A and L275A), suggesting that it binds to a different pore site than RTG (Xiong et al., 2008a). ZnPy and RTG also showed combinatorial effects in KCNQ2 activation, supporting the idea that they bind to independent sites on the channel (Xiong et al., 2008a). ZnPy induces a -24mV leftward shift in channel gating, and increases current magnitude by roughly 5-fold on KCNQ2 channels (Xiong et al., 2008a). The compound's pyrithione moiety, in a complex with zinc, binds to an extracellular pore site on the channel to increase single-channel open probability and increase overall conductance (Gao et al., 2017; Xiong et al., 2007). Furthermore, ZnPy is a zinc ionophore that delivers free zinc ions to activate KCNQ current, although it remains unclear whether concentrations of zinc accumulation reach physiological relevance (Gao et al., 2017). Its proposed mechanism of action is to increase channel sensitivity to PIP₂ and facilitate interactions between the channel and the lipid (Gao et al., 2017). KCNQ3, which has high affinity for PIP₂, is insensitive to ZnPy since PIP₂ levels are already saturating (Gao et al., 2017). Consistent with this hypothesis, mutations in KCNQ3 that disrupt PIP₂ interactions in the Helix A-B linker and at other proposed PIP₂ binding sites resulted in channels with enhanced sensitivity to ZnPy (Gao et al., 2017).

ML213 is another KCNQ activator based on a novel chemical scaffold, as it lacks a heteroaryl moiety present in ICA-27243 (Yu et al., 2010). It was originally reported to be a potent KCNQ2 and KCNQ4 activator, and selective against KCNQ1, 3, and 5 (Yu et al., 2010). In thallium flux assays, the compound exhibited >80 fold selectivity for KCNQ2 over KCNQ1, KCNQ1/E1, KCNQ3, KCNQ5, and 6.7 fold selectivity for KCNQ2 over KCNQ4 (Yu et al., 2010). Since then, however, other studies have reported effects in KCNQ3 and KCNQ5 channels (Brueggemann et al., 2014; Kim et al., 2015). Like other activators, ML-213 induces a leftward shift in the voltage dependence of channel activation, potentiates current, and slows channel deactivation (Brueggemann et al., 2014; Yu et al., 2010).

Voltage sensing domain activators

Other than the pore activators, another class of compounds, called gating modifiers, bind to a different channel site – the voltage sensing domain. These modifiers can be further broken down into two groups of structurally unrelated compounds – *N*-pyridyl and pyrimidine benzamides (ICA compounds, and ztz240) and *N*-phenylanthranilic acid derivatives (diclofenac, meclofenamic acid, and NH29) (Brueggemann et al., 2014; Wickenden et al., 2008).

ICA acts at the voltage sensing domain

Out of the family of ICA compounds, ICA-27243 is the best characterized in animal models, and shown to be a more potent and selective KCNQ2 channel opener than RTG. ICA-27243 exhibits selectivity for KCNQ2 and KCNQ4 with little or no effect on KCNQ1, KCNQ3, or KCNQ5 (Wickenden et al., 2008). In ex vivo and in vivo models of epilepsy, ICA-27243 is an effective anticonvulsant, suppressing seizure-like activity in hippocampal slices and in maximal electroshock-induced mice (Wickenden et al., 2008). ICA-27243 is most potent on Q2/Q3 channels endogenously ($EC_{50} = 0.4\mu M$), is significantly less potent on KCNQ3/5 channels ($EC_{50} = >100\mu M$), and has no effect on KCNQ1/KCNE1 channels (Wickenden et al., 2008). Despite being a RTG analog, ICA-27243 potentiates KCNQ2 W236L currents, strongly hinting at a distinct binding site from RTG (Blom et al., 2010; Padilla et al., 2009a). The ICA binding site most likely resides in the voltage sensing domain. Chimeras between KCNQ2 and KCNQ5 showed that ICA-27243 potentiated KCNQ current in channels containing KCNQ2 voltage sensing domains (Padilla et al., 2009a). Subsequent sequence alignment between the voltage sensors of the two channels showed greatest diversity in the extracellular/membrane interfaces of one region closer to S2, and another closer to S3 (Padilla et al., 2009a). While more specific chimeras generated at the S3 region yielded nonfunctional channels, chimeras generated at the S2 region led to channels that had 17 fold less sensitivity to ICA-27243 (Padilla et al., 2009a). In confirmation with these findings, past work from our lab using a similar chimeric approach between KCNQ2 and KCNQ3

showed that the KCNQ2 voltage sensing domain was necessary to impart ICA73 sensitivity (Wang et al., 2017). Single point mutations at divergent residues in the voltage sensing domain identified two mutants in the S3 helix, F168L and A181P, that had diminished ICA73 sensitivity (Wang et al., 2017).

Other voltage sensor activators

Ztz240, a structural analog of ICA-27243, was identified in a screen of 20 000 compounds to isolate drugs that retained effects on KCNQ2 W236L (Gao et al., 2010). Ztz240 potentiated KCNQ2, 4, and 5 current, and dramatically prolonged deactivation (Gao et al., 2010). Mutation of the alanine in the PAG motif, previously mentioned as a conserved KCNQ gating hinge, eliminated ztz240 effect, while the effects of RTG and ZnPy were retained (Gao et al., 2010). Other KCNQ2 voltage sensing domain residues also important for ztz240 effect include F137, E130, I134, G138, R207, and R210; these residues may form a gating charge pathway in the channel to accommodate ztz240 (Li et al., 2013). Meclofenamic acid and diclofenac are another class of KCNQ openers. Both are anti-inflammatory drugs widely used as non-steroidal anti-inflammatory agents to non-selectively inhibit COX-1 and COX-2 enzymes (Peretz et al., 2005). They activate channels by causing a hyperpolarizing shift in the voltage dependence of channel activation and slowing channel deactivation, leading to an overall potentiation of potassium conductance (Peretz et al., 2005). In cultured cortical neurons, the drugs enhanced M-current and were able to reduce both evoked and spontaneous action potentials in vivo and ex vivo (Peretz et al., 2005).

Our current understanding of KCNQ modulators is mostly limited to their binding sites, overall macroscopic effects on channel activity, and disrupting mutations. Very little is known about how these drugs bind to channels to elicit a gating shift and current potentiation, and an in-depth exploration of the interplay between drug interactions to different channel states is severely lacking. Research in this area will provide valuable insights into the mechanism of KCNQ drug interaction with channels, which we could take advantage of to treat pathological conditions.

STATE- AND USE-DEPENDENCE

Use-dependent activity of ion channel modulators is recognized as an important and desirable feature, because it allows the drug to more selectively target hyperexcitable cells (eg. in an epileptic seizure, or at a site of injury). The use-dependent properties of KCNQ channel activators, however, are currently largely unexplored. Use-dependence is a phenomenon whereby the excitability of the membrane progressively changes with repeated depolarization. Drugs may act on ion channels in a use-dependent manner because channels act as modulated receptors that have a voltage-dependent change in the affinity of their drug binding site (Modulated Receptor Hypothesis) (Hille, 1977). Channels exist in “normal” states as well as “modified” states. “Normal” states include resting (R), activated and open (O), or inactivated (I) states, while “modified” states include drug bound to R, O, and I states to yield R^* , O^* , and I^* states respectively (Hille, 1977). The rate of transition and equilibria among these channel states may differ, and the rates of drug interaction with each channel state is therefore different (Hille, 1977). Drug access to its binding site may also be restricted (Guarded Receptor Hypothesis) (Starmer and Courtney, 1986). In fact, the structural basis for use-dependent block or activation comes from the fact that large or hydrophilic drugs cannot access the drug binding site unless the intracellular activation gate is opened (i.e. channels must first be opened) (Hille, 1977). Hydrophobic drugs, however, may be able to bind to resting, closed channel states by accessing hydrophobic pathways in the membrane (Hille, 1977). Thus, drug accessibility to its binding site is variable and dependent on the hydrophobicity and pKa of the drug, as well the pH of the solution; these factors, along with experimental parameters such as holding potential, frequency and duration of stimulation, collectively determine the pathways a drug molecule can access to bind to or diffuse from the channel (Hille, 1977; Starmer and Courtney, 1986).

The classic example of use-dependence of ion channels is the use-dependent blockade of voltage-gated sodium channels by quaternary and amine local anesthetics (LAs). LAs

preferentially bind to open and inactivated channel states rather than resting, closed channels (Ragsdale et al., 1994). With a repetitive train of depolarizations, progressively more channels are opened and inactivated, leading to an accumulation of drug bound to open and inactivated channels and an overall greater drug effect (Ragsdale et al., 1994). This means that application of LAs yields a progressive reduction in peak I_{NaV} currents that becomes stronger at higher frequencies, showing drug-modified use-dependent inhibition of channels. Other well documented examples of use-dependence also occur with block of potassium channels by quaternary ammonium ions, and opening of sodium channels by DDT and scorpion venom (Hille, 1977). Sodium channels are broadly expressed throughout body, partaking in important physiological processes such as generating the rhythm of the heartbeat, sensing acute and chronic pain, and at regulating neuronal excitability (Wang et al., 2015). Sodium channel blockers such as verapamil, carbamazepine, phenytoin, lidocaine and mexiletine are thus hugely important therapies for diseases involving cardiac arrhythmia, pain, and seizures (Ragsdale et al., 1991; Wang et al., 2015).

How does use-dependent block translate into a clinically useful property for the treatment of arrhythmias and seizures? The use-dependence of block can be broken down into two components: first, drugs should have an increased on-rate when channels gate, and second, drugs should have a sufficiently slow off-rate so that block of channels accumulate (Sheets et al., 2010). Drugs that only display one of these two characteristics, such as benzocaine, which has an increased on-rate but does not accumulate, are not use-dependent (Sheets et al., 2010). The use-dependent mechanism translates into a clinically useful tool because cells in seizure or at arrhythmic foci tend to have more depolarized resting potentials than normal cells, and fire rapid bursts of action potentials (Ragsdale et al., 1991). Drugs that exhibit pronounced state-dependent binding can preferentially target hyperactive cells without affecting normal cells, and may be more valuable therapies in the context of antiepileptic drug design.

SCOPE OF THESIS INVESTIGATION

KCNQ channel openers are an emerging drug class approved for the treatment of epilepsy. However, retigabine (the only KCNQ opener previously approved as an antiepileptic for use in humans) activates both neuronal KCNQ2/3, and more peripherally-expressed KCNQ4/5 in the bladder detrusor smooth muscle, resulting in side effects such as urinary retention. Little is known about the mechanism(s) of how RTG and its analogs bind and act to open KCNQ channels, and better characterization of these drugs will be enormously useful in tuning their properties to minimize side effects, improve their selectivity, and increase their potency. I investigated three specific questions, addressed in the following three chapters:

Chapter Three: How does channel gating influence interactions with KCNQ openers? Taking an electrophysiological approach, we found that retigabine (a pore-targeted activator) and ICA73 (a voltage sensor-targeted gating modifier) exhibit markedly different affinities for different channel states. ICA73 exclusively binds to channels during depolarized potentials, when channels are open and activated. Conversely, RTG displays less voltage-dependence of binding, and is able to bind across a wider range of potentials, including more hyperpolarized potentials when channels are predominantly closed. These findings highlight fundamental differences in the mechanism of action of these KCNQ activators.

Chapter Four: Might ICA73 and RTG, two drugs with different mechanisms and binding sites, display synergistic effects in activating KCNQ channels? Using two-electrode voltage clamp experiments on *Xenopus* oocytes, we showed the potential of pore site activators, such as RTG, to display synergistic effects with voltage sensing domain activators, such as ICA73. In vivo studies conducted on zebrafish larvae induced to have seizures confirmed the anticonvulsant activity of RTG, not but ICA73. These studies further led to the identification of ML-213 as an extremely potent anticonvulsant.

Chapter Five: What is the molecular basis for differential selectivity and potency of ICA73 and RTG on KCNQ subtypes? To address this question, I conducted a sequence alignment of the voltage sensing domains of drug-sensitive KCNQ2 and drug-insensitive KCNQ5; this domain was previously identified as a region important for imparting ICA73 sensitivity. Whole-cell patch clamp electrophysiology was used to characterize these mutants. These experiments identified several residues that had altered ICA73 sensitivity, and support the hypothesis that residues in the KCNQ2 voltage sensing are critical for ICA73 sensitivity.

Overall Significance: Findings from this thesis address gaps in our understanding of KCNQ activators, and highlight how we may be able to take advantage of their differences in mechanism and binding site to aid in the development of more potent therapeutics. In the longer term, improvement of the KCNQ activators may lead to valuable additional therapeutic options for patients suffering from poorly managed epilepsy.

CHAPTER 2 : MATERIALS AND METHODS

Whole cell patch clamp

Patch pipettes were manufactured from soda lime capillary glass (Fisher), using a Sutter P-97 puller (Sutter Instrument). When filled with standard recording solutions, pipettes had a tip resistance of 1-3 M Ω . Recordings were filtered at 5 kHz, sampled at 10 kHz, with manual capacitance compensation and series resistance compensation between 70-90%, and stored directly on a computer hard drive using Clampex 10 software (Molecular Devices). Bath solution had the following composition: 135 mM NaCl, 5 mM KCl, 1 mM CaCl₂, 1 mM MgCl₂, 10 mM HEPES, and was adjusted to pH 7.4 with NaOH. Pipette solution had the following composition: 135 mM KCl, 5 mM K-EGTA, 10 mM HEPES and was adjusted to pH 7.2 using KOH. Chemicals were purchased from Sigma-Aldrich or Fisher. Solutions were delivered at room temperature by pressure-driven flow, through a multi-barreled solution delivery turret, driven by the RSC-200 (BioLogic) rapid solution exchanger to enable solution jumps.

Two-electrode voltage clamp

Recording pipettes were manufactured from borosilicate glass (Harvard Apparatus LTD), using a Sutter P-97 puller (Sutter Instrument) to pull to a tip resistance between 0.1-1 M Ω . Recordings were filtered at 5 kHz, and sampled at 10 kHz using a Digidata 1440A (Molecular Devices) controlled by pClamp 10 software (Molecular Devices). Oocytes were recorded using an OC-725C oocyte clamp (Warner) in modified Ringers solution (in mM): 116 NaCl, 2KCl, 1 MgCl₂, 0.5 CaCl₂, 5 HEPES (pH 7.4). Internal pipette solution was 3M KCl. Chemicals were purchased from Sigma-Aldrich or Fisher.

Fast-solution switching

Recording pipette with cell attached was positioned directly in front of capillary tubes containing control solutions or drug solutions. Capillaries were attached to a stepper motor,

allowing us to “step” in either direction so that cells are rapidly exposed to control or drug solutions. Timescale for drug wash-on or wash-off was 20-30ms. See image below:

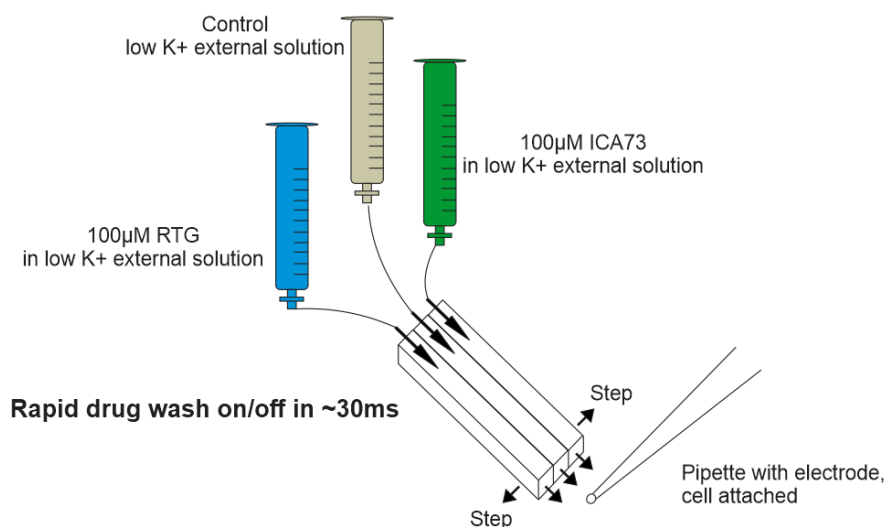


Figure 2.1 Fast-solution switching

Drug solutions

Retigabine was obtained from Toronto Research Chemicals, and ICA73 and ML-213 were obtained from Tocris. Drugs were dissolved in DMSO to yield stock concentrations of 100mM (retigabine and ICA73) or 50mM (ML-213). Stock solutions were diluted in extracellular solutions to appropriate concentrations for experiments the same day.

Chemical structures of drugs

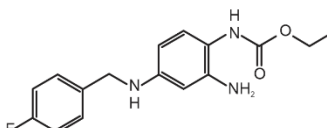
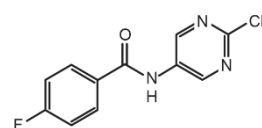
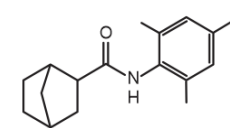
Retigabine	ICA069673	ML-213
		

Table 2.1 Chemical structures of drugs

Ion channel constructs and transfection in cells

Human KCNQ2 DNA originally expressed in pTLN vectors, obtained from Dr. M. Taglialatela and Dr. T. Jentsch, were subcloned into pcDNA3.1 (-). The point mutants KCNQ2[A181P], [W236F], and [F168L] were generated using a 2-step overlapping PCR method, then subcloned into pcDNA3.1 using NheI and EcoRI restriction enzymes. Sequences were verified by Sanger sequencing approaches (Genewiz or University of Alberta Applied Genomics Core).

HEK293 cells were maintained in DMEM media supplemented with 10% FBS and 1% penicillin/streptomycin. Cells were grown in Falcon™ tissue culture treated flasks, in an incubator at 5% CO₂ and 37°C. Cells were plated onto 12 well plates and allowed to settle for 24-48 hours prior to transfection. Cells were transiently transfected with 1µg of DNA encoding channel of interest, 500ng of GFP, using jetPRIME DNA transfection reagent (Polyplus). Cells sat in transfection media for ~24 hours, before being re-plated onto coverslips for electrophysiology experiments the following day.

Harvesting oocytes & mRNA injections

Oocytes were harvested from mature female *Xenopus laevis*, obtained from the University of Alberta Biology Department. Frogs were handled in accordance with animal care procedures implemented at the University of Alberta. Oocyte lobes were placed into OR2 solution for dissection into smaller pieces containing ~10-20 oocytes. These fragments were transferred into a collagenase solution made of 3µg/ml Type IV collagenase (Worthington Biochemical Corporation) in OR2. A 1:5 mixture of oocyte to collagenase solution, not exceeding 25mL, was transferred to a 50mL Falcon tube, and placed on a rotator which inverted the tube at a frequency of 0.5Hz to allow for sufficient contact between collagenase and oocytes. Oocytes were checked periodically starting at 2 hours to see if their follicular layer was removed. De-folliculated oocytes were placed into OR2 solution and back on the rotator for 30 minutes to rinse away remaining

follicular layers. Oocytes were incubated at 17°C in OR3 solution (500 mL Leibovitz's L15 Medium, 3.57 g HEPES, 5 mL Glutamine, 5 mL Gentamycin, 500 mL H₂O, pH 7.6, filtered) until the following morning, when they were sorted for injections.

Complementary RNA was transcribed from cDNA using mMessage mMachine kit (Ambion). DNA constructs were linearized with BglII (KCNQ2, KCNQ2/3 dimer) or BamHI (KCNQ3), and transcribed using a T7 primer (KCNQ2, KCNQ2/3 dimer) or SP6 primer (KCNQ3). Oocytes were injected with KCNQ2 and KCNQ3 mRNA (20ng each), or KCNQ2/KCNQ3 dimer mRNA (20ng), or KCNQ5 mRNA (100ng), and incubated for 48-72h at 17 °C before recording.

Zebrafish activity measurements

Zebrafish were maintained according to standard procedures. Experiments were conducted on larvae maintained in typical embryonic E3 growth media (0.03% Instant Ocean (Aquarium Systems)) in deionized water containing 0.0002% methylene blue as a fungicide). Zebrafish larvae were arrayed in 96 well plates, each well containing 650uL of E3 media. Behavioral tracking software quantified activity of larvae. Larvae were acclimatized for three hours before baseline recording for one hour, followed by a treatment dose of 10mM PTZ, and subsequent addition of ICA73, RTG, and/or ML-213. 96-well plates were placed on top of an infrared backlight source (Noldus) and below Basler GenICaM (Basler acA 1300-60) scanning camera (Noldus), which were used to track locomotor activity of an individual larvae within each well. EthoVision ® XT-11.5 software (Noldus) used to quantify locomotor activity, which was defined as % pixel change within a corresponding well between samples (motion was captured by taking 25 samples (frames) per second).

Statistics

Statistics for zebrafish seizure activities were performed using GraphPad Prism Software (Version 6). For seizure activity at different concentrations of drug, asterisks indicate statistical significance ($p < 0.05$) with one-way ANOVA compared to convulsant control (PTZ control).

Data analysis

Conductance-voltage relationships were normalized to the peak conductance in control conditions and fit with a Boltzmann equation:

$$\frac{I}{I_{max}} = \frac{A}{1 + e^{-(V-V_{1/2})/k}}$$

A is the ratio of the peak conductance (normalized to peak conductance in control conditions), I/I_{max} is the normalized current, V is the voltage applied, $V_{1/2}$ is the half activation voltage, and k is a slope factor reflecting the steepness of the curve. Conductance-voltage relationships from individual cells were fit, followed by statistical calculations for individual fit parameters. Time constants of activation and/or deactivation were fit to an exponential equation of the form:

$$F(t) = \sum_{i=1}^n A_i (1 - e^{-\frac{t}{\tau}})^a$$

where n is the number of activation or deactivation components, A is the amplitude of the peak current, τ is the time constant, t is the time elapsed, and a is the exponential power.

CHAPTER 3 : STATE- AND USE-DEPENDENT BINDING OF KCNQ CHANNEL OPENERS

INTRODUCTION

Voltage-gated potassium channels in the KCNQ (Kv7) family encode the ‘M-current’, a prominent neuronal potassium current with dual regulation by voltage and PIP₂ (Suh and Hille, 2007; Suh et al., 2006). The M-current was first named because of its identification as a potassium current that was inhibited by extracellular ligands of muscarinic acetylcholine receptors, although these currents are now recognized as important regulators of neuronal excitability in response to a variety of extracellular signals (Adams and Brown, 1980; Brown and Adams, 1980; Brown et al., 2007; Hernandez et al., 2008). KCNQ channels also have unique pharmacological properties, highlighted by their susceptibility to pronounced activation by an emerging class of voltage-gated potassium channel openers (Barrese et al., 2018; Miceli et al., 2017). The prototype drug in this class, retigabine, causes a hyperpolarizing shift of the voltage-dependence of activation of channels that contain KCNQ2-5 subtypes, and this effect depends on the presence of a conserved Trp residue (Trp 236 in KCNQ2) in retigabine sensitive KCNQ channels (Kim et al., 2015; Lange et al., 2009; Schenzer et al., 2005; Wuttke et al., 2005).

The primary clinical application of KCNQ channel activators has been the treatment of pharmaco-resistant epilepsy, and this is partly related to the recognition that KCNQ2 and KCNQ3 are associated with inheritable forms of epilepsy, varying in severity from BFNS (benign familial neonatal seizures) to EE (epileptic encephalopathy) (Biervert et al., 1998; Charlier et al., 1998; Martyn-St James et al., 2012; Singh et al., 1998). Mutations in KCNQ4 channels have also been linked to age-related deafness (Kharkovets et al., 2006; Kubisch et al., 1999). In addition to utility in epilepsy, applications for treatment of tinnitus, hypertension, pain, and neurodegenerative diseases are also being explored (Kalappa et al., 2015; Kumar et al., 2016; Mackie and Byron, 2008; Vicente-Baz et al., 2016; Wanger et al., 2014; Xu et al., 2010). Although retigabine was

recently discontinued due to low usage, the identification of Kv7 channels as targets for diseases of hyperexcitability has led to the development of a variety of openers (Miceli et al., 2008, 2017; Xiong et al., 2008b) including phenamates (diclofenac and meclofenamic acid derivatives) (Peretz et al., 2010); zinc pyrithione, (Xiong et al., 2007); BMS-204352 and the acrylamide compound (S)-1 (Bentzen et al., 2006). Lastly, a class of substituted benzamides including ICA-069673, ICA-27234, ICA-110381, ztz-240, and ML-213 exhibit activity as Kv7 openers (Gao et al., 2010; Wickenden et al., 2008; Yu et al., 2010). Of these, the most well-documented in preclinical anticonvulsant models is ICA-27243, while our group has primarily used ICA-069673 ('ICA73') to investigate the mechanism of action on KCNQ channels (Padilla et al., 2009a; Wang et al., 2017).

Recognition of diverse mechanisms of action of KCNQ openers originated with the demonstration that ICA-27243 retained activity on mutant channels lacking the conserved pore Trp residue known to be essential for retigabine activity (Gao et al., 2010; Padilla et al., 2009a; Peretz et al., 2010; Xiong et al., 2008b). Moreover, ICA-27243 exhibited greater subtype specificity, enhancing Q2/3 current, but not Q3/5 or Q3 homomeric current (Blom et al., 2010; Wickenden et al., 2008). A series of chimeric channels between drug sensitive and insensitive subunits revealed that residues in the KCNQ2 VSD were important for ICA73 and ICA-27243 effects, and our group recently identified two residues in the S3 helix of the KCNQ2 VSD that are critical for ICA sensitivity: A181 and F168 (Padilla et al., 2009a; Wang et al., 2017). Mutations at either of these positions weaken or abolish ICA73 mediated gating effects but retain retigabine sensitivity. This provides further support that ICA73 and retigabine have distinct binding sites and may act through different mechanisms.

Use-dependent interactions are often considered to be a useful property of small molecule ion channel modulators. The most widely studied example is use-dependent actions of many voltage-dependent sodium channel blockers, which preferentially stabilize the inactivated

channel state, and thereby exert stronger effects in hyperexcitable cells (Ragsdale et al., 1994). Although the anti-convulsant properties of KCNQ openers are well known, their use-dependent properties and fundamental mechanisms of action have not been described in detail. In this study, we characterized the state-dependence of interaction of retigabine and ICA73 with homomeric KCNQ2 channels. Our findings demonstrate that in addition to acting via different binding sites, these compounds also have fundamentally different mechanisms of action. ICA73 appears to bind almost exclusively to activated channel states and is occluded from resting channels. In contrast, retigabine exhibits less prominent state-dependent accessibility. Taken together with the differences in mutations that alter sensitivity to these drugs, our findings demonstrate the presence of at least two distinct mechanisms of action of KCNQ channel openers. We also characterize the effects of a voltage sensor mutation that alters sensitivity to ICA73.

RESULTS

ICA73 binding is occluded in the KCNQ2 closed state

Application of ICA73 to homomeric KCNQ2 channels causes a dramatic hyperpolarizing gating shift, ~50% current potentiation at voltages where the activation curve is saturated, and deceleration of channel deactivation (Fig. 3.1A and (Wang et al., 2017)). We investigated state-dependent interaction of ICA73 and KCNQ2 by applying 30 μ M ICA73 for approximately 1 minute while holding the membrane potential at various negative voltages (Fig. 3.1B, C). 30 μ M ICA73 was chosen because at this concentration, currents are visibly potentiated, and deactivation prolonged. We assessed drug interactions with the channel during the wash-in and incubation, by the development of a standing current. When cells are held at -120 mV, incubation in 100 μ M ICA73 fails to generate any apparent standing current (or instantaneous current upon depolarization) until after the first depolarizing pulse following drug application (Fig. 3.1B). However, upon the first depolarization in the presence of ICA73, there is development of a potentiated outward current, and a dramatically decelerated tail current (Fig. 3.1B, green) that prevents channel closure before a subsequent pulse four seconds later, leading to a large instantaneous current in subsequent pulses (Fig. 3.1B, grey). Application of ICA73 at more depolarized holding voltages caused development of a more prominent standing current during the drug incubation period (Fig. 3.1C). These findings indicate that ICA73 interactions with KCNQ2 are influenced by the holding potential, and access to the channel is excluded at sufficiently negative voltages.

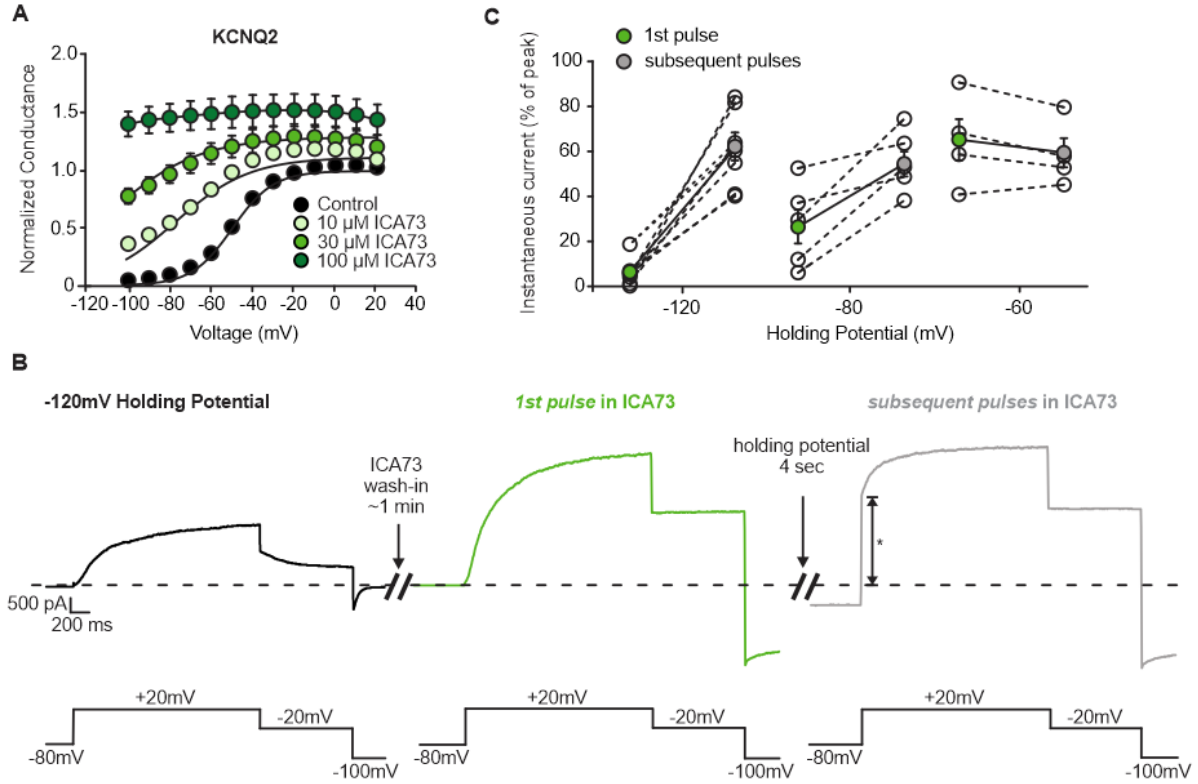


Figure 3.1 ICA73 is excluded from channel closed states and binds to open channel states. (A) Conductance-voltage relationships for WT KCNQ2 channels expressed in *X. laevis* oocytes in a control solution and in increasing concentrations of ICA73, normalized to peak current in control for each cell. KCNQ2 parameters of activation were: control $V_{1/2} = -48.7 \pm 1.0$ mV, $k = 9.9 \pm 0.4$ mV; 10 μ M ICA73 $V_{1/2} = -76.4 \pm 2.2$ mV, $k = 17.9 \pm 0.5$ mV; 30 μ M ICA73 $V_{1/2} = -108.6 \pm 3.0$ mV, $k = 21.3 \pm 0.7$ mV, $n = 10$. 100 μ M ICA73 could not be fit by a Boltzmann equation. (B) Exemplar patch clamp current traces of WT KCNQ2 channels expressed in HEK293 cells. Under control conditions, cells were held at a holding potential of -120 mV, depolarized to +20 mV, stepped to -20 mV, then hyperpolarized to -100 mV. During this time, 10 μ M ICA73 was applied extracellularly for about one minute. Cells were then re-depolarized to +20 mV for the first time ('1st pulse in ICA73') and in subsequent sweeps ('subsequent pulses in ICA73'). Voltage protocol shown underneath. (C) Amount of instantaneous current (marked by asterisks in (A)) in the 1st pulse and in subsequent pulses as a percentage of the peak current, calculated from cells which had drug applied at holding potentials of -120 mV, -80 mV, and -60 mV ($n = 4-7$).

ICA73 binding site access tracks voltage-dependent activation

ICA73 interactions with the channel were investigated with greater time resolution using rapid solution exchange over a range of voltages (Fig. 3.2). Cells were stepped to voltages ranging from -100 mV to 40 mV in 20mV increments, for 1 s, followed by rapid application of 100 μ M ICA73 (Fig. 3.2A). Based on calibrations with K⁺ concentration jumps, we estimate that the time constant of solution exchange in these experiments is ~20 ms (Zhang et al., 2015). The rate of ICA73 interaction with KCNQ2 channels was estimated using the rate of current increase upon drug application. In the absence of clear channel opening (at very negative voltages), we could also roughly infer the extent of drug binding based on the properties of current activation in a subsequent pulse to -60 mV (Fig. 3.2A).

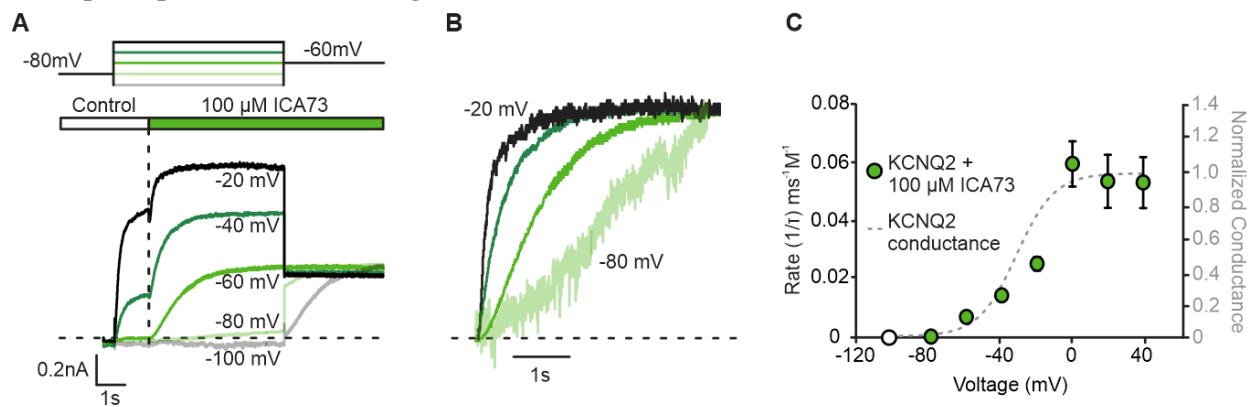


Figure 3.2 ICA73 binding tracks KCNQ2 channel opening. (A) Voltage protocol and exemplar current traces for KCNQ2 channels in HEK293 cells are shown. Cells were bathed in a control solution and held at -80mV, before being pulsed to a range of voltages between -120mV to 40mV for 5s. During these voltage steps, 100 μ M ICA73 was applied rapidly, before cells were pulsed to a subsequent voltage of -60mV. (B) A magnified view of the current traces immediately following drug addition, normalized to the peak current at -20mV. (C) Rates of ICA73 binding are plotted (green circles, left axis) against the KCNQ2 channel conductance in HEK293 cells (dotted line, right axis) at various membrane voltages. The unfilled circle represents drug binding rates of approximately 0 $\text{ms}^{-1}\text{M}^{-1}$, inferred from data (n = 4-6).

In the absence of ICA73, only a small fraction of KCNQ2 channels are activated at -60 mV. Upon rapid application of 100 μ M ICA73, there is a slow but resolvable current increase (Fig. 3.2A). At more positive voltages, the rate of ICA73 current enhancement is accelerated, as exemplified in normalized traces (Fig. 3.2B). In contrast, at -100 mV or more negative voltages, ICA73 appears to be occluded from the channel, because the subsequent pulse to -60 mV exhibits little or no instantaneous current, and the time course of activation is similar to activation after rapid drug application at -60 mV (Fig. 3.2A). This observation implies that drug application at -100 mV (or more negative voltages) has a minimal effect until the step to -60 mV, at which point channels behave as if they were rapidly exposed to the drug. We quantified the rate of interaction as a function of membrane voltage at the time of drug application (Fig. 3.2B, C), and plotted this data together with the conductance-voltage relationship, highlighting that the rate of ICA73 interaction closely tracks the voltage-dependence of channel activation. The implication of this observation is that the degree of channel activation limits the rate of ICA73 access to its binding site. An important related finding is that the conductance-voltage relationship of KCNQ channels has been previously shown to closely overlap with the voltage-dependence of voltage sensor movement (Kim et al., 2017; Osteen et al., 2012). We suggest that voltage sensor movement gates access to a binding site for ICA73.

Retigabine readily accesses KCNQ2 closed states

As mentioned, previous reports have suggested a distinct binding site for ICA73 (in the voltage sensor) vs retigabine (in the pore) (Padilla et al., 2009a; Wang et al., 2017). To compare the mechanism of action of retigabine and ICA73, we performed similar wash-in experiments with retigabine, revealing significant differences in channel responses at hyperpolarizing voltages. The effects of retigabine on the KCNQ2 conductance-voltage relationship and deactivation kinetics are much less pronounced than ICA73 (Fig. 3.3A). However, incubation in 30 μ M retigabine caused development of a prominent standing current over a wide voltage range (-120 mV to -60 mV). In contrast to ICA73 (Fig. 3.1), these findings indicate that retigabine can more readily access resting states of the channel.

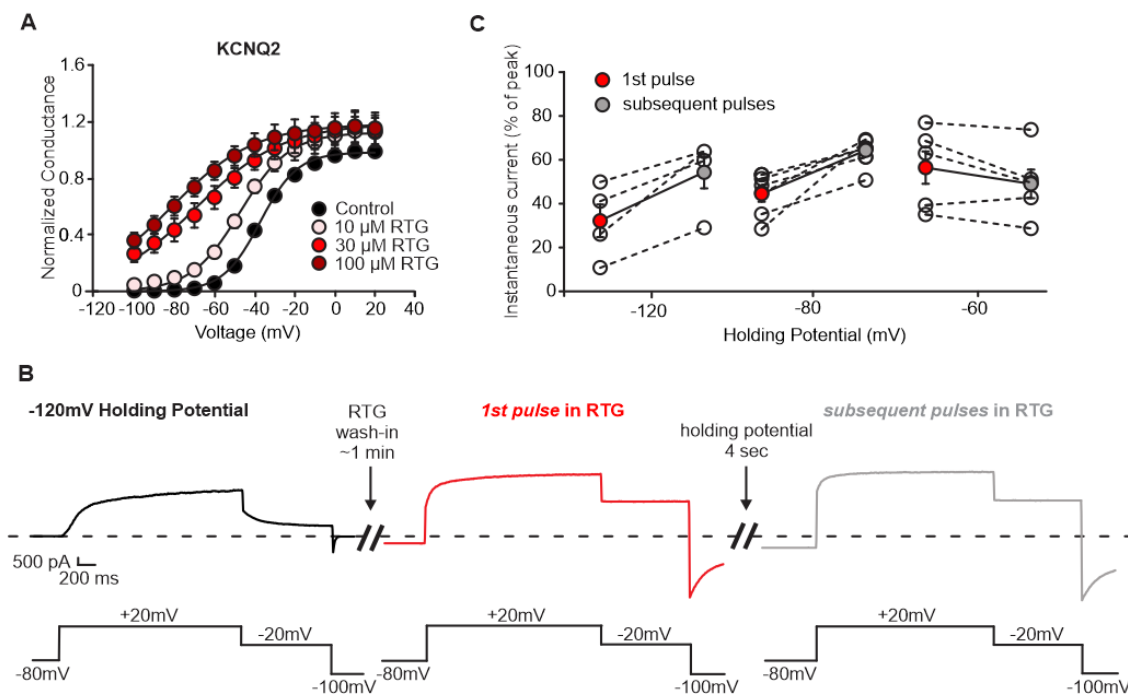


Figure 3.3 RTG can bind to both open and closed channel states. (A) Conductance-voltage relationships for WT KCNQ2 channels expressed in *X. laevis* oocytes in a control solution and in increasing concentrations of RTG, normalized to peak current in control for each cell. KCNQ2 parameters of activation were: control $V_{1/2} = -36.8 \pm 1.1$ mV, $k = 9.2 \pm 0.4$ mV; 10 μ M RTG $V_{1/2} = -47.6 \pm 2.0$ mV, $k = 12.2 \pm 1.1$ mV; 30 μ M RTG $V_{1/2} = -69.5 \pm 5.4$ mV, $k = 21.6 \pm 2.0$ mV; 100 μ M RTG $V_{1/2} = -81.7 \pm 3.6$ mV, $k = 20.7 \pm 1.4$ mV, $n = 6$. (B) Wash-in experiment described in Fig. 3.1B was performed using 30 μ M RTG. (C) Amount of instantaneous current as a percentage of the peak current, calculated from cells which had drug applied at holding potentials of -120 mV, -80 mV, and -60 mV ($n = 4-6$).

Using rapid solution exchange for time-resolved retigabine application, we confirmed that drug association is rapid even at negative voltages (Fig. 3.4). At -80 mV, although currents are small (close to the reversal potential for potassium), the onset of the retigabine effect can still be resolved and is only modestly slower than at -20 mV (Fig. 3.4A, B). At more negative voltages it is difficult to observe the rate of retigabine association because channels are predominantly closed. However, we infer that there is significant association even at negative voltages because there is accelerated channel activation in subsequent steps to -60 mV (Fig. 3.4A). We compared the rate of retigabine interaction at different membrane voltages to the conductance-voltage relationship (Fig. 3.4B, C). Unlike ICA73, retigabine influences channels even at negative voltages where conductance is minimal. At -60mV for example, the normalized channel conductance is <20%, but the rate of drug association is nearly maximal (Fig. 3.4C). Over the range of voltages tested, the data does not indicate strong occlusion from channel resting states, in contrast to ICA73.

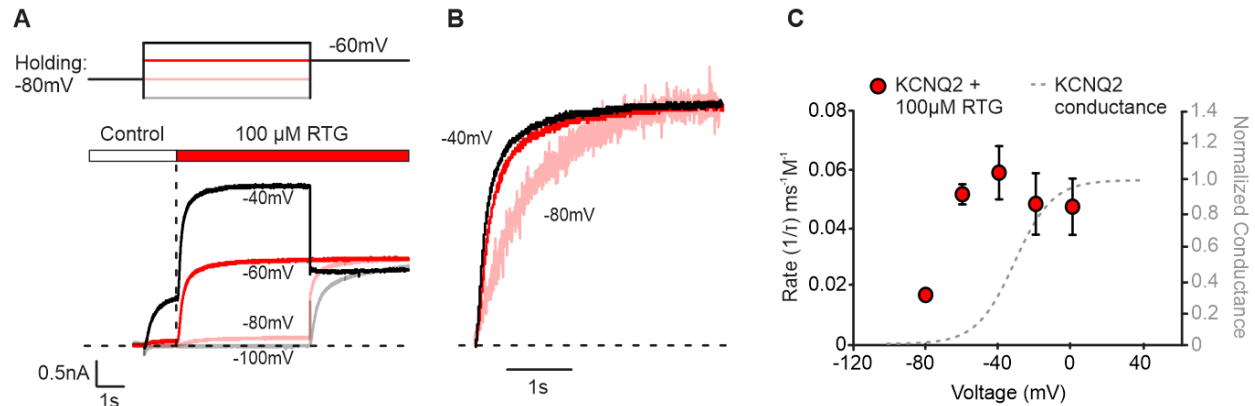


Figure 3.4 RTG binds before channels open. (A) Voltage protocol described in Fig. 3.2A was performed using 100 μ M RTG. Exemplar current traces from cells expressing WT KCNQ2 channels are shown. (B) A magnified view of the current traces immediately following drug addition, normalized to the peak current. (C) Rates of RTG binding are plotted (red circles, left axis) against the KCNQ2 channel conductance in HEK293 cells (dotted line, right axis) at various membrane voltages (n = 2-7).

Channel closure requires ICA73 unbinding

Findings thus far suggest marked differences in the state accessibility of ICA73 and retigabine. We further investigated the state accessibility of these KCNQ openers by examining channel reopening in the presence of retigabine and ICA73. We had noted that activation kinetics of KCNQ2 in the presence of ICA73 were not altered significantly from control conditions, in contrast to the pronounced acceleration of channel activation observed in the presence of retigabine (Figs. 3.1, 3.3). We reasoned that this may reflect different closed state binding properties of these drugs. That is, accelerated activation kinetics in the presence of retigabine might reflect binding and destabilization of resting states. In contrast, closed KCNQ2 channels appear unable to bind ICA73, and therefore would be predicted to activate with kinetics similar to control (and subsequently bind the drug after they reach an activated state). To test this difference, we delivered a depolarizing stimulus (0 mV) in the presence of each drug, repolarized for varying durations (Δ time in Fig. 3.5A, C), to allow varying degrees of channel closure, and then depolarized again. We compared the activation kinetics of channels that closed during the repolarizing interpulse interval, with activation kinetics in control conditions (normalized traces in Fig. 3.5B, D). In retigabine, the activating fraction consistently exhibited accelerated activation kinetics (Fig. 3.5B and inset), suggesting that retigabine remains associated with channels during repolarization-induced closure, leading to accelerated activation during subsequent depolarizations.

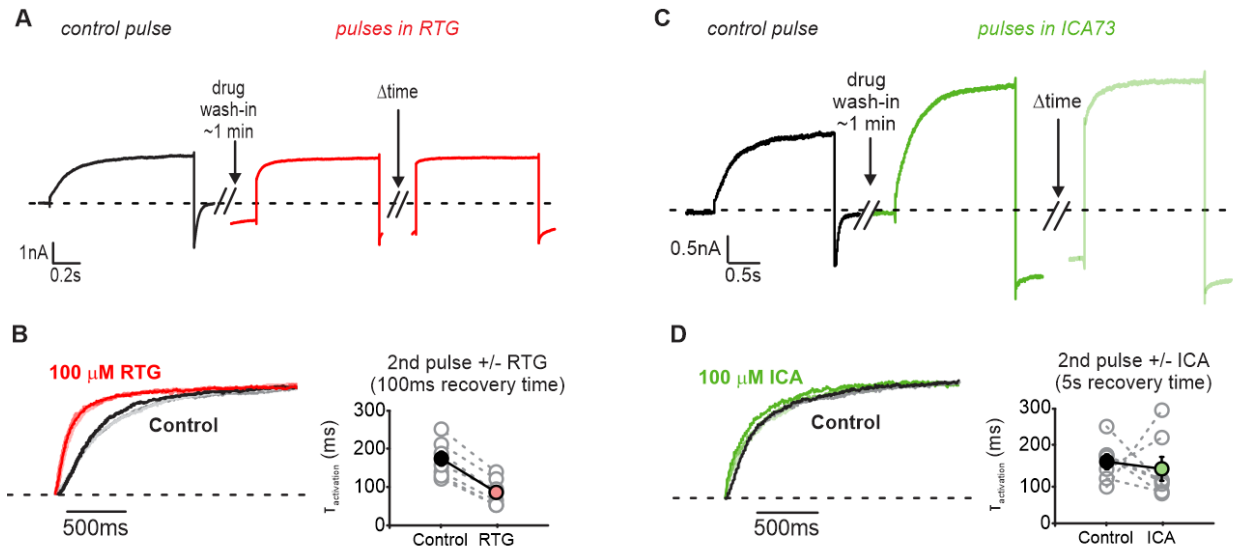


Figure 3.5 RTG increases the speed of channel opening and re-opening while ICA73 does not affect channel opening kinetics. (A, C) Sample current traces from cells expressing WT KCNQ2 channels before and after exposure to RTG or ICA73. Under control conditions, cells were held at a holding potential of -100mV, depolarized to 0mV, and then repolarized to -100mV. During this time, drug was applied extracellularly for one minute. Cells were then re-pulsed to 0mV before being repolarized to -100mV for varying amounts of time (Δ time) to induce varying amounts of channel closure. (B, D) Exemplar current traces from one cell showing first-time activation kinetics in RTG or ICA73 solution (red and green respectively) or control solution (black), normalized to the peak current post-drug. Time constants for the onset of current in control solution versus drug solution were calculated for the 2nd pulse ($n = 7$).

ICA73 has much more prominent effects on channel deactivation, requiring up to 25 s repolarizations for complete channel closure at -120 mV (Fig. 3.5C). Using longer interpulse intervals to achieve intermediate levels of channel closure, we observed that activation kinetics were unchanged relative to the control condition. We interpret this result to mean that channel closure requires ICA73 unbinding. Thus, channels that close during the interpulse interval are no longer bound to ICA73, and therefore exhibit activation kinetics identical to control conditions (Fig. 3.5D).

A voltage sensor mutation accelerates ICA73 unbinding

We recently described the KCNQ2[A181P] mutation that attenuates ICA73-mediated gating effects, but preserves current potentiation (Wang et al., 2017). Specifically, KCNQ2[A181P] mutant channels exhibit modest deceleration of channel deactivation in the presence of ICA73, leading to a weaker apparent shift of the conductance-voltage relationship relative to WT KCNQ2. The specific mechanism underlying this effect was not clear, and we speculated this weaker gating effect might reflect a loss of the strict state-dependence of ICA73 (allowing KCNQ2[A181P] channels to close even when bound to ICA73), or alternatively, a faster unbinding rate reflecting weakened affinity.

We tested these possibilities using rapid solution application, as described in Figs. 3.2, 3.4. This experiment demonstrates quite clearly that ICA73 is occluded from interactions with the resting state of KCNQ2[A181P] channels, similar to what was observed for WT KCNQ2 (Figs. 3.2, 3.6). There is a pronounced voltage-dependence of the rate of ICA73 interaction with KCNQ2[A181P] channels, that tracks the voltage-dependence of A181P conductance. The onset of ICA73 effects are extremely slow or absent at voltages more negative than -80mV (Fig. 3.6B, C).

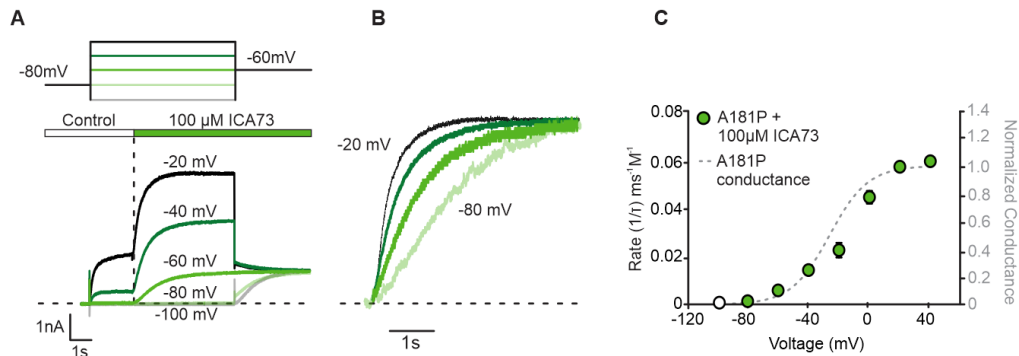


Figure 3.6 ICA73 binding to KCNQ2[A181P] also tracks channel opening. (A) Voltage protocol described in Fig. 3.2A was performed using 100 μ M ICA73 on KCNQ2[A181P]. Exemplar current traces from cells expressing these channels are shown. (B) A magnified view of the current traces immediately following drug addition, normalized to the peak current. (C) Rates of RTG binding are plotted (green circles, left axis) against the KCNQ2[A181P] channel conductance in HEK293 cells (dotted line, right axis) at various membrane voltages. The unfilled circle represents drug binding rates of approximately 0, inferred from data ($n = 2-6$).

We also compared the association and dissociation rates of ICA73 in WT KCNQ2 and KCNQ2[A181P] channels using rapid solution exchange (Figs. 3.7, 3.8). Drug binding at 0 mV had similar time constants of ~500ms between WT KCNQ2 and KCNQ2[A181P] channels, suggesting that ICA73 binding is not strongly affected by the A181P mutation. This experiment differs slightly from Fig. 3.6 in that we focused on applying the drug at voltages where channels were fully activated and the ICA73 binding site was maximally accessible. Thus, channel transitions between resting and activated states would not influence the observed rate of interaction.

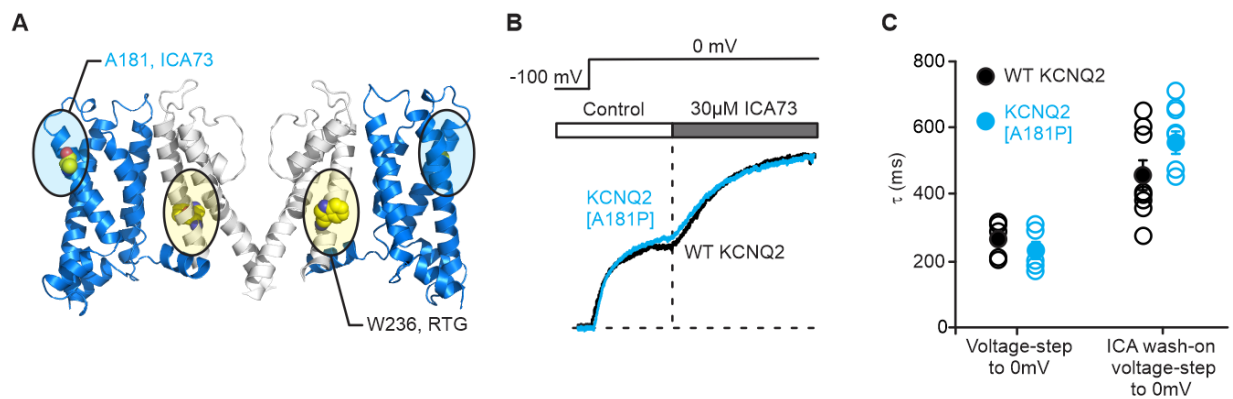


Figure 3.7 Rate of ICA73 binding to WT KCNQ2 and KCNQ2[A181P] channels. (A) Model of KCNQ2 channel structure showing A181, a residue important for ICA73 effects, in the voltage sensing domain (highlighted in blue) and W236, a residue essential for RTG effects, in the pore domain (shown in white). (B) Sample current traces for WT KCNQ2 channels (black) and KCNQ2[A181P] channels (blue) when cells were held at -100mV, then depolarized to 0mV during which time 30μM ICA73 was rapidly applied extracellularly. (C) Activation time constants for wildtype and mutant channel opening at 0mV in control solution and following drug addition (n = 5-6).

When ICA73 is rapidly washed off, there is very slow relaxation of currents in WT KCNQ2 channels, ranging from a time constant of ~6s (at 0 mV) to ~2s (at -150 mV) (Fig. 3.8). This likely reflects very slow dissociation of ICA73 from the channels. Across all voltages tested, ICA73 dissociation from A181P channels was considerably faster (~10-fold) than dissociation from WT KCNQ2, suggesting that the primary mechanism underlying the weakened ICA73 gating effects in KCNQ2[A181P] channels is accelerated unbinding reflecting weakened affinity, allowing for more rapid channel closure at negative voltages.

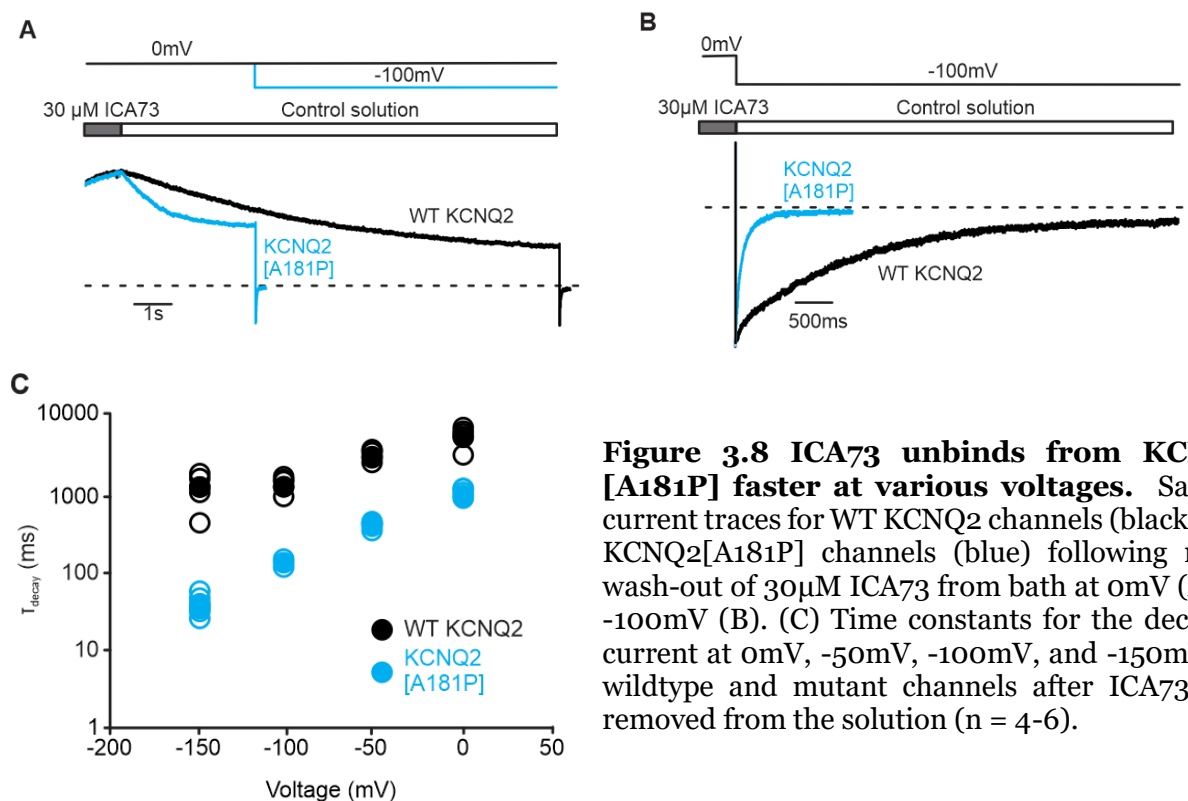


Figure 3.8 ICA73 unbinds from KCNQ2 [A181P] faster at various voltages. Sample current traces for WT KCNQ2 channels (black) and KCNQ2[A181P] channels (blue) following rapid wash-out of 30 μ M ICA73 from bath at 0mV (A) or -100mV (B). (C) Time constants for the decay of current at 0mV, -50mV, -100mV, and -150mV for wildtype and mutant channels after ICA73 was removed from the solution (n = 4-6).

Both RTG and ICA73 promote channel opening with high frequency stimulation

The effects of both ICA73 and retigabine were enhanced when cells were depolarized with a train of brief, high frequency stimulations. The amount of current passing through WT KCNQ2 channels increased by ~3 fold in ICA73 or RTG solution, when cells were stimulated at 10Hz, compared to stimulation at 1Hz (Fig. 3.9A, B). In contrast, A181P channels exhibited attenuated use-dependent activation of the channel in ICA73 solution (Fig. 3.9C). This difference between A181P and WT KCNQ2 is likely most attributable to the more rapid unbinding rate of ICA73 from A181P channels, allowing for more prominent channel closure during the inter-pulse interval.

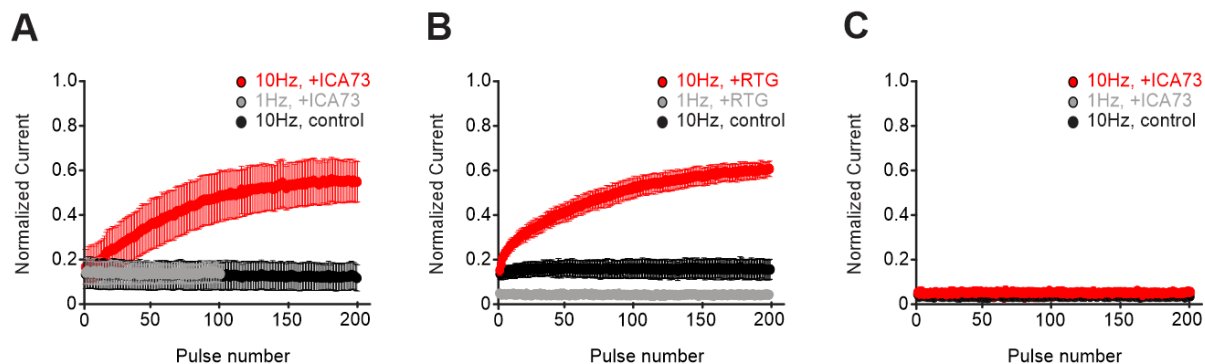


Figure 3.9 Use-dependent activation by ICA73 and RTG. Cells expressing WT KCNQ2 channels or mutant KCNQ2 [A181P] channels were given 100-200 square wave pulses to +20mV at 1Hz or 10Hz in control or drug solutions. Inter-pulse intervals were 100ms long. Current values were normalized to peak current in drug solution for each cell, $n = 3-4$. (A) Use-dependent activation assessed with 10 μ M ICA73 on WT KCNQ2 channels, with 20ms pulse durations. (B) Use-dependent activation assessed with 30 μ M RTG on WT KCNQ2 channels, with 20ms pulse durations. (C) Use-dependent activation assessed with 30 μ M ICA73 on KCNQ2 [A181P] channels, with 10ms pulse durations.

DISCUSSION

Retigabine-sensitive KCNQ channel isoforms (KCNQ2-5) have been targeted in the development of voltage-gated potassium channel openers (Barrese et al., 2018; Miceli et al., 2017). Large compound libraries have been screened in recombinant systems and animal models, and several reports have documented openers with enhanced subtype specificity and increased potency towards certain KCNQ channel types (Blom et al., 2010; Brueggemann et al., 2014; Padilla et al., 2009a). Some openers, such as ICA73, cause extremely large gating effects relative to retigabine on certain KCNQ subtypes. Although many KCNQ channel openers act on the canonical retigabine site formed by a conserved Trp residue in the pore domain (Bentzen et al., 2006; Lange et al., 2009), it is now recognized that certain KCNQ openers are resistant to mutation of the retigabine site, and instead act at an alternative voltage sensor site (Gao et al., 2010; Li et al., 2013; Padilla et al., 2009a; Peretz et al., 2010; Wang et al., 2017). Consistent with this finding, point mutations in the voltage sensor (KCNQ2 A181 and F168) alter sensitivity to VSD-targeted drugs like ICA73, but not retigabine.

These structure-function approaches provide strong evidence for an alternative site for KCNQ openers, formed by the voltage sensor, which is distinct from the pore-delimited retigabine site. In this study, we used rapid solution switching to demonstrate a fundamentally different mechanism of action for pore and voltage sensor-targeted KCNQ openers like ICA73. Most convincingly, the rate of ICA73 association with KCNQ2 closely tracks the voltage-dependence of channel activation, whereas the rate of retigabine access is less affected by membrane voltage (Figs. 3.2, 3.4, 3.6). ICA73 appears to be completely occluded from interacting with resting states of the channel, as incubation of KCNQ2 for minutes in ICA73 has no effect on channel opening, until a depolarization is delivered, channels open, and the binding site becomes accessible (Fig. 3.1). In contrast, retigabine association with KCNQ2 does not follow the same strict dependence on channel activation, and drug effects are apparent during retigabine incubation at negative

voltages where most channels are closed. Hints of this dependence on channel activation have appeared in pharmacological investigations of DRG reflexes, in which pore-targeted activators (retigabine, ML-213) rapidly suppress evoked responses in the DRG, whereas ICA73 has a slower onset (many action potentials fire before the drug effect becomes apparent) (Vicente-Baz et al., 2016).

Synthesizing data from mutagenesis and rapid solution perfusion, a reasonable explanation for our findings is that ICA73 (and likely related compounds like ICA-27243) binds nearly exclusively to activated states of the voltage sensing domain. Thus, when channels are at rest, very few (if any) bind to ICA73, and activation kinetics are comparable to control conditions. After a voltage sensor reaches an active state, ICA73 can bind and dramatically decelerate voltage sensor deactivation, causing homomeric KCNQ2 channels to be trapped in an activated conformation for extended durations (Fig. 3.10). This pronounced state-dependence differs significantly from retigabine (Fig. 3.10). The distinct mechanisms of action of these drugs is consistent with our recent findings that the stoichiometric requirement for channel activation is different for pore vs. VSD-targeted openers. KCNQ3 activation by retigabine is nearly maximal in tetramers with a single retigabine sensitive subunit. In contrast, ICA73 activation of KCNQ2 requires four drug-sensitive subunits for maximal drug effect, leading us to suggest that this multi-subunit dependence may be due to unique features of VSD-pore coupling in KCNQ channels (Wang et al., 2018; Yau et al., 2018). That is, activation of intermediate numbers of voltage sensors may underlie channel states with intermediate open probability or conductance.

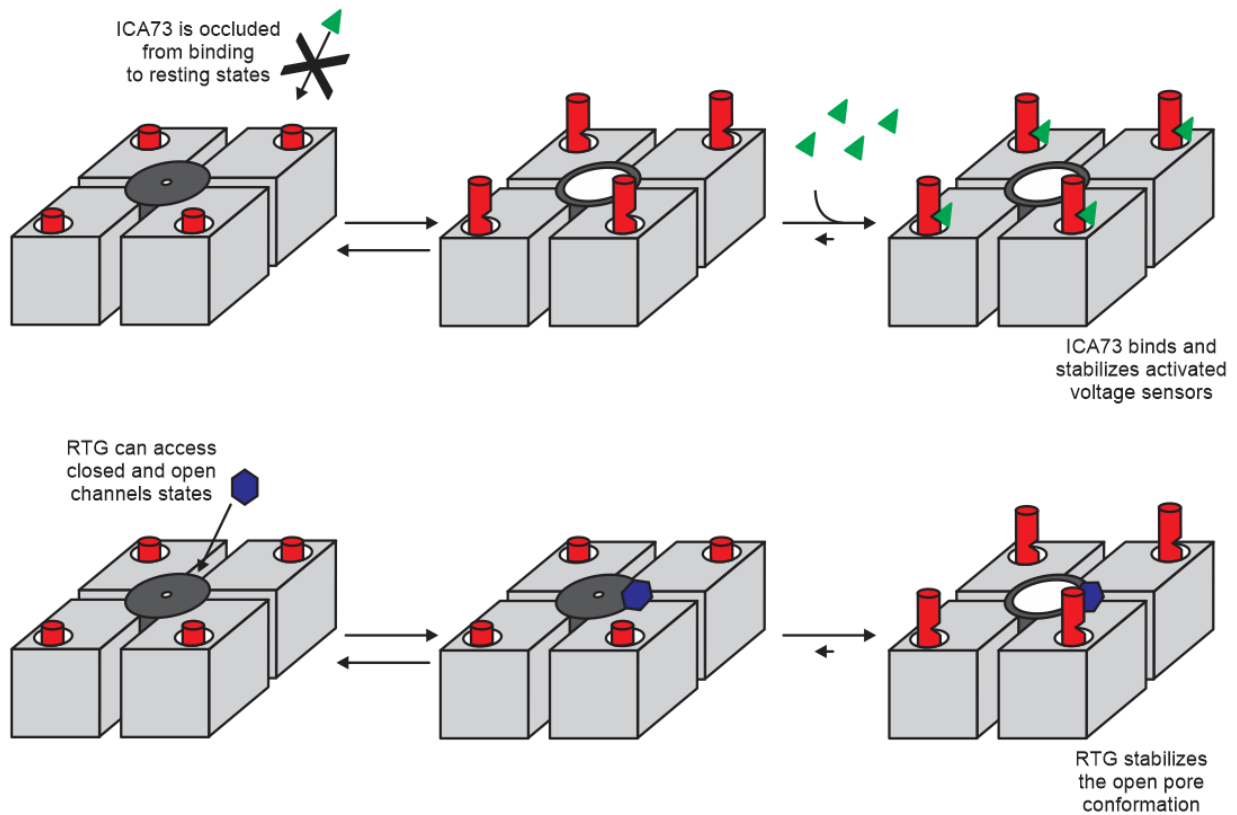


Figure 3.10 Model of ICA73 versus RTG binding. When voltage sensors are inactivated, ICA73 cannot bind. Upon voltage sensor activation and pore opening, ICA73 preferentially binds to activated voltage sensors. RTG can still access its site in the closed pore when voltage sensors are inactivated. Upon voltage sensor activation and pore opening, RTG stabilizes the open pore.

Although the existence of an alternative VSD-delimited binding site is supported by several findings, details of the structural determinants of this binding site have been more difficult to describe with certainty. Our sequence comparison study between KCNQ2 and KCNQ3 led to the identification of KCNQ2 residues A181 and F168 as important determinants of sensitivity, but did not demonstrate whether they directly contribute to binding (Wang et al., 2017). Based on the recent KCNQ1 Cryo-EM structure, the predicted alpha-carbon distance between these two amino acid positions is ~ 18 Å, while the ‘end-to-end’ length of ICA73 is ~ 12 Å, so it is unlikely that both amino acids contribute to a binding site (Sun and MacKinnon, 2017). More importantly, we have also demonstrated that ICA73 sensitivity persists in many A181 mutants (L, G), while the constrained A181P substitution is required to diminish ICA73 effects. Other amino acids in the

vicinity of A181 (E130, Y127, R207) have also been suggested to play a role in a class of diclofenac derivatives that target the voltage sensor, and so a possible explanation for our findings is that the A181P substitution distorts the conformation of this region and weakens the affinity for ICA73 (leading to a faster dissociation rate as reported here), rather than making essential direct contacts with the drug. Although the effects of mutating F168 are more prominent, leading to complete loss of ICA73 sensitivity, it is more distant from this cluster of residues, and has also been suggested to influence stability of the activated voltage sensor (Miceli et al., 2013). Thus, mutation of F168 may have indirect effects on voltage sensor activation that prevent ICA73 binding or effects. Further functional and structural studies of the mechanisms of voltage sensor-targeted KCNQ openers will be required to describe the binding site of these compounds in more detail.

Interestingly, despite the different mechanisms of action of retigabine and ICA73, the effects of both drugs are enhanced by repetitive stimulation. In the case of retigabine, this is likely best attributed to drug-mediated acceleration of activation, allowing more channels to activate during a brief depolarization. In contrast, ICA73 dramatically decelerates voltage sensor deactivation, and so use-dependent accumulation of activation in ICA73 is best attributed to the effect of ‘trapping’ the activated voltage sensor conformation. Overall, use-dependent interactions of KCNQ activators have not been investigated with the same detail as the effects of sodium channel inhibitors, for example. One might predict that use-dependent actions of these drugs could contribute to their therapeutic benefit, and this property might be considered in development of future drugs in this class.

In summary, our study illustrates critical mechanistic differences between pore and voltage sensor-targeted activators. These findings compliment previous structure-function experiments delineating different structural requirements for sensitivity to these different drugs, and also reveal important details related to drug binding to specific channel states.

CHAPTER 4 : SYNERGISTIC ACTIONS OF ANTICONVULSANT KCNQ CHANNEL OPENERS

BACKGROUND

Findings presented in Chapter 3 and elsewhere highlight the recent classification of KCNQ activators into two broad categories, depending on where they act (refer to Table 1). Pore-targeted activators include RTG, BMS-204352, and acrylamide-S1. All of these rely on an essential pore tryptophan (KCNQ2 W236, KCNQ3 W265), and mutation of this tryptophan renders channels insensitive to the drugs (Bentzen et al., 2006; Gao et al., 2017; Lange et al., 2009; Schröder et al., 2001; Wuttke et al., 2005). This tryptophan side chain is proposed to form a hydrogen bond with the carbonyl group present on RTG and its derivatives (Kim et al., 2015). Moreover, the carbonyl group and the tryptophan side chain can be modulated to tune the hydrogen bond interaction between the drug and the channel, with corresponding effects on drug potency (Kim et al., 2015). For example, fluorination of the tryptophan side chain withdraws electron density from the indole nitrogen, increasing its ability to donate a hydrogen bond (Kim et al., 2015). Likewise, addition of electron donating groups surrounding the carbonyl group on the drug increases its propensity to accept a hydrogen bond (Kim et al., 2015). Such properties of drug-channel interaction explain why ML213, a RTG analog, is a more potent KCNQ3 activator than RTG itself (Kim et al., 2015). ML-213 has a series of methyl groups that donate electron density to the carbonyl group, resulting in increased polarity and a stronger hydrogen bond interaction between the drug and the tryptophan in the pore (see Table 2, Pg.73) (Kim et al., 2015).

Other than the pore site activators, a second subtype of KCNQ openers act on a distinct site in the voltage sensor. These include the ICA compounds, as well as others, such as ztz240 and the NSAIDs diclofenac and meclofenamic acid (Gao et al., 2010; Peretz et al., 2005; Wickenden et al., 2008). These compounds do not rely on the pore tryptophan, and retain drug effects on channels carrying the tryptophan pore mutation. Mutations in the voltage sensor, however, alter

channel sensitivity to these compounds, suggesting that the voltage sensor may comprise their binding sites and underlie their actions (Padilla et al., 2009b; Wang et al., 2017). Moreover, certain ICA compounds display weak polarity in their carbonyl group (see Table 2) (Kim et al., 2015). This likely reflects their weakened ability to participate in a hydrogen bond with the tryptophan side chain, causing reduced potency at the pore site (Kim et al., 2015).

In this chapter, we have investigated whether ICA73, a voltage sensor site activator, can act synergistically with RTG, a pore site activator, to open KCNQ channels and suppress seizure activity. Using two-electrode voltage clamp experiments of *Xenopus laevis* oocytes expressing KCNQ2/KCNQ3 channels, we recorded currents from heteromeric channels at various membrane voltages. We chose to record from heteromeric channels because they form the M-current in native systems. These experiments were performed under control conditions, or in the presence of 10 μ M ICA73 alone, 10 μ M RTG alone, or a mixture of ICA73 and RTG. We found that intermediate concentrations (10 μ M) of ICA73 alone or of RTG alone shifted the voltage dependence of KCNQ2/3 by \sim -10 mV. This leftward shift was enhanced by 10mV by adding small concentrations (1 μ M) of the complementary drug (that have little or no effect alone). These findings suggest that the KCNQ2/3 channel response to ICA73 or RTG can be sensitized by sub-effective concentrations of a KCNQ channel opener with an alternative mechanism and binding site. Combinations of KCNQ openers were also tested in 7 days post fertilized (dpf) zebrafish larvae to investigate potential enhancement of anticonvulsant activity. Contrary to our findings in vitro, ICA73 was not anticonvulsive across the concentration range tested. Another KCNQ opener, ML-213, strongly activated KCNQ2/3 channels in vitro and potently suppressed seizures in larvae. Closer examination of ML-213 effects in vitro showed that channel sensitivity to ML-213 is diminished most in pore mutants, and less so in voltage sensor mutants. Collectively, this suggests that ML-213 actions are mediated via the pore site.

RESULTS

ICA73 and RTG have synergistic actions in oocytes expressing KCNQ2/3 channels

Given that ICA73 and RTG act at distinct sites and via different mechanisms, we tested whether a combination of these drugs could produce enhanced activation of the channel. We tested potential synergistic interactions between ICA73 and RTG on *Xenopus* oocytes co-injected with KCNQ2 and KCNQ3 mRNA. Oocytes were exposed to ICA73 or RTG alone, and in combination (Fig. 4.1A, B). 1 μ M RTG minimally shifted or potentiated the activation curve (Fig. 4.1A). 10 μ M ICA73 potentiated current by ~1.5 fold, and shifted the voltage dependence of channel activation by approximately 15mV in the hyperpolarizing direction. The combination of 1 μ M RTG and 10 μ M ICA73 resulted in an enhanced hyperpolarizing gating shift that was greater than the sum of the effects of the two drugs in isolation. Average $V_{1/2}$ values shifted from -34mV in control to -84.7mV in combination solution, compared to -35.8mV in 1 μ M RTG and -49.5mV in 10 μ M ICA73. The magnitude of this enhancement is particularly prominent at voltages < -60mV, when channels are more likely to be closed. For example, more than 50% of channels remained opened at -100mV following combination wash-in, compared to ~10% after 10 μ M ICA73 wash-in. We also measured the voltage dependence of channel activation following application of 1 μ M ICA73, 10 μ M RTG, or a combination of 1 μ M ICA73 and 10 μ M RTG (Fig. 4.1B). 1 μ M ICA73 minimally affected the activation curve. 10 μ M RTG shifted the voltage dependence of channel activation by approximately 10mV in the hyperpolarizing direction. Average $V_{1/2}$ values shifted from -32.9mV in control to -79.4mV in combination solution, compared to -38.2mV in 1 μ M ICA73 and -43.7mV in 10 μ M RTG. Fig. 4.1C illustrates the conductance at -80mV following application of a drug mixture containing 1 μ M RTG and 1, 3, or 10 μ M ICA73. The conductance magnitude increased in a synergistic manner at all concentrations of ICA73 tested; moreover, the synergistic effect became stronger at higher concentrations of ICA73 tested. Fig. 4.1D shows the same experiment using 1 μ M ICA73 and 1, 3, or 10 μ M RTG. As with before, the drug mixture

retained synergistic activation of KCNQ2/3 heteromeric channels, with stronger synergism occurring at higher concentrations of RTG used.

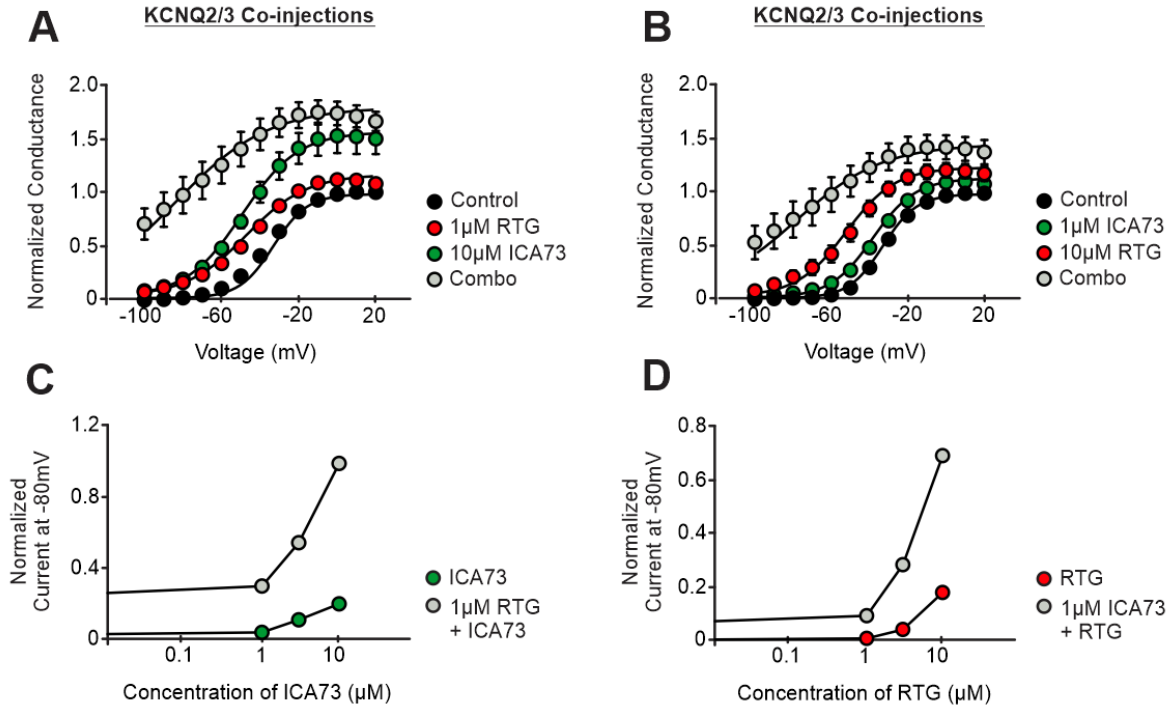


Figure 4.1 Low to intermediate concentrations of ICA73 and RTG synergistically activate KCNQ channels. Activation curves recorded from oocytes co-injected with KCNQ2 and KCNQ3 mRNA in control conditions and following wash-ins of ICA73, RTG, or a combination of both drugs. (A) The conductance voltage relationships of oocytes co-injected with KCNQ2 and KCNQ3 mRNA. Currents were normalized to peak current in control for each cell. KCNQ2/3 parameters of activation were: control $V_{1/2} = 34.0 \pm 1.3\text{mV}$, $k = 8.5 \pm 0.2\text{mV}$; 1μM RTG $V_{1/2} = -35.8 \pm 1.2\text{mV}$, $k = 9.6 \pm 0.2\text{mV}$; 10μM ICA73 $V_{1/2} = -49.5 \pm 1.1\text{mV}$, $k = 15.0 \pm 0.5\text{mV}$; Combo $V_{1/2} = -84.7 \pm 7.1\text{mV}$, $k = 24.6 \pm 0.5\text{mV}$ ($n = 4-5$). (B) Similar experiments described in (A) performed using 1μM ICA73 and 10μM RTG. KCNQ2/3 parameters of activation were: control $V_{1/2} = -32.9 \pm 1.6\text{mV}$, $k = 9.1 \pm 0.3\text{mV}$; 1μM ICA73 $V_{1/2} = -38.2 \pm 2.4\text{mV}$, $k = 11.2 \pm 0.2\text{mV}$; 10μM RTG $V_{1/2} = -43.7 \pm 3.6\text{mV}$, $k = 11.5 \pm 1.2\text{mV}$; Combo $V_{1/2} = -79.4 \pm 7.4\text{mV}$, $k = 23.2 \pm 1.4\text{mV}$ ($n = 4-5$). (C) Oocytes were held at a holding potential of -80mV, before being pulsed to +20mV down to -100mV in 10mV decreases. The current magnitude at -80mV, normalized to peak current in control, was compared between oocytes that were exposed to different concentrations of ICA73 alone, or in combination with 1μM RTG. (D) Similar experiments described in (C) performed using RTG alone (at 1, 3, and 10μM), or in combination with 1μM ICA73.

KCNQ channel opener effects in an *in vivo* model

We also tested KCNQ channel opener effects using 7 days post fertilized (dpf) zebrafish larvae as an *in vivo* model. Larvae have a basal amount of activity under control conditions, which is increased by addition of 10mM pentylenetetrazole (PTZ), a proconvulsive drug that induces seizures (Baraban et al., 2005). Activity of larvae following drug treatment was compared to larvae treated with 10mM PTZ alone. ICA73 was not anticonvulsive at 1 μ M or 3 μ M, and was actually proconvulsive at 10 μ M (Fig. 4.2A, D). In contrast, retigabine elicited a clear, dose-dependent inhibition of larvae activity (Fig. 4.2B, E). Drug mixtures of ICA73 and RTG in different ratios did not show synergistic actions (Fig. 4.2C, F).

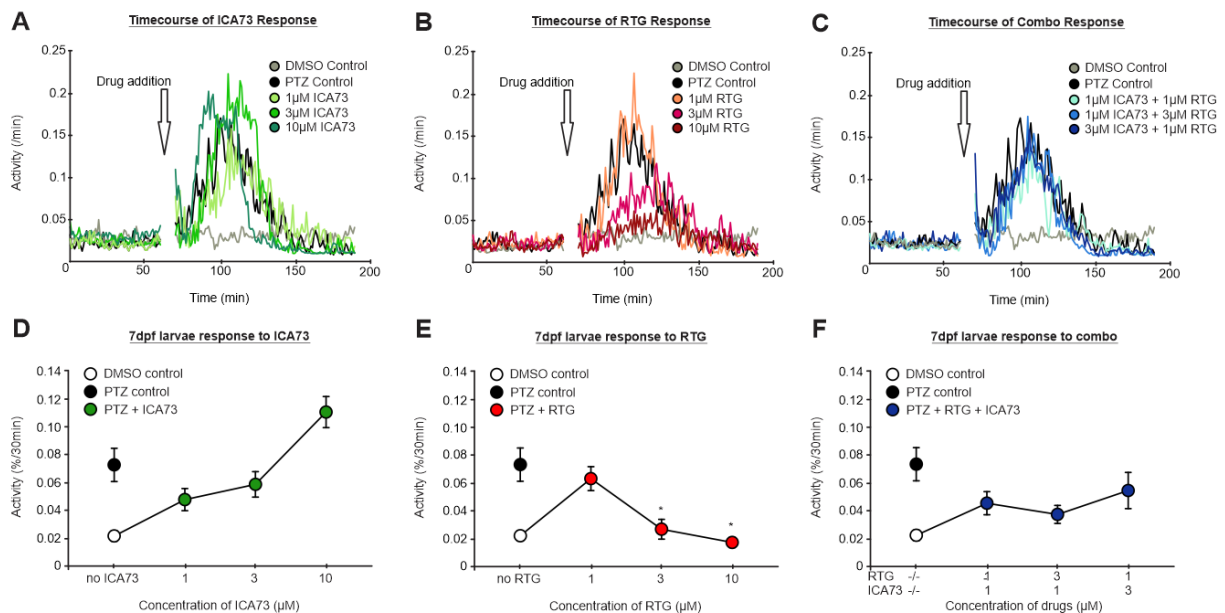


Figure 4.2 KCNQ opener effects in zebrafish larvae. The activity of 7 days post fertilized (dpf) zebrafish larvae was measured in control conditions or following drug treatment. Larval activity over time (A-C), or at 30min post drug treatment (D-F) in response to increasing concentrations of ICA73 (A, D), RTG (B, E), and varying concentrations of a mixture of ICA73 and RTG (C, F), $n = 11-12$. Control conditions for A-F were: DMSO (vehicle control) and 10mM PTZ control. Drugs were administered at 60-75 minutes, indicated by the arrow.

These findings led us to characterize additional KCNQ openers including ML-213. *Xenopus* oocytes expressing heteromeric KCNQ2/3 channels were exposed to ML-213; Fig. 4.3A shows the activation curve of these channels in the absence and presence of the drug. Average $V_{1/2}$

values shifted from -37.9mV in control to -79.8mV in 30 μ M ML-213. This represents a shift of ~42mV in the hyperpolarizing direction, compared to a shift of ~25mV in an equimolar concentration of RTG and ICA73 respectively. In HEK cells, ML-213 had a greater effect on channels compared to RTG and ICA73 (Fig. 4.3B). Average $V_{1/2}$ values shifted from -32.7mV in control to -118.7mV in 30 μ M ML-213, an overall shift of ~86mV in the hyperpolarizing direction. The unusual shape of the G_v seen at higher voltages with 30 μ M ML-213 is likely due to less reliable voltage clamp with large outward currents following drug-induced potentiation. We also investigated the effects of a range of ML-213 concentrations (0.1, 1, 10, 30, 100, and 1000nM) in larvae (Fig. 4.3D). Concentrations of ML-213 as low as 1nM suppressed PTZ-induced hyperactivity. Fig. 4.3C compares larvae activity over time before and after administration of 10 μ M RTG, 10 μ M ICA73, or 10 μ M ML-213. While ICA73 increased activity post drug administration, both RTG and ML-213 decreased activity compared to PTZ-control.

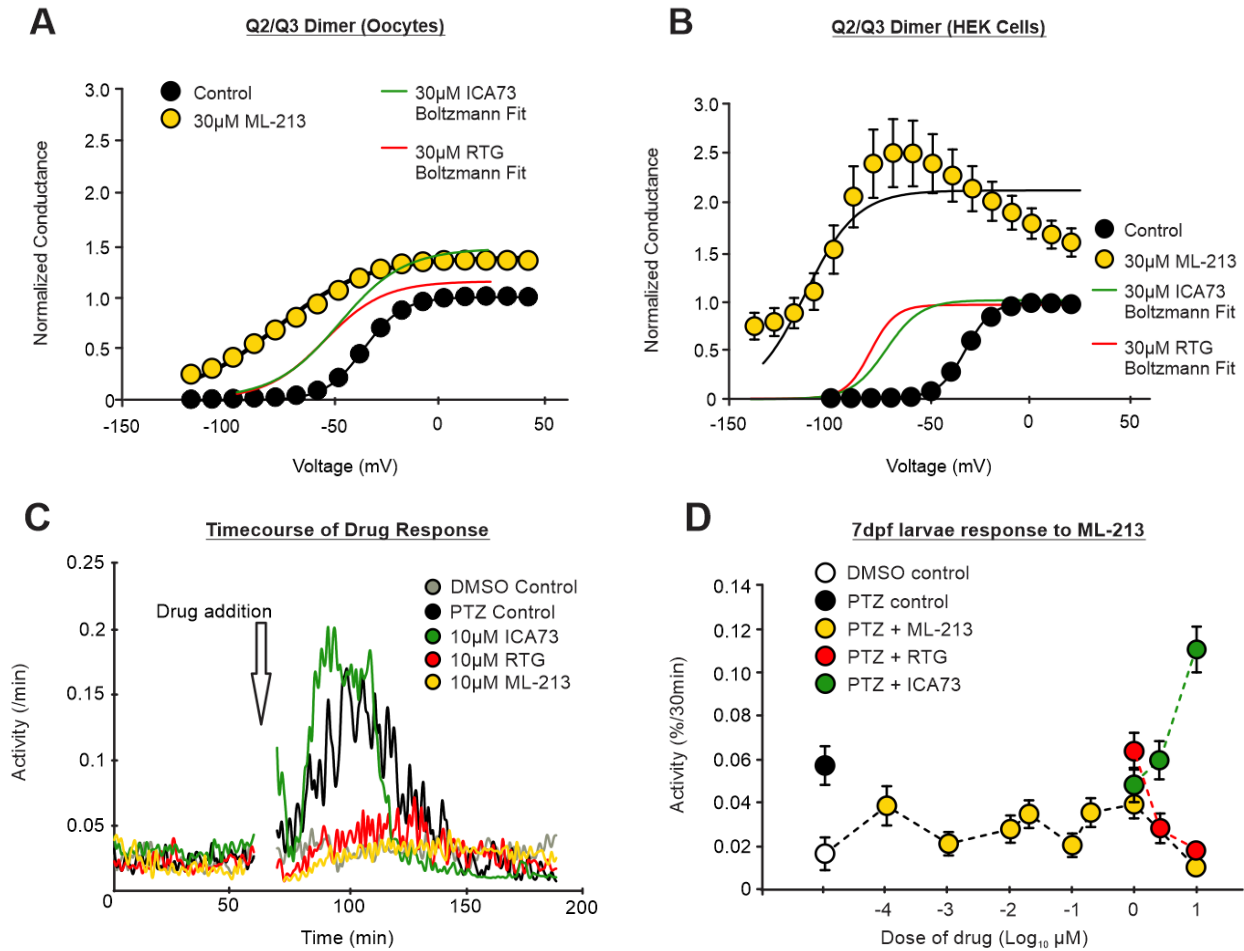


Figure 4.3 ML-213 is a strong KCNQ channel opener and effective anticonvulsant. In oocytes (A) and HEK cells (B): the conductance voltage relationships of heteromeric KCNQ2/3 channels in control conditions, and following wash-in of 30μM ML-213. Currents were normalized to peak current in control for each egg or cell. KCNQ2/3 parameters of activation in oocytes were: control $V_{1/2} = -37.9 \pm 1.6\text{mV}$, $k = 9.2 \pm 0.4\text{mV}$; 30μM ML213 $V_{1/2} = 79.8 \pm 4.8\text{mV}$, $k = 21.7 \pm 0.9\text{mV}$ ($n = 8$). KCNQ2/3 parameters of activation were in HEK were: control $V_{1/2} = -32.7 \pm 2.2\text{mV}$, $k = 6.6 \pm 0.3\text{mV}$; 30μM ML213 $V_{1/2} = -118.7 \pm 5.8\text{mV}$, $k = 13.0 \pm 0.7\text{mV}$ ($n = 5$). Boltzmann fits of KCNQ2/3 channel response to 30μM ICA73 (green) and to 30μM RTG (red) in oocytes are overlaid for comparison. (C) The activity of 7dpf zebrafish larvae in control conditions, following PTZ addition, and 30 minutes after exposure to increasing concentrations of ML-213. Asterisks indicate concentrations of ML-213 for which activity was significantly lower compared to PTZ control. (D) Larval activity over time in control conditions and in response to 10μM ICA73, 10μM RTG, or 10μM ML-213 are overlaid for comparison.

ML213 effects on pore and voltage sensor mutants

We tested the effects of previously characterized mutations in the pore and voltage sensor on ML-213 sensitivity to investigate where ML-213 might be acting. In the pore mutant (W236F, Fig. 4.4C), channels lost drug-induced hyperpolarizing shifts in voltage dependence of channel activation, and were only minimally potentiated. In the voltage sensor mutant (F168L, Fig. 4.4B), the ML-213 mediated gating shift and current potentiation was largely preserved, although there were small reductions ($\sim 20\text{mV}$) in gating shift.

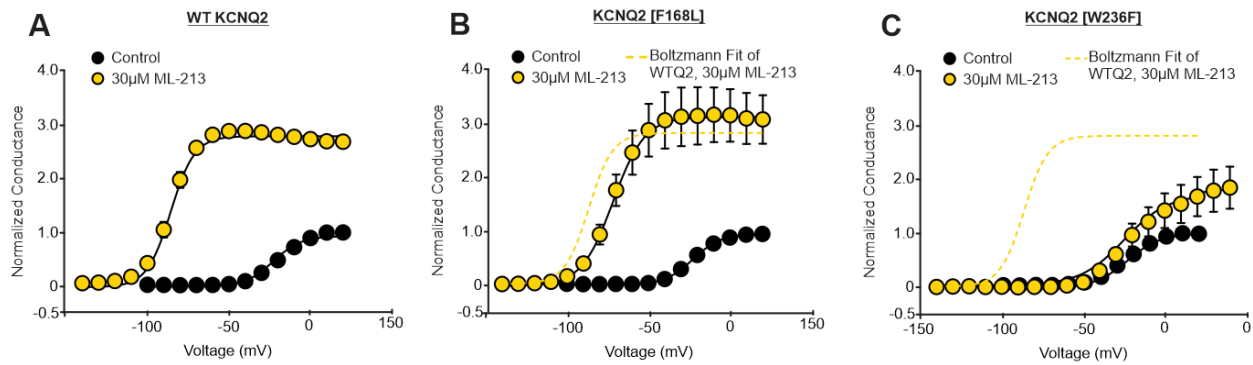


Figure 4.4 ML213 sensitivity in pore and voltage sensor mutants. The conductance voltage relationships of WT KCNQ2 (A), KCNQ2 [F168L] (B), and KCNQ2 [W236F] (C) were measured in HEK293 cells in control conditions, and following wash-in of 30 μM ML-213. Currents were normalized to peak current in control for each cell. WT KCNQ2 parameters of activation were: control $V_{1/2} = -18.3 \pm 2.8\text{mV}$, $k = 8.6 \pm 0.3\text{mV}$; 30 μM ML213 $V_{1/2} = -86.8 \pm 1.8\text{mV}$, $k = 7.3 \pm 0.7\text{mV}$ ($n = 4$). KCNQ2 [F168L] parameters of activation were: control $V_{1/2} = -22.8 \pm 0.8\text{mV}$, $k = 8.5 \pm 0.5\text{mV}$; 30 μM ML213 $V_{1/2} = -71.9 \pm 2.4\text{mV}$, $k = 9.6 \pm 1.2\text{mV}$ ($n = 6$). KCNQ2 [W236F] parameters of activation were: control $V_{1/2} = -24.0 \pm 1.8\text{mV}$, $k = 10.0 \pm 0.6\text{mV}$; 30 μM ML213 $V_{1/2} = -17.8 \pm 3.3\text{mV}$, $k = 15.1 \pm 2.3\text{mV}$ ($n = 4$).

DISCUSSION

This chapter illustrates the potential for synergistic actions of KCNQ openers that act on different regions of the channel and that work through different mechanisms. We have shown that ICA73 and RTG demonstrate synergistic effects in enhancing KCNQ current in *Xenopus* oocytes, and that RTG is a powerful anticonvulsant in zebrafish larvae induced with seizures. Surprisingly, ICA73 did not have anticonvulsant activity and was actually pro-convulsive at higher concentrations. We also found that ML-213, another KCNQ channel opener, exhibited potent anticonvulsive activity.

The rationale of simultaneously applying two drugs is that if the two drugs can bind at the same time to the channel, overall net effects might be non-additive and display unique characteristics. If, however, both compounds occupy the same site, then they would compete for binding. The compound having the greatest affinity for the site would produce a “dominant” effect by occupying the site and preventing binding of the second compound. In isolation, ICA73 and RTG produced a hyperpolarizing shift in KCNQ2/3 activation. In combination, ICA73 and RTG produced an enhanced hyperpolarizing shift, greater than the mere sum of the effects from each drug. This effect was seen with inverse ratios of ICA73 and RTG, suggesting that in each case, a low concentration of one drug is enough to sensitize channel response to intermediate concentrations of the other. The synergistic effects are most pronounced at hyperpolarized membrane potentials when channels are predominantly closed. The observation that RTG and ICA73 have synergistic actions *in vitro* is consistent with the hypothesis that these two compounds bind to different channel sites and work through different mechanisms. This method has been used to suggest that other KCNQ openers (ztz240 and RTG, for example) act at different sites (Gao et al., 2010).

In both *in vitro* and *in vivo* assays, ML-213 stood out as an extremely potent KCNQ activator and anticonvulsant. In oocytes, ML-213 dramatically potentiated Q2/Q3 heteromeric

channel currents, with >80% of channels remaining open at -100mV, compared to <20% and <40% for the same concentration of RTG and ICA73 respectively. The dramatic opener effects of ML213 were accentuated in HEK cells, where 30 μ M ML-213 induced a roughly two-fold greater hyperpolarizing shift in channel activation than an equimolar concentration of RTG or ICA73. The enhanced potency of ML-213 in cells compared to oocytes may be due to differences in drug application between the two systems. In eggs, drug solution was pipetted in for several seconds before immediately recording. In cells, drug solution was washed on continuously for one minute. Depending on drug accessibility to its binding site at a holding potential of -80 to -100mV, ML-213 may exert its most prominent effects when given more time to access the channel.

In vivo, ICA73 was not anticonvulsive at low concentrations, and actually increased excitability when administered at 10 μ M. This may be due to off-target effects of the drug, such as activation of GABA-A receptors (since RTG is known to activate GABA-A receptors at concentrations >10 μ M, (Gunthorpe et al., 2012)). Additionally, VS residues important for ICA73 sensitivity in human KCNQ may not be present in the zebrafish homolog. For example, zebrafish KCNQ contains a serine at the 181 position instead of an alanine. This is unlikely to account for complete ICA73 sensitivity (A181 mutated to a leucine or a glycine still retains ICA73 sensitivity, and it seems a proline mutation is necessary to disrupt drug actions (Wang et al., 2017)), but potentially other VS residues necessary for ICA73 actions, currently unknown, may also be absent.

In contrast to ICA73, ML-213 suppressed seizures at concentrations as low as 1nM. Our experiments did not measure EC₅₀ specifically, but other papers note ML-213 as being a more potent activator of KCNQ3 than RTG (Kim et al., 2015; Vicente-Baz et al., 2016). Despite being originally identified as selective for KCNQ2 and ineffective on KCNQ3, our group has shown that it is a potent activator of KCNQ3 subunits. The carbonyl group in ML213 is extremely polar, and acts as a strong hydrogen bond acceptor to interact with the pore tryptophan essential for retigabine and other pore site activators (Kim et al., 2015). Heteromeric Q2/Q3 channels generate

native M-current in neurons, so taken together, there is potential for ML-213 to depress neuronal excitation much more potently than the current anticonvulsant drug RTG. Potential difficulties with using ML-213 clinically, however, may arise from its extensive metabolism in the liver (Yu et al., 2010).

To investigate ML213 binding in greater detail, we tested the effect of the drug on a KCNQ2 pore mutant (W236F) that abolishes RTG effect, and a KCNQ2 voltage sensor (F168L) mutant that abolishes ICA73 effect. In comparison to other KCNQ channel activators, RTG and ICA73, which are affected by mutations in one channel region but not the other (Wang et al., 2017), ML-213 appears primarily affected by the pore mutation, and less so by the voltage sensor mutation. In the F168L mutant, ML-213 effects are moderately diminished. The magnitude of this disruption in F168L compared to WT KCNQ2 (~20mV reduction in drug-mediated hyperpolarizing shift) is not as dramatic as with W236F, and could arise from changes in channel gating or VS-pore coupling introduced by the mutation itself that alters channel response to ML-213. Since both the gating shift and potentiation are largely preserved, it seems unlikely that F168L disrupts ML-213 binding specifically. Additionally, A181P, another voltage sensor mutation that disrupts ICA73 effect, also largely retains ML-213 effects (data not shown). Taken together, this suggests that like RTG, ML-213 relies on the conserved pore tryptophan for its actions. This is consistent with experiments showing the propensity of ML-213 to participate in a hydrogen bond with W236, and that removal of this hydrogen bond eliminates ML-213 effects (Kim et al., 2015).

Using zebrafish larvae proved to be a useful and valuable tool for drug screening and for investigating the effects of these drugs in vivo. 7dpf zebrafish larvae express KCNQ2, 3, and 5 genes in diffuse patterns corresponding to the central nervous system, and have robust locomotor activity that can be enhanced by selective KCNQ blockers linopirdine and XE-991, or reduced by RTG (Chege et al., 2012). As shown with the unexpected pro-convulsive effects of ICA73 in larvae,

however, caution must be used when translating data from an in vitro model to an in vivo prediction. A drug that has potent effects in vitro may have off-target effects and unexpected results in an in vivo model. One valuable future direction would be to test the effect of ML-213 in combination with other KCNQ openers to see if we can obtain even greater effects. Experimental data has so far shown that ML-213 is a powerful pore site activator; might a mixture of ML-213 and a voltage sensor activator, such as another ICA compound with anticonvulsant activity, have synergistic effects? Additionally, further experiments clarifying the residues important in ML-213 binding will be useful in furthering our understanding of KCNQ pharmacology. The overall trajectory of future experiments would be to characterize specific features of ML-213 that differentiate it from both ICA73 and RTG as an exceptionally strong heteromeric KCNQ2/3 channel activator, and to exploit these differences in future drug design.

CHAPTER 5 : PROBING FOR SPECIFIC VOLTAGE SENSOR RESIDUES REQUIRED FOR ICA₇₃ EFFECT

BACKGROUND

The voltage-gated potassium channels represent an exciting new target in the treatment of epilepsy, a disease characterized by a high percentage of drug-resistant patients. Following the development of retigabine as the prototype KCNQ opener for use in epilepsy, a number of other KCNQ-targeted drugs are undergoing development in the hopes of improving upon retigabine's shortcomings. These include CNS-related side effects such as drowsiness, fatigue, dizziness, and confusion (Amabile and Vasudevan, 2013; Brodie et al., 2010; French et al., 2011). Other side effects, however, are more peripherally localized, including urinary retention and precipitation of RTG metabolites in the skin and retinal epithelium (Amabile and Vasudevan, 2013; Millichap et al., 2016). The main explanation for this is due to the lack of selectivity of retigabine. In addition to potentiating neuronal KCNQ isoforms to exert its anticonvulsant activity, the drug also activates peripherally-concentrated KCNQ4 and KCNQ5 subtypes which are expressed in the bladder detrusor muscle (Gunthorpe et al., 2012; Svalø et al., 2015; Wang and Li, 2016). Oxidation of RTG's aniline ring is also hypothesized to form colored deposits in the skin and eye (Kumar et al., 2016). As development of retigabine analogs moves forward, drug selectivity and design of less metabolically reactive drugs will be an important consideration for a newer and better generation of KCNQ channel openers.

The ICA compounds are a class of pyridinyl benzamides that exhibit greater selectivity for KCNQ2 subunits (Blom et al., 2010; Wickenden et al., 2008). They are significantly less effective on other subunits, displaying EC₅₀'s of >100μM on KCNQ3/Q5 channels in rubidium efflux assays, and are ineffective on KCNQ1/E1 (Wickenden et al., 2008). The actions of ICA rely on residues in the KCNQ2 voltage sensing domain. Chimeric channels between drug sensitive and drug insensitive subunits showed that the KCNQ2 voltage sensing domain is required for the

channel to remain sensitive to ICA73 (Padilla et al., 2009; Wang et al., 2017). Furthermore, our lab identified two specific residues in the S3 helix of the voltage sensor, A181 and F168, which were critical for imparting full ICA73 sensitivity (Wang et al., 2017). Mutation of these residues to their KCNQ3 equivalents showed diminished ICA73 sensitivity: F168L completely abolished the current potentiation and hyperpolarizing shift induced by the drug, while A181P exhibited strongly attenuated gating shift although current potentiation and deceleration of channel closure was maintained (Wang et al., 2017). Reverse mutation of the corresponding residues in KCNQ3 to their KCNQ2 equivalents (L198F and P211A) partially restored ICA73 sensitivity (Wang et al., 2017). An inconsistency with these findings is that KCNQ5 retains both the essential phenylalanine and alanine residues, yet remains insensitive to ICA73. Collectively, these results suggest that additional residues in the VSD are important for ICA73 effects (Wang et al., 2017).

In this chapter, we sought to further narrow down our understanding of the structural determinants of ICA73 sensitivity and selectivity. Past work from our lab has shown that residues in the voltage sensing domain influence ICA73 effect. These were determined by comparing the KCNQ2 VSD with the KCNQ3 VSD to identify specific residues that differed between the two channels. In order to identify additional voltage sensor residues that may be important for ICA73 sensitivity, we identified sequence differences in the voltage sensor of KCNQ2 and the ICA73-insensitive subunit KCNQ5. Using site-directed mutagenesis, we mutated KCNQ2 residues to their KCNQ5 equivalents, and tested for alterations in channel sensitivity to ICA73. The findings from our work identify several mutations that had modest effects on channel sensitivity to ICA73, although no individual mutation completely abolished drug sensitivity. These findings suggest that ICA73 sensitivity likely involves multiple residues.

RESULTS

KCNQ5 is insensitive to ICA73

In wildtype KCNQ2 channels, ICA73 produced a strong, concentration-dependent increase in current amplitude and shifted the channel's voltage-dependence of opening leftward (Fig. 5.1A). In wildtype KCNQ5 channels, ICA73 concentrations as high as 100 μ M had minimal effect on both current amplitude and channel gating (Fig. 5.1B), consistent with data reporting ICA73 as a KCNQ2-selective channel opener. Sequence alignment between the VSD of KCNQ5 and KCNQ2 showed several divergent residues (Fig. 5.1C). We created single point mutations at these sites, with KCNQ2 residues mutated to their KCNQ5 equivalents. The mutations tested were scattered throughout the VSD (S1-S4) of the channel. These included mutations in the S1-S2 linker (K116P, Y118H, E119T, S122A, E123S, G124S), the S2 helix (T133M), the S2-S3 linker (A147S, R158Q), the S3 helix (I173T, M174I, A184S, G186K, S187T), the S3-S4 linker (V191I), and the S4 helix (I209V). A final mutation in the S5 helix (Y226C) was made based on molecular simulations suggesting that ICA73 may bind to a pocket created by aromatic residues in this area.

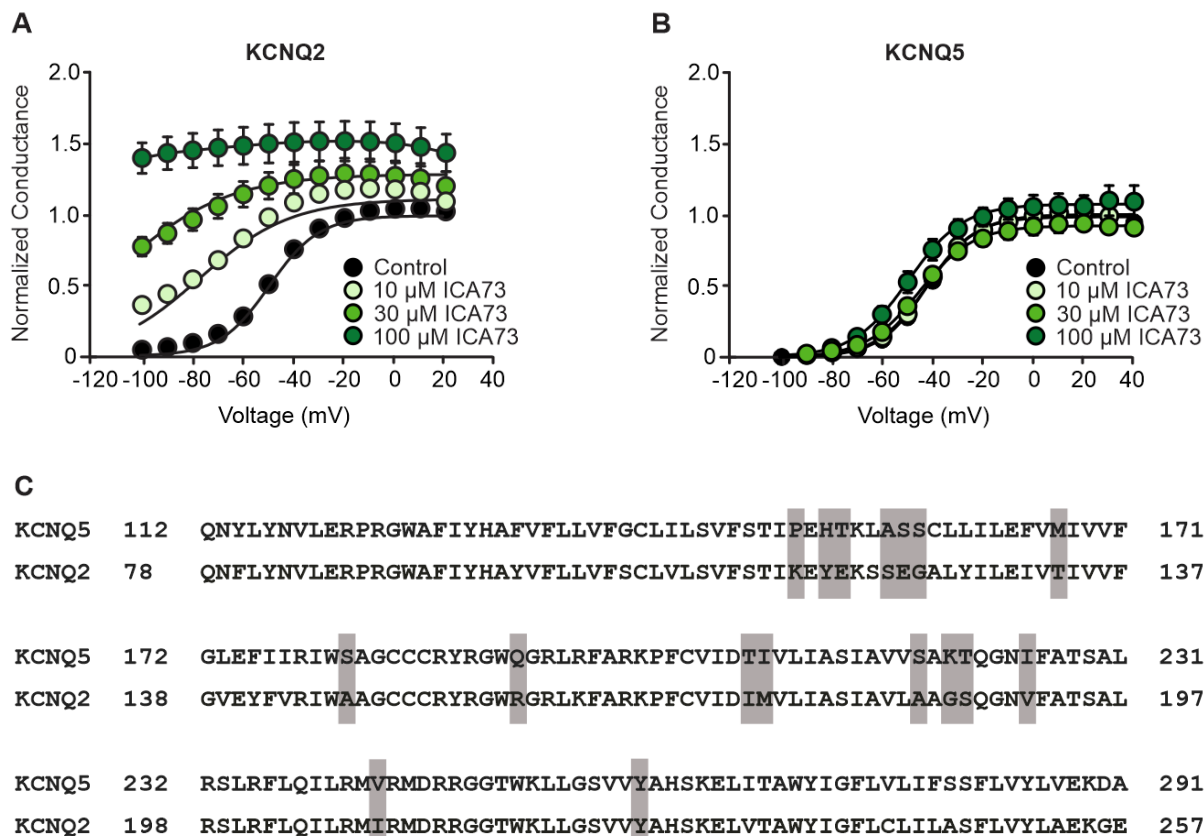


Figure 5.1 ICA73 sensitivity of KCNQ5 and residue differences. (A-B) Current levels of KCNQ2 and KCNQ5 expressed in oocytes under indicated drug conditions were normalized to peak current levels in control. KCNQ2 parameters of activation were: control $V_{1/2} = -48.7 \pm 1.0$ mV, $k = 9.9 \pm 0.4$ mV; 10 μ M ICA73 $V_{1/2} = -76.4 \pm 2.2$ mV, $k = 17.9 \pm 0.5$ mV; 30 μ M ICA73 $V_{1/2} = -108.6 \pm 3.0$ mV, $k = 21.3 \pm 0.7$ mV, $n = 10$. 100 μ M ICA73 could not be fit by a Boltzmann equation. KCNQ5 parameters of activation were: control $V_{1/2} = 41.6 \pm 1.3$ mV, $k = 9.4 \pm 0.3$ mV; 10 μ M ICA73 $V_{1/2} = -41.5 \pm 1.0$ mV, $k = 10.1 \pm 0.1$ mV; 30 μ M ICA73 $V_{1/2} = -44.6 \pm 1.5$ mV, $k = 10.7 \pm 0.2$ mV; 100 μ M ICA73 $V_{1/2} = -49.0 \pm 2.9$ mV, $k = 10.9 \pm 0.7$ mV, $n = 4$. (C) Sequence alignment of KCNQ2 and KCNQ5 VSD. Grey highlights indicate residues in KCNQ2 mutated to their KCNQ5 equivalents.

ICA73 effects are diminished in three voltage sensor mutants

Channel sensitivity to ICA73 was assessed mainly by alterations in channel gating (i.e. shifts in the voltage dependence of channel activation, and changes in the steepness of the curve). Mutant channel sensitivity to ICA73 was compared to wildtype KCNQ2 sensitivity to 30 μ M ICA73, shown in Fig. 5.2A. Out of all the mutations tested, three mutations showed greatest disruptions to ICA73 sensitivity. In the S1-S2 linker, KCNQ2[K116P] had an attenuated hyperpolarizing shift

in channel gating caused by ICA73 (Fig. 5.2D). In the S3 helix, KCNQ2[I173T] and KCNQ2 [G186K] both showed a reduced response to ICA73-induced hyperpolarizing shift (Fig. 5.2E, F). Additionally, under control conditions, I173T had a slightly left-shifted $V_{1/2}$.

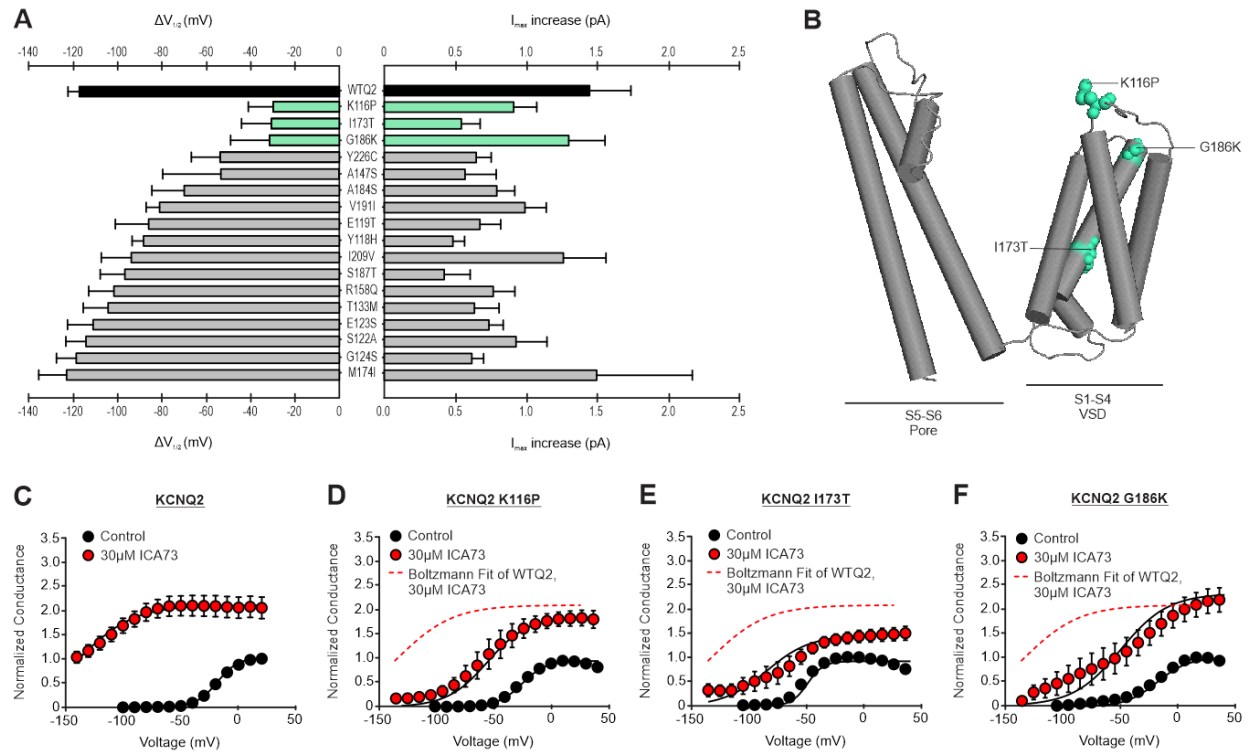


Figure 5.2 ICA73 effects in three voltage sensor mutants. (A) Summary of response of mutant channels to 30μM ICA73 application. Left: shift in $V_{1/2}$ values for each mutant following ICA73 addition; right: amount of current potentiation following 30 μM ICA73 addition (average \pm SEM). Values for each mutant are quantified as change in average $V_{1/2}$ or current compared to that in control. Cyan indicates the changes in the current-voltage relationship of the three most disrupted mutants: K116P, I173T, and G186K. (B) Location of disrupting mutations. K116P is in the S1-S2 linker, I173T is in the S3 helix, and G186K is at extracellular end of S3. (C-F) The conductance voltage relationships in HEK cells for wildtype KCNQ2 (C), K116P (D), I173T (E), and G186K (F) in the absence and presence of 30μM ICA73. Activation protocol was a holding potential of -100mV, pulses to +40mV that decreased in 10mV increments, then repolarization to -20mV for tail current data. Current levels in the drug were normalized to peak current levels in control. KCNQ2 parameters of activation were: control $V_{1/2} = -18.5 \pm 2.3$ mV, $k = 9.1 \pm 0.3$ mV; 30μM ICA73 $V_{1/2} = -136.1 \pm 4.6$ mV, $k = 23.4 \pm 0.7$ mV, $n = 5$. K116P parameters of activation were: control $V_{1/2} = -25.9 \pm 3.1$ mV, $k = 10.3 \pm 1.9$ mV; 30μM ICA73 $V_{1/2} = -55.7 \pm 10.7$ mV, $k = 17.2 \pm 2.8$ mV, $n = 4$. I173T parameters of activation were: control $V_{1/2} = -48.9 \pm 0.9$ mV, $k = 6.8 \pm 0.4$ mV; 30μM ICA73 $V_{1/2} = -79.5 \pm 13.4$ mV, $k = 18.7 \pm 3.2$ mV, $n = 5$. G186K parameters of activation were: control $V_{1/2} = -18.1 \pm 4.1$ mV, $k = 13.4 \pm 1.3$ mV; 30μM ICA73 $V_{1/2} = -49.5 \pm 17.0$ mV, $k = 20.4 \pm 1.9$ mV, $n = 6$.

DISCUSSION

One inconsistency encountered with the results were variable amounts of gating shift for the mutants identified as having altered ICA73 sensitivity (K116P, I173T, G186K). Some cells displayed drastically shifted conductance-voltage relationships, while others showed minimal gating shifts for the same mutant. This suggests inconsistencies in drug access to the channel, possibly through inconsistent drug wash-in times.

We also encountered variability with the amount of current potentiation induced by ICA73 for the same mutant. Since the amount of current potentiation is likely affected by levels of PIP_2 in the membrane, as well as sensitivity of the channel to PIP_2 , the variability in current potentiation could be explained by inconsistent PIP_2 levels in cells. KCNQ3 is very sensitive to PIP_2 , and hence does not show increases in channel open probability and hence, macroscopic current, when factors that increase PIP_2 concentrations (ATP, PI kinases) are added (Li et al., 2005). On the other hand, KCNQ2 is less sensitive to PIP_2 (Li et al., 2005). Presumably because the concentration of PIP_2 in the membrane falls within the dynamic range of channel opening, slight increases or decreases in PIP_2 levels could result in dramatically different responses to channel openers such as ICA73. Thus, in a cell with slightly higher PIP_2 levels, ICA73 would not be able to increase channel open probability by much, as the concentration of PIP_2 has already saturated KCNQ2 open probability. In a cell with slightly lower PIP_2 levels, ICA73 would greatly increase channel open probability, leading to a macroscopic increase in current. Worthwhile future experiments include standardizing PIP_2 concentrations by adding ATP or $\text{PI}_{4/5}$ -kinase to the internal solution to increase PIP_2 levels across all cells, or alternatively, by adding wortmannin to decrease PIP_2 levels uniformly.

All of the mutants identified that alter ICA73 sensitivity exhibited attenuated hyperpolarizing shifts in the presence of the drug. This suggests multiple possibilities. The drug may have reduced affinity for binding to the channel, and dissociate from the channel faster

resulting in less stabilization of the open channel state (as in the case of A181P). Alternatively, the drug may have reduced state-dependent binding to the channel, with either a reduced propensity to bind to the open channel state, or a greater propensity to bind to the closed channel state. A closer investigation of which of these two possibilities may be at play can be done through fast solution switching experiments to assess the kinetics of drug binding and unbinding at a range of membrane voltages.

G186K also exhibited shallower conductance voltage relationships in the absence and presence of ICA73. This suggests a reduction in the charge displacement between the closed and open channel states, resulting in a channel that is less sensitive to voltage. Further experiments with VCF, which report voltage sensor activation and deactivation directly and in relation to channel opening, will clarify the extent of these alterations. In general, mutations that affect channel sensitivity to ICA73 do not cluster in a specific area of the voltage sensor; rather, they are widely dispersed throughout all four helices. This differs from predictions that the S1-S2 linker and S3-S4 linker, which had the most differences between KCNQ2 and KCNQ5, may be where mutations would be most disruptive for ICA73 effect. K116P is in the S1-S2 linker, I173T is buried in the middle of the S3 helix, and G186K is on the extracellular side at the top of the S3 helix. While multiple residues affected ICA73 sensitivity, there was not one residue that completely eliminated ICA73 effect consistently. This suggests that rather than single point residues, *regions* of the voltage sensing domain may be more important in modulating channel sensitivity to ICA73. An important next step would be to test ICA73 sensitivity in channels carrying multiple mutations.

CHAPTER 6 : GENERAL DISCUSSION & CONCLUSION

General discussion

The umbrella term of “KCNQ opener” is now recognized to encompass a variety of binding sites and mechanisms of drug action. Retigabine, the prototype KCNQ channel opener indicated for use in pharmaco-resistant epileptic patients, was first approved for use <10 years ago (Martyn-St James et al., 2012). Since that time, there has been ongoing investigation and development of analogs, but many questions persist related to the molecular mechanism of action of these drugs. Findings presented in this thesis begin to unravel some of the fundamental differences in the mechanisms of action of two KCNQ openers, RTG and ICA73. Additionally, I investigated how another KCNQ opener, ML213, acts as a powerful KCNQ2/3 channel opener and anticonvulsant.

In chapter 3, I explored the distinct mechanisms of ICA73 and RTG actions on KCNQ2 channels. I demonstrated that ICA73 exhibits strong voltage dependence of drug binding, with the drug preferentially binding at depolarized voltages when its binding site in the voltage sensor becomes accessible (Figs. 3.1, 3.2). In contrast, RTG accesses channels across a wider voltage range of voltages, and binds at hyperpolarized potentials where channels are predominantly closed (Figs. 3.4, 3.5). Preference for binding to activated voltage sensor states also generates use-dependent activation of KCNQ2 channels as frequent, repetitive depolarizations in the presence of ICA73 caused channels to gradually accumulate in a drug bound active state (Fig. 3.9). I also found that ICA73 had attenuated effects on the KCNQ2 voltage sensor mutant A181P. Closer inspection of drug-channel interactions using fast solution switching demonstrated that ICA73 unbinds more rapidly from KCNQ2[A181P] channels relative to WT KCNQ2 (Fig. 3.8). This results in a weaker stabilization of the open channel state, leading to more rapid drug unbinding and channel closure, and an overall attenuated use-dependent potentiation during repetitive pulse trains (Fig. 3.9). Similar to effects in WT KCNQ2, ICA73 maintains strong voltage

dependence of binding to A181P, with a strong preference for binding activated channel conformations achieved with depolarization (Fig. 3.7).

In Chapter 4, I investigated potential synergistic effects of KCNQ openers. KCNQ channels expressed in *Xenopus* oocytes displayed enhanced channel opening with a combination of low to intermediate concentrations of ICA73 and RTG, compared to either drug in isolation (Fig. 4.1). The effect of ICA73 and RTG alone and in combination was also tested in 7 dpf zebrafish larvae. While RTG displayed a strong, concentration-dependent anticonvulsant effect, ICA73 had no effects at low concentrations and was pro-convulsive at higher concentrations (Fig. 4.2). In combination, RTG and ICA73 displayed no synergistic anticonvulsant effect. The unexpected results from ICA73 led us to test other KCNQ openers. Of these, ML-213 emerged as a consistently potent anticonvulsant with activity at concentrations as low as 1 nM (Fig. 4.3). A closer examination of the effects of ML-213 on KCNQ channels in cells and oocytes showed that mutations in the pore and to a lesser extent, the voltage sensor, diminished ML-213 effects, raising the possibility that ML-213 may act at both the pore and VSD sites (Fig. 4.4). Importantly, ML-213 exhibited a strong effect on heteromeric KCNQ2/3 channels, the most common heteromeric channel responsible for generating M-current in native neurons. ML-213 induces a dramatic hyperpolarizing shift in the voltage dependence of heteromeric KCNQ2/3 channel activation, to a greater extent than a similar concentration of either ICA73 or RTG (Fig. 4.3).

Finally, in chapter 5, I built upon past findings from our group to further identify residues important for ICA73 sensitivity. Previously, a sequence comparison of KCNQ2 (ICA73-sensitive) and KCNQ3 (ICA73-insensitive) motivated the identification and testing of specific residues in the KCNQ2 voltage sensor with altered ICA73 sensitivity (Wang et al., 2017). To identify other residues important for ICA73 sensitivity, I compared voltage sensor sequences between KCNQ2 and another ICA73 insensitive subunit, KCNQ5. I used site-directed mutagenesis to substitute individual residues in the KCNQ2 voltage sensor with their KCNQ5 equivalents. These mutations

were scattered throughout the voltage sensor (Fig. 5.1C). While most mutant channels retained the current potentiation and gating shift induced by the drug, several mutations had noticeably altered ICA73 sensitivity (Fig. 5.2). These mutations were: K116P, I173T, and G186K. Each of these mutations resulted in a channel with variable but overall diminished ICA73-induced hyperpolarizing shift. No single point mutation was sufficient to completely eliminate drug effect, suggesting that multiple residues may contribute to ICA73 sensitivity to ICA73. A useful next step would be to test the effect of multiple VS mutations together on ICA73 sensitivity.

To date, much of the work in the field has focused on characterizing drug binding sites through mutagenesis and chimeric approaches, supplemented with molecular modelling. However, few studies investigate how these drugs interact with the channel to stabilize the open state. Using a fast solution switching apparatus I was able to monitor the kinetics of drug binding and unbinding, yielding valuable information regarding drug:channel interactions at different membrane voltages. Going forward, fast solution switching will be a valuable tool to describe ligand-channel interactions in the context of KCNQ channels.

Findings presented in this thesis highlight gaps in knowledge that should be addressed in the continued development of better antiepileptic drugs. While use-dependent properties of sodium channel blockers are well characterized, these features of KCNQ openers remain largely unexplored. In sodium channels, quaternary and amine local anesthetics (LAs) preferentially bind to open and inactivated channel states rather than resting, closed channels (Ragsdale et al., 1991, 1994). With a repetitive train of depolarizations, progressively more channels are opened and inactivated, leading to an accumulation of drug bound to open and inactivated channels and an overall greater drug effect (Ragsdale et al., 1991, 1994). As highlighted in chapter 3, a similar phenomenon occurs for KCNQ channel interactions with RTG or ICA73. In this case, RTG and ICA73 preferentially bind and stabilize active conformations of either the pore or voltage sensor, respectively. For either drug, a train of brief, repetitive stimulations leads to progressively more

drug binding and accumulation of channels in activated states. Use-dependent activation of ion channels is recognized as an important and desirable feature, because it allows the drug to more selectively target hyperexcitable cells present at an epileptic trigger site (Ragsdale et al., 1991). A deeper understanding of the mechanisms underlying state- and use dependent actions may offer a new perspective or property to monitor in the development of future KCNQ activators.

Aside from state- and use-dependence, it may also be desirable to develop anticonvulsants with increased potency and/or selectivity. In my investigation of KCNQ activators, ML-213 stood out as a strong enhancer of KCNQ current *in vitro* and a powerful seizure suppressant *in vivo*. An unanswered question is what features of ML-213 make it such a potent and effective drug (at least in these pre-clinical assays)? Some of the evidence I have collected suggests that it may act primarily on residues in the pore site (essential for RTG binding) rather than the voltage sensor site (essential for ICA73 binding). However, the disruptive effect of the F168L mutation is presently yet unclear, and it remains uncertain if the small reduction in gating shift (~20mV) compared to WT KCNQ2 is due to disruptions in drug effect from altered channel biophysics, or drug binding specifically. In the future, it will be useful to characterize the residues that constitute the ML-213 binding site, and features of ML-213 that allow it to be such a potent anticonvulsant. An ideal drug may be a hybrid of different types of KCNQ openers, incorporating desirable features from both pore- and voltage sensor-targeted KCNQ activator subtypes.

Similar to considering the features that make certain drugs effective anticonvulsants, we can consider the characteristics of the drug target, the KCNQ channel, that underlie selectivity and potency. My findings illustrate that while individual residues may have some effect on drug sensitivity and selectivity, it is likely that multiple residues contribute to drug sensitivity. The exact identity of these residues and how they work together, however, remains unclear. A181 and F168 (KCNQ2 numbering) are two residues previously identified as important for full ICA73 sensitivity (Wang et al., 2017). However, both residues are retained in the ICA73-insensitive

KCNQ5 subunit, suggesting more residues are involved. These residues may be directly responsible for drug effects by reconstituting a binding site. Indirectly, they could be responsible for coupling of drug binding to channel activation, or by contributing to attractive/repulsive forces that may make the drug more/less likely to bind, or by impacting the interaction of the channel with other molecular factors that could then affect the interaction of the channel with the drug.

The voltage-gated potassium channels represent an exciting target in the treatment of epilepsy, a disease characterized by a high percentage of drug-resistant patients. The development of new KCNQ-targeted anti-epileptic drugs is ongoing, with retigabine at its forefront. A major disadvantage of retigabine use, however, is its common and numerous side effects, including urinary retention and precipitation of metabolites in retinal and skin epithelia (Millichap et al., 2016). At fault are two factors of retigabine pharmacology. First, the drug is nonselective, and binds to KCNQ4 and KCNQ5, subtypes expressed in the bladder detrusor muscle and retinal epithelium (Amabile and Vasudevan, 2013). Second, improvements in RTG potency may also improve its side effect profile. Thus, a drug that can simultaneously target specific isoforms of the channel (i.e. be selective) while having large anticonvulsant effect at minimal concentrations (i.e. be potent) would diminish side effects from off-target effects and high doses. This is the principle underlying why combinations of KCNQ openers may be a valuable therapy. In a cocktail of KCNQ openers, only small to intermediate concentrations of each drug would be required. Presumably, such low amounts of the individual drugs alone would reduce the likelihood of binding to off target sites, but when administered together, can exert therapeutic effects in the brain. Additionally, the effects would be limited to regions of the body that express the specific KCNQ isoform targeted by all drugs in the mixture. In a mixture of ICA73 and RTG, for example, this biases drug effects towards channels containing KCNQ2, the subunit targeted by both drugs. As development of KCNQ openers moves forward, these features will be important considerations with potential for therapeutic application.

Going forward, it will also become increasingly important to show drug efficacy in more physiologically relevant targets. The finding that ICA73 was not an effective anticonvulsant in vivo despite its potent activation of KCNQ channels in vitro serves as a humble reminder that effects in one model system do not necessarily translate well to another model system. Indeed, even transitioning between HEK cells and oocytes, we noticed differences in parameters of channel gating and drug-induced changes in channel gating, although overall responses to drugs were preserved. Care should thus be taken to not inflate the importance of findings, especially in a model that is not primary. If possible, future experiments using heterologous expression systems should be done using the most physiologically relevant targets. While experiments with homomeric KCNQ2 or KCNQ3 may yield useful insights, experiments with heteromeric KCNQ2/Q3 channels, with possible contribution from KCNQ5, may be most clinically significant because they form the M-current in native neurons. Thus, while RTG and ICA73 are potent activators of certain homomeric KCNQ channels, their effects on heteromeric Q2/Q3 are weaker, explaining their diminished effects in an in vivo model.

Conclusion

KCNQ openers are emerging as a more complex and diverse group of ion channel modulators than originally anticipated. This thesis highlights some of the fundamental differences underlying how different KCNQ openers work to activate their ion channel targets, which if exploited, may have valuable therapeutic implications in KCNQ-targeted AED development.

REFERENCES

- Adams, P.R., and Brown, D.A. (1980). Luteinizing hormone-releasing factor and muscarinic agonists act on the same voltage-sensitive K⁺-current in bullfrog sympathetic neurones. *Br. J. Pharmacol.* 68, 353–355.
- Aggarwal, S.K., and MacKinnon, R. (1996). Contribution of the S4 Segment to Gating Charge in the Shaker K⁺ Channel. *Neuron* 16, 1169–1177.
- Amabile, C.M., and Vasudevan, A. (2013). Ezogabine: a novel antiepileptic for adjunctive treatment of partial-onset seizures. *Pharmacotherapy* 33, 187–194.
- Anderson, U.A., Carson, C., Johnston, L., Joshi, S., Gurney, A.M., and McCloskey, K.D. (2013). Functional expression of KCNQ (Kv7) channels in guinea pig bladder smooth muscle and their contribution to spontaneous activity. *Br. J. Pharmacol.* 169, 1290–1304.
- Armstrong, C.M., and Hille, B. (1998). Voltage-Gated Ion Channels and Electrical Excitability. *Neuron* 20, 371–380.
- Baraban, S.C., Taylor, M.R., Castro, P.A., and Baier, H. (2005). Pentylentetrazole induced changes in zebrafish behavior, neural activity and c-fos expression. *Neuroscience* 131, 759–768.
- Barhanin, J., Lesage, F., Guillemare, E., Fink, M., Lazdunski, M., and Romey, G. (1996). K(V)LQT1 and IsK (minK) proteins associate to form the I(Ks) cardiac potassium current. *Nature* 384, 78–80.
- Barrese, V., Stott, J.B., and Greenwood, I.A. (2018). KCNQ-Encoded Potassium Channels as Therapeutic Targets. *Annu. Rev. Pharmacol. Toxicol.* 58, 625–648.
- Bentzen, B.H., Schmitt, N., Calloe, K., Dalby Brown, W., Grunnet, M., and Olesen, S.-P. (2006). The acrylamide (S)-1 differentially affects Kv7 (KCNQ) potassium channels. *Neuropharmacology* 51, 1068–1077.
- Bezannilla, F. (2008). How membrane proteins sense voltage. *Nat. Rev. Mol. Cell Biol.* 9, 323–332.
- Biervert, C., Schroeder, B.C., Kubisch, C., Berkovic, S.F., Propping, P., Jentsch, T.J., and Steinlein, O.K. (1998). A Potassium Channel Mutation in Neonatal Human Epilepsy. *Science* 279, 403–406.
- Blom, S.M., Schmitt, N., and Jensen, H.S. (2010). Differential effects of ICA-27243 on cloned K(V)7 channels. *Pharmacology* 86, 174–181.
- Brodie, M.J., Lerche, H., Gil-Nagel, A., Elger, C., Hall, S., Shin, P., Nohria, V., Mansbach, H., and RESTORE 2 Study Group (2010). Efficacy and safety of adjunctive ezogabine (retigabine) in refractory partial epilepsy. *Neurology* 75, 1817–1824.
- Brown, D.A., and Adams, P.R. (1980). Muscarinic suppression of a novel voltage-sensitive K⁺ current in a vertebrate neurone. *Nature* 283, 673–676.
- Brown, D.A., and Passmore, G.M. (2009). Neural KCNQ (Kv7) channels. *Br. J. Pharmacol.* 156, 1185–1195.

- Brown, D.A., Hughes, S.A., Marsh, S.J., and Tinker, A. (2007). Regulation of M(Kv7.2/7.3) channels in neurons by PIP(2) and products of PIP(2) hydrolysis: significance for receptor-mediated inhibition. *J. Physiol.* *582*, 917–925.
- Brueggemann, L.I., Haick, J.M., Cribbs, L.L., and Byron, K.L. (2014). Differential Activation of Vascular Smooth Muscle Kv7.4, Kv7.5, and Kv7.4/7.5 Channels by ML213 and ICA-069673. *Mol. Pharmacol.* *86*, 330–341.
- Chadha, P.S., Jepps, T.A., Carr, G., Stott, J.B., Zhu, H.-L., Cole, W.C., and Greenwood, I.A. (2014). Contribution of Kv7.4/Kv7.5 Heteromers to Intrinsic and Calcitonin Gene-Related Peptide-Induced Cerebral Reactivity Significance. *Arterioscler. Thromb. Vasc. Biol.* *34*, 887–893.
- Charlier, C., Singh, N.A., Ryan, S.G., Lewis, T.B., Reus, B.E., Leach, R.J., and Leppert, M. (1998). A pore mutation in a novel KQT-like potassium channel gene in an idiopathic epilepsy family. *Nat. Genet.* *18*, 53–55.
- Chege, S.W., Hortopan, G.A., Dinday, M.T., and Baraban, S.C. (2012). Expression and function of KCNQ channels in larval zebrafish. *Dev. Neurobiol.* *72*, 186–198.
- Constanti, A., and Brown, D.A. (1981). M-Currents in voltage-clamped mammalian sympathetic neurones. *Neurosci. Lett.* *24*, 289–294.
- Delmas, P., and Brown, D.A. (2005). Pathways modulating neural KCNQ/M (Kv7) potassium channels. *Nat. Rev. Neurosci.* *6*, 850.
- Doyle, D.A., Cabral, J.M., Pfuetzner, R.A., Kuo, A., Gulbis, J.M., Cohen, S.L., Chait, B.T., and MacKinnon, R. (1998). The Structure of the Potassium Channel: Molecular Basis of K⁺ Conduction and Selectivity. *Science* *280*, 69–77.
- French, J.A., Abou-Khalil, B.W., Leroy, R.F., Yacubian, E.M.T., Shin, P., Hall, S., Mansbach, H., Nohria, V., and RESTORE 1/Study 301 Investigators (2011). Randomized, double-blind, placebo-controlled trial of ezogabine (retigabine) in partial epilepsy. *Neurology* *76*, 1555–1563.
- Gao, H., Boillat, A., Huang, D., Liang, C., Peers, C., and Gamper, N. (2017). Intracellular zinc activates KCNQ channels by reducing their dependence on phosphatidylinositol 4,5-bisphosphate. *Proc. Natl. Acad. Sci. U. S. A.* *114*, E6410–E6419.
- Gao, Z., Zhang, T., Wu, M., Xiong, Q., Sun, H., Zhang, Y., Zu, L., Wang, W., and Li, M. (2010). Isoform-specific Prolongation of Kv7 (KCNQ) Potassium Channel Opening Mediated by New Molecular Determinants for Drug-Channel Interactions. *J. Biol. Chem.* *285*, 28322–28332.
- Gómez-Posada, J.C., Etxeberria, A., Roura-Ferrer, M., Areso, P., Masin, M., Murrell-Lagnado, R.D., and Villarreal, A. (2010). A Pore Residue of the KCNQ3 Potassium M-Channel Subunit Controls Surface Expression. *J. Neurosci.* *30*, 9316–9323.
- Gu, N., Vervaeke, K., Hu, H., and Storm, J.F. (2005). Kv7/KCNQ/M and HCN/h, but not KCa2/SK channels, contribute to the somatic medium after-hyperpolarization and excitability control in CA1 hippocampal pyramidal cells. *J. Physiol.* *566*, 689–715.
- Gunthorpe, M.J., Large, C.H., and Sankar, R. (2012). The mechanism of action of retigabine (ezogabine), a first-in-class K⁺ channel opener for the treatment of epilepsy. *Epilepsia* *53*, 412–424.

- Heginbotham, L., Lu, Z., Abramson, T., and MacKinnon, R. (1994). Mutations in the K⁺ channel signature sequence. *Biophys. J.* *66*, 1061–1067.
- Heidenreich, M., Lechner, S.G., Vardanyan, V., Wetzel, C., Cremers, C.W., De Leenheer, E.M., Aránguez, G., Moreno-Pelayo, M.Á., Jentsch, T.J., and Lewin, G.R. (2012). KCNQ4 K⁺ channels tune mechanoreceptors for normal touch sensation in mouse and man. *Nat. Neurosci.* *15*, 138–145.
- Hernandez, C.C., Zaika, O., Tolstikh, G.P., and Shapiro, M.S. (2008). Regulation of neural KCNQ channels: signalling pathways, structural motifs and functional implications. *J. Physiol.* *586*, 1811–1821.
- Hille, B. (1977). Local anesthetics: hydrophilic and hydrophobic pathways for the drug-receptor reaction. *J. Gen. Physiol.* *69*, 497–515.
- Horowitz, L.F., Hirdes, W., Suh, B.-C., Hilgemann, D.W., Mackie, K., and Hille, B. (2005). Phospholipase C in living cells: activation, inhibition, Ca²⁺ requirement, and regulation of M current. *J. Gen. Physiol.* *126*, 243–262.
- Jepps, T.A., Olesen, S.P., Greenwood, I.A., and Dalsgaard, T. (2016). Molecular and functional characterization of Kv 7 channels in penile arteries and corpus cavernosum of healthy and metabolic syndrome rats. *Br. J. Pharmacol.* *173*, 1478–1490.
- Jervell, A., and Lange-Nielsen, F. (1957). Congenital deaf-mutism, functional heart disease with prolongation of the Q-T interval, and sudden death. *Am. Heart J.* *54*, 59–68.
- Joshi, S., Sedivy, V., Hodyc, D., Herget, J., and Gurney, A.M. (2009). KCNQ modulators reveal a key role for KCNQ potassium channels in regulating the tone of rat pulmonary artery smooth muscle. *J. Pharmacol. Exp. Ther.* *329*, 368–376.
- Kalappa, B.I., Soh, H., Duignan, K.M., Furuya, T., Edwards, S., Tzingounis, A.V., and Tzounopoulos, T. (2015). Potent KCNQ2/3-specific channel activator suppresses in vivo epileptic activity and prevents the development of tinnitus. *J. Neurosci. Off. J. Soc. Neurosci.* *35*, 8829–8842.
- Kharkovets, T., Hardelin, J.-P., Safieddine, S., Schweizer, M., El-Amraoui, A., Petit, C., and Jentsch, T.J. (2000). KCNQ4, a K⁺ channel mutated in a form of dominant deafness, is expressed in the inner ear and the central auditory pathway. *Proc. Natl. Acad. Sci. U. S. A.* *97*, 4333–4338.
- Kharkovets, T., Dedek, K., Maier, H., Schweizer, M., Khimich, D., Nouvian, R., Vardanyan, V., Leuwer, R., Moser, T., and Jentsch, T.J. (2006). Mice with altered KCNQ4 K⁺ channels implicate sensory outer hair cells in human progressive deafness. *EMBO J.* *25*, 642–652.
- Kim, R.Y., Yau, M.C., Galpin, J.D., Seeböhm, G., Ahern, C.A., Pless, S.A., and Kurata, H.T. (2015). Atomic basis for therapeutic activation of neuronal potassium channels. *Nat. Commun.* *6*.
- Kim, R.Y., Pless, S.A., and Kurata, H.T. (2017). PIP₂ mediates functional coupling and pharmacology of neuronal KCNQ channels. *Proc. Natl. Acad. Sci.* *114*, E9702–E9711.

- Kubisch, C., Schroeder, B.C., Friedrich, T., Lütjohann, B., El-Amraoui, A., Marlin, S., Petit, C., and Jentsch, T.J. (1999). KCNQ4, a novel potassium channel expressed in sensory outer hair cells, is mutated in dominant deafness. *Cell* 96, 437–446.
- Kumar, M., Reed, N., Liu, R., Aizenman, E., Wipf, P., and Tzounopoulos, T. (2016). Synthesis and Evaluation of Potent KCNQ2/3-Specific Channel Activators. *Mol. Pharmacol.* 89, 667–677.
- Lange, W., Geißendörfer, J., Schenzer, A., Grötzinger, J., Seeböhm, G., Friedrich, T., and Schwake, M. (2009). Refinement of the Binding Site and Mode of Action of the Anticonvulsant Retigabine on KCNQ K⁺ Channels. *Mol. Pharmacol.* 75, 272–280.
- Large, C.H., Sokal, D.M., Nehlig, A., Gunthorpe, M.J., Sankar, R., Crean, C.S., Vanlandingham, K.E., and White, H.S. (2012). The spectrum of anticonvulsant efficacy of retigabine (ezogabine) in animal models: implications for clinical use. *Epilepsia* 53, 425–436.
- Larsson, H.P., Baker, O.S., Dhillon, D.S., and Isacoff, E.Y. (1996). Transmembrane Movement of the Shaker K⁺ Channel S4. *Neuron* 16, 387–397.
- Lehman, A., Thouta, S., Mancini, G.M.S., Naidu, S., van Slegtenhorst, M., McWalter, K., Person, R., Mwenifumbo, J., Salvarinova, R., Guella, I., et al. (2017). Loss-of-Function and Gain-of-Function Mutations in KCNQ5 Cause Intellectual Disability or Epileptic Encephalopathy. *Am. J. Hum. Genet.* 101, 65–74.
- Leppert, M., Anderson, V.E., Quattlebaum, T., Stauffer, D., O’Connell, P., Nakamura, Y., Lalouel, J.M., and White, R. (1989). Benign familial neonatal convulsions linked to genetic markers on chromosome 20. *Nature* 337, 647–648.
- Lerche, C., Scherer, C.R., Seeböhm, G., Derst, C., Wei, A.D., Busch, A.E., and Steinmeyer, K. (2000). Molecular cloning and functional expression of KCNQ5, a potassium channel subunit that may contribute to neuronal M-current diversity. *J. Biol. Chem.* 275, 22395–22400.
- Lewis, T.B., Leach, R.J., Ward, K., O’Connell, P., and Ryan, S.G. (1993). Genetic heterogeneity in benign familial neonatal convulsions: identification of a new locus on chromosome 8q. *Am. J. Hum. Genet.* 53, 670–675.
- Li, P., Chen, Z., Xu, H., Sun, H., Li, H., Liu, H., Yang, H., Gao, Z., Jiang, H., and Li, M. (2013). The gating charge pathway of an epilepsy-associated potassium channel accommodates chemical ligands. *Cell Res.* 23, 1106.
- Li, Y., Gamper, N., Hilgemann, D.W., and Shapiro, M.S. (2005). Regulation of Kv7 (KCNQ) K⁺ channel open probability by phosphatidylinositol 4,5-bisphosphate. *J. Neurosci. Off. J. Soc. Neurosci.* 25, 9825–9835.
- Littleton, J.T., and Ganetzky, B. (2000). Ion Channels and Synaptic Organization: Analysis of the *Drosophila* Genome. *Neuron* 26, 35–43.
- Liu, Y., Holmgren, M., Jurman, M.E., and Yellen, G. (1997). Gated Access to the Pore of a Voltage-Dependent K⁺ Channel. *Neuron* 19, 175–184.
- Long, S.B., Campbell, E.B., and Mackinnon, R. (2005). Voltage sensor of Kv1.2: structural basis of electromechanical coupling. *Science* 309, 903–908.

- Lu, Z., Klem, A.M., and Ramu, Y. (2001). Ion conduction pore is conserved among potassium channels. *Nature* *413*, 809–813.
- Mackie, A.R., and Byron, K.L. (2008). Cardiovascular KCNQ (Kv7) potassium channels: physiological regulators and new targets for therapeutic intervention. *Mol. Pharmacol.* *74*, 1171–1179.
- MacKinnon, R. (2003). Potassium channels. *FEBS Lett.* *555*, 62–65.
- Main, M.J., Cryan, J.E., Dupere, J.R.B., Cox, B., Clare, J.J., and Burbidge, S.A. (2000). Modulation of KCNQ2/3 Potassium Channels by the Novel Anticonvulsant Retigabine. *Mol. Pharmacol.* *58*, 253–262.
- Martire, M., Castaldo, P., D’Amico, M., Preziosi, P., Annunziato, L., and Tagliatela, M. (2004). M Channels Containing KCNQ2 Subunits Modulate Norepinephrine, Aspartate, and GABA Release from Hippocampal Nerve Terminals. *J. Neurosci.* *24*, 592–597.
- Martyn-St James, M., Glanville, J., McCool, R., Duffy, S., Cooper, J., Hugel, P., and Lane, P.W. (2012). The efficacy and safety of retigabine and other adjunctive treatments for refractory partial epilepsy: A systematic review and indirect comparison. *Seizure* *21*, 665–678.
- Miceli, F., Soldovieri, M.V., Martire, M., and Tagliatela, M. (2008). Molecular pharmacology and therapeutic potential of neuronal Kv7-modulating drugs. *Curr. Opin. Pharmacol.* *8*, 65–74.
- Miceli, F., Soldovieri, M.V., Ambrosino, P., Barrese, V., Migliore, M., Cilio, M.R., and Tagliatela, M. (2013). Genotype-phenotype correlations in neonatal epilepsies caused by mutations in the voltage sensor of K(v)7.2 potassium channel subunits. *Proc. Natl. Acad. Sci. U. S. A.* *110*, 4386–4391.
- Miceli, F., Soldovieri, M.V., Ambrosino, P., Manocchio, L., Medoro, A., Mosca, I., and Tagliatela, M. (2017). Pharmacological Targeting Of Neuronal Kv7.2/3 Channels: A Focus On Chemotypes And Receptor Sites. *Curr. Med. Chem.*
- Miller, C. (2000). An overview of the potassium channel family. *Genome Biol.* *1*, reviews0004.1-reviews0004.5.
- Millichap, J.J., Park, K.L., Tsuchida, T., Ben-Zeev, B., Carmant, L., Flamini, R., Joshi, N., Levisohn, P.M., Marsh, E., Nangia, S., et al. (2016). KCNQ2 encephalopathy: Features, mutational hot spots, and ezogabine treatment of 11 patients. *Neurol. Genet.* *2*, e96.
- Neyroud, N., Tesson, F., Denjoy, I., Leibovici, M., Donger, C., Barhanin, J., Fauré, S., Gary, F., Coumel, P., Petit, C., et al. (1997). A novel mutation in the potassium channel gene KVLQT1 causes the Jervell and Lange-Nielsen cardioauditory syndrome. *Nat. Genet.* *15*, 186–189.
- Osteen, J.D., Barro-Soria, R., Robey, S., Sampson, K.J., Kass, R.S., and Larsson, H.P. (2012). Allosteric gating mechanism underlies the flexible gating of KCNQ1 potassium channels. *Proc. Natl. Acad. Sci. U. S. A.* *109*, 7103–7108.
- Otto, J.F., Yang, Y., Frankel, W.N., White, H.S., and Wilcox, K.S. (2006). A spontaneous mutation involving Kcnq2 (Kv7.2) reduces M-current density and spike frequency adaptation in mouse CA1 neurons. *J. Neurosci. Off. J. Soc. Neurosci.* *26*, 2053–2059.

- Padilla, K., Wickenden, A.D., Gerlach, A.C., and McCormack, K. (2009a). The KCNQ2/3 selective channel opener ICA-27243 binds to a novel voltage-sensor domain site. *Neurosci. Lett.* **465**, 138–142.
- Padilla, K., Wickenden, A.D., Gerlach, A.C., and McCormack, K. (2009b). The KCNQ2/3 selective channel opener ICA-27243 binds to a novel voltage-sensor domain site. *Neurosci. Lett.* **465**, 138–142.
- Pan, Z., Kao, T., Horvath, Z., Lemos, J., Sul, J.-Y., Cranstoun, S.D., Bennett, V., Scherer, S.S., and Cooper, E.C. (2006). A Common Ankyrin-G-Based Mechanism Retains KCNQ and NaV Channels at Electrically Active Domains of the Axon. *J. Neurosci.* **26**, 2599–2613.
- Park, K.-H., Piron, J., Dahimene, S., Mérot, J., Baró, I., Escande, D., and Loussouarn, G. (2005). Impaired KCNQ1-KCNE1 and phosphatidylinositol-4,5-bisphosphate interaction underlies the long QT syndrome. *Circ. Res.* **96**, 730–739.
- Passmore, G.M., Selyanko, A.A., Mistry, M., Al-Qatari, M., Marsh, S.J., Matthews, E.A., Dickenson, A.H., Brown, T.A., Burbidge, S.A., Main, M., et al. (2003). KCNQ/M Currents in Sensory Neurons: Significance for Pain Therapy. *J. Neurosci.* **23**, 7227–7236.
- Peretz, A., Degani, N., Nachman, R., Uziyel, Y., Gibor, G., Shabat, D., and Attali, B. (2005). Meclofenamic Acid and Diclofenac, Novel Templates of KCNQ2/Q3 Potassium Channel Openers, Depress Cortical Neuron Activity and Exhibit Anticonvulsant Properties. *Mol. Pharmacol.* **67**, 1053–1066.
- Peretz, A., Pell, L., Gofman, Y., Haitin, Y., Shamgar, L., Patrich, E., Kornilov, P., Gourgy-Hacohen, O., Ben-Tal, N., and Attali, B. (2010). Targeting the voltage sensor of Kv7.2 voltage-gated K⁺ channels with a new gating-modifier. *Proc. Natl. Acad. Sci. U. S. A.* **107**, 15637–15642.
- Peters, H.C., Hu, H., Pongs, O., Storm, J.F., and Isbrandt, D. (2005). Conditional transgenic suppression of M channels in mouse brain reveals functions in neuronal excitability, resonance and behavior. *Nat. Neurosci.* **8**, 51–60.
- Ragsdale, D.S., Scheuer, T., and Catterall, W.A. (1991). Frequency and voltage-dependent inhibition of type IIA Na⁺ channels, expressed in a mammalian cell line, by local anesthetic, antiarrhythmic, and anticonvulsant drugs. *Mol. Pharmacol.* **40**, 756–765.
- Ragsdale, D.S., McPhee, J.C., Scheuer, T., and Catterall, W.A. (1994). Molecular determinants of state-dependent block of Na⁺ channels by local anesthetics. *Science* **265**, 1724–1728.
- Rhee, S.G. (2001). Regulation of phosphoinositide-specific phospholipase C. *Annu. Rev. Biochem.* **70**, 281–312.
- Robbins, J. (2001a). KCNQ potassium channels: physiology, pathophysiology, and pharmacology. *Pharmacol. Ther.* **90**, 1–19.
- Robbins, J. (2001b). KCNQ potassium channels: physiology, pathophysiology, and pharmacology. *Pharmacol. Ther.* **90**, 1–19.
- Rodriguez-Menchaca, A.A., Adney, S.K., Tang, Q.-Y., Meng, X.-Y., Rosenhouse-Dantsker, A., Cui, M., and Logothetis, D.E. (2012). PIP₂ controls voltage-sensor movement and pore opening of Kv channels through the S4-S5 linker. *Proc. Natl. Acad. Sci. U. S. A.* **109**, E2399–2408.

- Romano, C. (1965). CONGENITAL CARDIAC ARRHYTHMIA. *Lancet Lond. Engl.* *1*, 658–659.
- Rundfeldt, C. (1997). The new anticonvulsant retigabine (D-23129) acts as an opener of K⁺ channels in neuronal cells. *Eur. J. Pharmacol.* *336*, 243–249.
- Sanguinetti, M.C., Curran, M.E., Zou, A., Shen, J., Specter, P.S., Atkinson, D.L., and Keating, M.T. (1996). Coassembly of KVLQT1 and minK (IsK) proteins to form cardiac IKS potassium channel. *Nature* *384*, 80–83.
- Schenzer, A., Friedrich, T., Pusch, M., Saftig, P., Jentsch, T.J., Grötzinger, J., and Schwake, M. (2005). Molecular determinants of KCNQ (Kv7) K⁺ channel sensitivity to the anticonvulsant retigabine. *J. Neurosci. Off. J. Soc. Neurosci.* *25*, 5051–5060.
- Schoppa, N.E., McCormack, K., Tanouye, M.A., and Sigworth, F.J. (1992). The size of gating charge in wild-type and mutant Shaker potassium channels. *Science* *255*, 1712–1715.
- Schrøder, R.L., Jespersen, T., Christophersen, P., Strøbæk, D., Jensen, B.S., and Olesen, S.-P. (2001). KCNQ4 channel activation by BMS-204352 and retigabine. *Neuropharmacology* *40*, 888–898.
- Schroeder, B.C., Kubisch, C., Stein, V., and Jentsch, T.J. (1998). Moderate loss of function of cyclic-AMP-modulated KCNQ2/KCNQ3 K⁺ channels causes epilepsy. *Nature* *396*, 687–690.
- Schroeder, B.C., Hechenberger, M., Weinreich, F., Kubisch, C., and Jentsch, T.J. (2000). KCNQ5, a novel potassium channel broadly expressed in brain, mediates M-type currents. *J. Biol. Chem.* *275*, 24089–24095.
- Seeböhm, G., Strutz-Seeböhm, N., Ureche, O.N., Baltaev, R., Lampert, A., Kornichuk, G., Kamiya, K., Wuttke, T.V., Lerche, H., Sanguinetti, M.C., et al. (2006). Differential Roles of S6 Domain Hinges in the Gating of KCNQ Potassium Channels. *Biophys. J.* *90*, 2235–2244.
- Seoh, S.-A., Sigg, D., Papazian, D.M., and Bezanilla, F. (1996). Voltage-Sensing Residues in the S2 and S4 Segments of the Shaker K⁺ Channel. *Neuron* *16*, 1159–1167.
- Sheets, M.F., Fozzard, H.A., Lipkind, G.M., and Hanck, D.A. (2010). Sodium channel molecular conformations and antiarrhythmic drug affinity. *Trends Cardiovasc. Med.* *20*, 16–21.
- Singh, N.A., Charlier, C., Stauffer, D., DuPont, B.R., Leach, R.J., Melis, R., Ronen, G.M., Bjerre, I., Quattlebaum, T., Murphy, J.V., et al. (1998). A novel potassium channel gene, KCNQ2, is mutated in an inherited epilepsy of newborns. *Nat. Genet.* *18*, 25–29.
- Starmer, C.F., and Courtney, K.R. (1986). Modeling ion channel blockade at guarded binding sites: application to tertiary drugs. *Am. J. Physiol.* *251*, H848–856.
- Steinlein, O., Schuster, V., Fischer, C., and Häussler, M. (1995). Benign familial neonatal convulsions: confirmation of genetic heterogeneity and further evidence for a second locus on chromosome 8q. *Hum. Genet.* *95*, 411–415.
- Suh, B.-C., and Hille, B. (2002). Recovery from Muscarinic Modulation of M Current Channels Requires Phosphatidylinositol 4,5-Bisphosphate Synthesis. *Neuron* *35*, 507–520.
- Suh, B.-C., and Hille, B. (2007). Regulation of KCNQ channels by manipulation of phosphoinositides. *J. Physiol.* *582*, 911–916.

- Suh, B.-C., and Hille, B. (2008). PIP₂ is a necessary cofactor for ion channel function: How and why? *Annu. Rev. Biophys.* *37*, 175–195.
- Suh, B.-C., Inoue, T., Meyer, T., and Hille, B. (2006). Rapid chemically induced changes of PtdIns(4,5)P₂ gate KCNQ ion channels. *Science* *314*, 1454–1457.
- Sun, J., and MacKinnon, R. (2017). Cryo-EM Structure of a KCNQ1/CaM Complex Reveals Insights into Congenital Long QT Syndrome. *Cell* *169*, 1042–1050.e9.
- Svalø, J., Sheykhzade, M., Nordling, J., Matras, C., and Bouchelouche, P. (2015). Functional and Molecular Evidence for Kv7 Channel Subtypes in Human Detrusor from Patients with and without Bladder Outflow Obstruction. *PLOS ONE* *10*, e0117350.
- Szelenyi, I. (2013). Flupirtine, a re-discovered drug, revisited. *Inflamm. Res.* *62*, 251–258.
- Tatulian, L., and Brown, D.A. (2003). Effect of the KCNQ potassium channel opener retigabine on single KCNQ2/3 channels expressed in CHO cells. *J. Physiol.* *549*, 57–63.
- Tatulian, L., Delmas, P., Abogadie, F.C., and Brown, D.A. (2001). Activation of Expressed KCNQ Potassium Currents and Native Neuronal M-Type Potassium Currents by the Anti-Convulsant Drug Retigabine. *J. Neurosci.* *21*, 5535–5545.
- Testai, L., Barrese, V., Soldovieri, M.V., Ambrosino, P., Martelli, A., Vinciguerra, I., Miceli, F., Greenwood, I.A., Curtis, M.J., Breschi, M.C., et al. (2016). Expression and function of Kv7.4 channels in rat cardiac mitochondria: possible targets for cardioprotection. *Cardiovasc. Res.* *110*, 40–50.
- Thomas, A.M., Harmer, S.C., Khambra, T., and Tinker, A. (2011). Characterization of a binding site for anionic phospholipids on KCNQ1. *J. Biol. Chem.* *286*, 2088–2100.
- Tinel, N., Diochot, S., Lauritzen, I., Barhanin, J., Lazdunski, M., and Borsotto, M. (2000). M-type KCNQ2-KCNQ3 potassium channels are modulated by the KCNE2 subunit. *FEBS Lett.* *480*, 137–141.
- Tobelaim, W.S., Dvir, M., Lebel, G., Cui, M., Buki, T., Peretz, A., Marom, M., Haitin, Y., Logothetis, D.E., Hirsch, J.A., et al. (2017). Competition of calcified calmodulin N lobe and PIP₂ to an LQT mutation site in Kv7.1 channel. *Proc. Natl. Acad. Sci.* *114*, E869–E878.
- Vicente-Baz, J., Lopez-Garcia, J.A., and Rivera-Arconada, I. (2016). Effects of novel subtype selective M-current activators on spinal reflexes in vitro: Comparison with retigabine. *Neuropharmacology* *109*, 131–138.
- Wainger, B.J., Kiskinis, E., Mellin, C., Wiskow, O., Han, S.S.W., Sandoe, J., Perez, N.P., Williams, L.A., Lee, S., Boulting, G., et al. (2014). Intrinsic membrane hyperexcitability of amyotrophic lateral sclerosis patient-derived motor neurons. *Cell Rep.* *7*, 1–11.
- Wang, J., and Li, Y. (2016). KCNQ potassium channels in sensory system and neural circuits. *Acta Pharmacol. Sin.* *37*, 25–33.
- Wang, A.W., Yang, R., and Kurata, H.T. (2017). Sequence determinants of subtype-specific actions of KCNQ channel openers. *J. Physiol.* *595*, 663–676.
- Wang, A.W., Yau, M.C., Wang, C.K., Yang, R., Pless, S.A., and Kurata, H.T. (2018). Functional stoichiometry of KCNQ channel openers II: voltage sensor-targeted openers. *J. Gen. Physiol.*

- Wang, H.S., Pan, Z., Shi, W., Brown, B.S., Wymore, R.S., Cohen, I.S., Dixon, J.E., and McKinnon, D. (1998a). KCNQ2 and KCNQ3 potassium channel subunits: molecular correlates of the M-channel. *Science* 282, 1890–1893.
- Wang, Q., Curran, M.E., Splawski, I., Burn, T.C., Millholland, J.M., VanRaay, T.J., Shen, J., Timothy, K.W., Vincent, G.M., Jager, T. de, et al. (1996). Positional cloning of a novel potassium channel gene: KVLQT1 mutations cause cardiac arrhythmias. *Nat. Genet.* 12, 17.
- Wang, Q., Chen, Q., and Towbin, J.A. (1998b). Genetics, molecular mechanisms and management of long QT syndrome. *Ann. Med.* 30, 58–65.
- Wang, Y., Mi, J., Lu, K., Lu, Y., and Wang, K. (2015). Comparison of Gating Properties and Use-Dependent Block of Nav1.5 and Nav1.7 Channels by Anti-Arrhythmics Mexiletine and Lidocaine. *PloS One* 10, e0128653.
- Weckhuysen, S., Mandelstam, S., Suls, A., Audenaert, D., Deconinck, T., Claes, L.R.F., Deprez, L., Smets, K., Hristova, D., Yordanova, I., et al. (2012). KCNQ2 encephalopathy: Emerging phenotype of a neonatal epileptic encephalopathy. *Ann. Neurol.* 71, 15–25.
- Weckhuysen, S., Ivanovic, V., Hendrickx, R., Van Coster, R., Hjalgrim, H., Møller, R.S., Grønborg, S., Schoonjans, A.-S., Ceulemans, B., Heavin, S.B., et al. (2013). Extending the KCNQ2 encephalopathy spectrum. *Neurology* 81, 1697–1703.
- Wickenden, A.D., Yu, W., Zou, A., Jegla, T., and Wagoner, P.K. (2000). Retigabine, A Novel Anti-Convulsant, Enhances Activation of KCNQ2/Q3 Potassium Channels. *Mol. Pharmacol.* 58, 591–600.
- Wickenden, A.D., Zou, A., Wagoner, P.K., and Jegla, T. (2001). Characterization of KCNQ5/Q3 potassium channels expressed in mammalian cells. *Br. J. Pharmacol.* 132, 381–384.
- Wickenden, A.D., Krajewski, J.L., London, B., Wagoner, P.K., Wilson, W.A., Clark, S., Roeloffs, R., McNaughton-Smith, G., and Rigdon, G.C. (2008). N-(6-Chloro-pyridin-3-yl)-3,4-difluorobenzamide (ICA-27243): A Novel, Selective KCNQ2/Q3 Potassium Channel Activator. *Mol. Pharmacol.* 73, 977–986.
- Wuttke, T.V., Seeböhm, G., Bail, S., Maljevic, S., and Lerche, H. (2005). The New Anticonvulsant Retigabine Favors Voltage-Dependent Opening of the Kv7.2 (KCNQ2) Channel by Binding to Its Activation Gate. *Mol. Pharmacol.* 67, 1009–1017.
- Xiong, Q., Sun, H., and Li, M. (2007). Zinc pyrithione-mediated activation of voltage-gated KCNQ potassium channels rescues epileptogenic mutants. *Nat. Chem. Biol.* 3, 287–296.
- Xiong, Q., Sun, H., Zhang, Y., Nan, F., and Li, M. (2008a). Combinatorial augmentation of voltage-gated KCNQ potassium channels by chemical openers. *Proc. Natl. Acad. Sci. U. S. A.* 105, 3128–3133.
- Xiong, Q., Gao, Z., Wang, W., and Li, M. (2008b). Activation of Kv7 (KCNQ) voltage-gated potassium channels by synthetic compounds. *Trends Pharmacol. Sci.* 29, 99–107.
- Xu, W., Wu, Y., Bi, Y., Tan, L., Gan, Y., and Wang, K. (2010). Activation of voltage-gated KCNQ/Kv7 channels by anticonvulsant retigabine attenuates mechanical allodynia of inflammatory temporomandibular joint in rats. *Mol. Pain* 6, 49.

- Yau, M.C., Kim, R.Y., Wang, C.K., Yang, R., Pless, S.A., and Kurata, H.T. (2018). Functional stoichiometry of KCNQ channel openers I: pore-targeted openers. *J. Gen. Physiol.*
- Yu, H., Wu, M., Hopkins, C., Engers, J., Townsend, S., Lindsley, C., McManus, O.B., and Li, M. (2010). A small molecule activator of KCNQ2 and KCNQ4 channels. In *Probe Reports from the NIH Molecular Libraries Program*, (Bethesda (MD): National Center for Biotechnology Information (US)), p.
- Yue, C., and Yaari, Y. (2004). KCNQ/M channels control spike afterdepolarization and burst generation in hippocampal neurons. *J. Neurosci. Off. J. Soc. Neurosci.* *24*, 4614–4624.
- Zaydman, M.A., and Cui, J. (2014). PIP2 regulation of KCNQ channels: biophysical and molecular mechanisms for lipid modulation of voltage-dependent gating. *Front. Physiol.* *5*.
- Zaydman, M.A., Silva, J.R., Delaloye, K., Li, Y., Liang, H., Larsson, H.P., Shi, J., and Cui, J. (2013a). Kv7.1 ion channels require a lipid to couple voltage sensing to pore opening. *Proc. Natl. Acad. Sci.* *110*, 13180–13185.
- Zaydman, M.A., Silva, J.R., Delaloye, K., Li, Y., Liang, H., Larsson, H.P., Shi, J., and Cui, J. (2013b). Kv7.1 ion channels require a lipid to couple voltage sensing to pore opening. *Proc. Natl. Acad. Sci. U. S. A.* *110*, 13180–13185.
- Zhang, H., Craciun, L.C., Mirshahi, T., Rohács, T., Lopes, C.M.B., Jin, T., and Logothetis, D.E. (2003). PIP2 Activates KCNQ Channels, and Its Hydrolysis Underlies Receptor-Mediated Inhibition of M Currents. *Neuron* *37*, 963–975.
- Zhang, R.S., Wright, J.D., Pless, S.A., Nunez, J.-J., Kim, R.Y., Li, J.B.W., Yang, R., Ahern, C.A., and Kurata, H.T. (2015). A Conserved Residue Cluster That Governs Kinetics of ATP-dependent Gating of Kir6.2 Potassium Channels. *J. Biol. Chem.* *290*, 15450–15461.